Stony Brook University

The official electronic file of this thesis or dissertation is maintained by the University Libraries on behalf of The Graduate School at Stony Brook University.

Inhibition of Chaperone/Usher Pilus Assembly by Nitazoxanide

A Dissertation Presented

by

Peter Nicholas Chahales

to

The Graduate School

in Partial Fulfillment of the

Requirements

for the Degree of

Doctor of Philosophy

in

Molecular Genetics and Microbiology

Stony Brook University

December 2015

Stony Brook University
The Graduate School

Peter Nicholas Chahales

We, the dissertation committee for the above candidate for the
Doctor of Philosophy degree, hereby recommend
acceptance of this dissertation.

David G. Thanassi Ph. D. – Dissertation Advisor
Professor, Department of Molecular Genetics and Microbiology

James B. Bliska Ph. D. - Chairperson of Defense
Professor, Department of Molecular Genetics and Microbiology

A. Wali Karzai Ph. D. – Committee Member
Associate Professor, Department of Biochemistry and Cell Biology

Peter J. Tonge Ph. D. - Committee Member
Professor, Department of Chemistry

Thomas J. Silhavy Ph. D. – Outside Committee Member
Warner-Lambert Parke-Davis Professor of Molecular Biology, Department of Molecular
Biology, Princeton University

This dissertation is accepted by the Graduate School

Charles Taber
Dean of the Graduate School

ii

Abstract of the Dissertation

Inhibition of Chaperone/Usher Pilus Assembly by Nitazoxanide

by

Peter Nicholas Chahales

Doctor of Philosophy

in

Molecular Genetics and Microbiology

Stony Brook University

2015

Increasing rates of antibiotic resistance are challenging the status quo and raising the possibility of a post-antibiotic era, in which even common infections could become life threatening. This looming health crisis highlights the immediate need for new and effective therapies, which not only neutralize bacterial pathogens but also limit the development of resistance. A new class of molecules known as anti-virulence therapeutics targets the bacterial virulence factors used to establish disease in the host. This is in contrast to traditional antibiotics, which disrupt essential processes required for bacterial survival. One such virulence target includes adhesive fibers, termed pili, assembled by a conserved mechanism known as the chaperone/usher (CU) pathway. P and type 1 pili are prototypical examples of pili assembled by the CU pathway. These pili are utilized by uropathogenic *Escherichia coli* to colonize host tissues and establish urinary tract infections (UTIs). UTIs are the second most common infection of the human body, and uropathogenic *E. coli* is a pathogen that displays high incidences of antibiotic resistance clinically. To address the need for new antimicrobial agents, I have

identified a new use and mechanism of action for the FDA approved anti-parasitic drug nitazoxanide (NTZ). I have shown that NTZ inhibits the assembly of adhesive pili on the surface of *E. coli* in a dose dependent manner. Using a combination of genetic and biochemical techniques, I demonstrated that NTZ prevents proper maturation the usher protein in the bacterial outer membrane (OM). The usher is an essential part of the CU pathway and serves as a platform for pilus assembly and secretion. Furthermore, I have obtained genetic evidence strongly suggesting that NTZ targets an essential OM complex known as the ß-barrel assembly machinery (Bam), which is required to fold the usher. This work not only identifies NTZ as a potential anti-virulence compound to treat pilus-mediated diseases such as UTIs, but also provides the first described chemical tool to investigate the functionality of the Bam complex. Additionally, this work highlights the value of both CU pili and the Bam complex as therapeutic targets.

Dedication

This dissertation is dedicated to the memory of my grandparents,

Christos and Sparti Nicholoudis,

whose sacrifice and devotion to the pursuit of higher education

formed the foundation for which my future will be built upon.

And to my parents,

Nicholas and Pauline Chahales,

who are the definition of unconditional love and support,

and the reason I am the man that I am today.

Table of Contents

List of Tables

List of Figures

Acknowledgments

There are many people I need to thank and recognize for their significant contributions towards helping me achieve this milestone in my life:

This work would have not been possible without the support and collaborative efforts of a number of individuals. **Dr. Paul Hoffmann** at the University of Virginia has been my primary collaborator throughout this project and the one responsible for introducing David and me to nitazoxanide. It is his initial work with the drug that set the foundation for my project. **Dr. Nathan Rigel** at Hofstra University provided insightful discussion and access to materials. **Dr. James Bliska** at Stony Brook University, **Dr. Ian Henderson** at the University of Birmingham and **Dr. Harris Bernstein** at the National Institutes of Health who also generously provided access materials. **Dr. Wali Karzai and the members of his laboratory** at Stony Brook University, including **Dr. Krithika Venkataramen**, **Dr. Perry Woo**, **Dr. Preeti Mehta**, and **Neha Puri** who provided protocols, reagents, materials (especially the Keio collection), and insightful discussion, in addition to being dear friends of mine. And lastly **Dr. Thomas Silhavy and the members of his laboratory** at Princeton University, who I have communicated with either via email or at conferences, for sharing materials and their wealth of knowledge about the Bam complex and for being an absolute pleasure to interact with over the years.

My fellow lab mates: **Nadine Henderson,** for keeping the lab organized and functional; **Dr. Vinaya Sampath,** who has been a wonderful desk mate these past five and a half years; **Dr. Sarah Alaei** for being a great friend and a someone who is always willing to listen; **Erik Kopping**, my Hudson Valley brother and fellow bar-b-que aficionado; **Glenn Werneburg**, for sharing my love of the usher and for introducing me to Heady Topper; our newest lab member

John Psonis, who will be taking over my project and undoubtedly will contribute greatly to the work; and our undergraduate student **Hemil Chauhan** for injecting some youthful humor into the lab. We have laughed together, cried together, and probably wanted to punch one another at some point in time, but there is no doubt that we view ourselves as part of a team and would be there to support each other in a moments notice.

I would like thank the administration of the Department of Molecular Genetics and Microbiology including: **Kate Bell**, for being the department mom, always listening, and being there whenever I had a question; **Dr. Janet Hearing**, for her guidance, support, and recognition of my efforts through letters of recommendation and award nominations; and the chairman of the department **Dr. Jorge Benach**, whose unwavering support for me, both academically and personally, I am extremely grateful for, and whose open door policy is a clear indicator of his commitment to the success of young scientists like myself.

I would like to acknowledge the members of my thesis committee **Dr. James Bliska (chair), Dr. Wali Karzai, Dr. Peter Tonge, and Dr. Thomas Silhavy**. Their insights and perspectives have not only guided me through this process but have challenged and inspired me in ways that have helped me to become a better scientist.

It has been an absolute honor to have **Dr. David Thanassi** as my thesis advisor. I could not have asked for a better mentor. His patience, intellect, and genuine interest in the success of his students have had, and will continue to have, an immeasurable impact on scientific career. It is a privilege to not only call him my boss but a colleague and a friend.

My career in science would not exist if it was not for **Dr. Vincent Fischetti** at The Rockefeller University. Vince provided me, at the age of 19, an opportunity to work in his

laboratory and literally changed the course of my life. To him and the rest of my Rockefeller family who have supported me throughout this journey I am forever grateful.

To all the friends I have made here at Stony Brook and on Long Island I want to extend a deep thanks for their friendship and support. I am exited to see all the amazing things they will go on to accomplish and do in their futures.

Without question, the greatest discovery I have made during my time here at Stony Brook is my amazing and loving girlfriend **Stephanie Mueller**. She has been my rock and number one cheerleader during this entire process. I cannot think of any better person to have shared this experience with and I am exited for the new adventures we will experience together in the future. I would also like to thank her parents **Gary and Tracy Mueller** who always generously supported me and made me feel as a member of their family.

To my grandparents, **Christos and Sparti Nicholoudis,** who immigrated to this country after escaping war torn Greece and sacrificed everything in the hopes that, one day, one of their own would go on to achieve the highest level of education possible. This is the realization of their dream.

And lastly, to my parents **Nicholas and Pauline Chahales and my sister Themi**, the words are not available to express how grateful I am for you all. You are the reason that I view myself as the luckiest man in the world and hope that one day I can repay you for the endless amounts of love and support you have given me throughout my life.

CHAPTER 1

Introduction

1.1 Antibiotic Resistance

Since Alexander Fleming's discovery of penicillin in 1928, antibiotics have been recognized as arguably the greatest advancement in human health. Prior to their introduction into society, common bacterial infections such as strep throat, pneumonia, or even a small infected cut carried with them a significant risk of severe disability and death. Today, the widespread use of antibiotics has not only made these, and many other infections, curable but is credited for extending the average human life expectancy by ten years (1). However, in his 1945 Nobel Prize lecture, Alexander Fleming shared with the public an almost prophetic warning about the use of antibiotics based on his own observations with penicillin: "The time may come when penicillin can be bought by anyone in the shops. Then there is the danger that the ignorant man may easily underdose himself and by exposing his microbes to non-lethal quantities of the drug make them resistant" (2). Seventy years later the threat of antibiotic resistance has become an ever-apparent global crisis.

The development of antibiotic resistance is not a novel phenomenon as it is a natural evolutionary process by which bacteria compete with each other. However, with the recent dwindling antibiotic pipeline, combined with overconsumption of these drugs, humans have dramatically accelerated this process, selecting for pathogens that are increasingly difficult to treat and leading to what is often referred to as a tragedy of the commons. Today it is estimated that at least 700,000 deaths per year worldwide are attributed to anti-microbial resistant infections, which results in an economic burden of $21-$34 billion annually in the United States alone (3, 4). A 2014 review on the subject commissioned by the British government predicts the number of deaths to increase to 10 million by the year 2050 and surpass more than $100 trillion in costs to the global economy if immediate action is not taken (3).

While antibiotic resistance is prevalent amongst pathogenic strains of both Gram-positive and Gram-negative bacteria, it is the latter that have become increasingly worrisome. This is because Gram-negative bacteria possess an additional protective barrier known as the outer membrane (OM), which restricts access to certain antibiotics, rendering the bacteria generally more resistant and harder to treat. Additionally, infections by these organisms are becoming commonplace within our healthcare facilities, putting already at risk patients in a very precarious position. Of the most urgent concern are isolates of stains such as *Klebsiella pneumoniae* and *Escherichia coli*, termed carbapenem-resistant enterobacteriaceae (CRE), which have been identified in hospitals and are resistant to all, or nearly all, available antibiotics (5). These "nightmare bacteria", as they have been deemed by the Centers for Disease Control and Prevention, have gained resistance to our last resort class of antibiotics, the carbapenems, leaving physicians with little-to-no options should a patient become infected (6). Further exemplifying the severity of these pathogens is the 50% mortality rate associated with them should an infection enter the bloodstream (7). CRE infections can manifest themselves in many sites throughout the human body; however, it is in the bladder and kidneys, in the form of a urinary tract infection, that incidences of these pathogens are on the rise.

1.2 Urinary Tract Infections

Urinary tract infections (UTIs) are the second most commonly acquired infections of the human body. Greater than 50% of women and 15% of men will experience at least one UTI during their lifetime. Moreover, 25% of those woman will go on to develop one or more additional UTIs at a later time highlighting the high rate of recurrence associated with the disease. UTIs also pose a significant burden to healthcare facilities, accounting for 40% of all

hospital-acquired infections (8-10). The frequency of these infections results in over 10.5 million doctors office visits per year at a cost of $3.5 billion annually in the United States alone (9, 11, 12).

A community-acquired, often referred to as uncomplicated, UTI is typically established when bacteria, or uropathogens, enter the urogenital tract through the opening in the urethra. Two common mechanisms of transmission are through sexual intercourse and/or the transfer of gut microbes present in fecal material (13). These modes of transmission also highlight the gender discrepancy seen with incidences of UTIs due to the fact that females have a shorter urethra than males. Once in the urethra, the bacteria ascend to the bladder where they can adhere to and colonize the bladder epithelium, triggering inflammation and leading to the development of cystitis. This initial adherence step is critical to the infection cycle as it prevents the bacteria from being cleared away by the natural flow of urine. Should the infection in the bladder remain unresolved, bacteria can then ascend the ureters and enter into the kidneys where adherence and colonization of kidney epithelia can occur leading to the development of pyelonephritis. If treatment or resolution of the infection fails at this stage the bacteria can progress to gain access to the blood supply leading to bacteremia (13, 14). Kidney infections are the third leading cause of sepsis behind respiratory and abdominal infections (15). Common symptoms of a UTI include urgency and frequency of urination, hematuria, back pain, and fever (16, 17).

Catheter-associated UTIs are another form of the disease predominantly found in the healthcare setting. These UTIs result from the improper usage of indwelling urinary catheters in patients. Some uropathogens are capable of colonizing the catheter surface using it as a vehicle to gain access to the urinary tract. Alternatively, the introduction of the catheter into the patient

can induce structural abnormalities in the urogenital tract epithelia increasing the patient's susceptibility to infection. This form of the infection is referred to as a complicated UTI (15).

A number of bacteria have been identified as causative agents of UTIs, including *Proteus mirabilis*, *Pseudomonas aeruginosa*, *Streptococcus agalactiae*, and *Enterococcus fecalis* (9). However, the primary causative agent responsible for ~85% of all uncomplicated and catheter-associated forms of the disease is uropathogenic *E. coli* (UPEC) followed by *K. pneumonia,* which is implicated in 6–17% of infections (13, 18, 19). UPEC is a member of the human commensal resident gut flora where it is not associated with any disease. It is only upon introduction of the bacterium into the urinary tract that it can employ its virulence mechanisms to establish a UTI.

1.3 Pili and the Chaperone/Usher Pathway

1.3.1 Introduction to bacterial adhesins. Bacteria assemble a variety of adhesive proteins (adhesins) on their surface to mediate binding to receptors and colonization of surfaces. For pathogenic bacteria, adhesins are critical for early stages of infection, allowing the bacteria to initiate contact with host cells, colonize different tissues, and establish a foothold within the host. Adhesins recognize specific receptors expressed by specific subsets of host cells. Therefore, the repertoire of adhesins expressed by a pathogen play a major role in dictating the tropism of the pathogen toward specific host tissues and organs. Moreover, binding of bacterial adhesins to host cell receptors influences subsequent events by triggering signaling pathways in both the host and bacterial cells. These signaling pathways may determine whether the bacteria remain extracellular or become internalized, and influence the intracellular trafficking of invaded bacteria and their ability to survive and replicate (20, 21). The adhesins expressed by a pathogen

are also critical for bacterial-bacterial interactions and the formation of bacterial communities such as biofilms. The ability to adhere to host tissues is particularly important for bacteria that colonize sites such as the urinary tract, where the flow of urine functions to maintain sterility by washing away non-adherent pathogens.

Adhesins vary from monomeric proteins that are directly anchored to the bacterial surface to polymeric, hairlike fibers that extend out from the cell surface. These latter fibers are termed pili or fimbriae, and were among the first identified virulence factors of UPEC (22). Uropathogenic bacteria have been closely associated with the discovery and characterization of pili. The chromosomal gene clusters responsible for expression of both type 1 and P pili were first cloned from the J96 UPEC strain (23), and the genes coding for S pili were isolated from UPEC strain 536 (24). Much of our current understanding of the structure, assembly, and functions of bacterial pili stems from studies of the type 1 and P pili originally isolated from UPEC.

Pili and other extended surface fibers increase the functional reach of adhesins, enabling the bacteria to act at a distance. Pili place adhesins outside capsular or other protective surface structures, allowing contact with receptors while maintaining the protective integrity of the bacterial envelope. The ability to initiate contact at a distance also provides a means for pathogenic bacteria to avoid detection or uptake by host cells.

1.3.2 Pili assembled by the chaperone/usher pathway. A wide range of Gram-negative bacteria use the chaperone/usher (CU) pathway to assemble a superfamily of virulence-associated adhesive surface fibers (25-28). The CU pathway takes its name from the components of its secretion machinery, which consist of a dedicated periplasmic chaperone and an integral outer membrane protein termed the usher. The CU pathway builds a diverse array of peritrichous

surface fibers, ranging from thin, flexible filaments to rigid, rod-like organelles. For uropathogenic bacteria, pili assembled by the CU pathway mediate adhesion to receptors in the urinary tract, initiating infection and promoting bacterial colonization. Pili are critical virulence factors of uropathogenic bacteria and have been the subject of intense study. The CU pili expressed by uropathogenic bacteria are exquisitely adapted to colonization within the urinary tract, engineered to withstand and take advantage of forces encountered during colonization such as the flow of urine (29-32). In addition to binding to host molecules, CU pili are important for bacterial-bacterial interactions, biofilm formation, and adhesion to abiotic surfaces. Moreover, binding of bacteria to host cells via CU pili modulates host signaling pathways and promotes subsequent stages of pathogenesis such as invasion inside host cells(33-39).

Genes coding for CU pili are found on both the bacterial chromosome and on plasmids, and are clustered together with a similar organization: a 5' regulatory region that is followed by a single downstream operon encoding the required pilus structural proteins and assembly components (Fig. 1). CU gene clusters are often associated together with other virulence determinants in pathogenicity islands, which have characteristics indicating acquisition by horizontal gene transfer (40). A single bacterial genome often contains multiple CU pathways, which presumably provides the ability to adhere to a variety of different receptors and surfaces (41-43). A recent genomic analysis found that *E. coli* strains encode as many as 17 CU gene clusters and that UPEC strains encode from 9-12 intact CU gene clusters (44). Many of the CU gene clusters present in a bacterial genome are not expressed under laboratory growth conditions and their functions remain unknown (42). The expression of CU gene clusters is typically highly regulated, subject to phase variation, and responsive to environmental cues (45, 46). Regulatory cross talk may occur among different CU gene clusters (47-49). This cross talk likely ensures

that a given bacterium only expresses a single pilus at a given time, thus controlling adhesive specificity. Furthermore, expression of adhesive pili has been shown to be inversely correlated with the expression of flagella for motility (50).

1.3.3 Structure of the CU pilus fiber. Pili assembled by the CU pathway range from 2-10 nm in diameter and generally 1-3 μm in length. The pili are linear fibers built from thousands of copies of non-covalently interacting subunit proteins, termed pilins. Some pili adopt a final helical quaternary structure, resulting in the formation of rigid, rod-like organelles. Alternatively, the pili may remain as linear, flexible fibers, which in some cases form amorphous or 'afimbrial' structures. Many pili assembled by the CU pathway are composite structures containing both a rigid, helical rod, which extends out from the bacterial surface, as well as a thin, flexible tip structure, which is located at the distal end of the rod and contains the adhesive activity. Type 1 and P pili expressed by UPEC are prototypical composite organelles with distinct rod and tip structures (Fig. 1.1). The Afa/Dr family of pili expressed by UPEC and other pathogenic *E. coli* are well studied examples of thin, flexible fibers that often have an amorphous appearance by electron microscopy (51).

The structures of pilins and many aspects of pilus assembly by the CU pathway are understood in atomic detail (27, 52-57). All pilins contain an immunoglobulin-like (Ig) fold termed the pilin domain (Fig. 1.2). Canonical Ig folds comprise seven ß-strands arranged into two sheets as a ß-sandwich (58). However, pilins lack the seventh, C-terminal ß-strand (the G strand) and thus are unable to complete their own fold (52-55). This missing strand results in a deep groove on the surface of the subunit, exposing its hydrophobic core. To complete their folds, pilins rely on structural information provided by interaction with the periplasmic

chaperone or with neighboring subunits in the pilus fiber.

Subunit-subunit interactions in the pilus fiber are mediated by a mechanism termed donor strand exchange(54, 55). Pilins contain a conserved N-terminal extension (Nte) in addition to the pilin domain. In the pilus fiber, the Nte of one pilus subunit is 'donated' to the preceding subunit, completing the Ig fold of the preceding subunit (Fig. 1.2). Therefore, the pilus fiber consists of an array of Ig folds, with each subunit noncovalently bound to the preceding subunit by donor strand exchange. This arrangement provides great mechanical strength and stability to the pili, which is reflected by the property that subunit-subunit interactions in the pilus are resistant to dissociation by heat and denaturants (59, 60). A high level of mechanical strength is essential for the pili to maintain adhesion in the face of shear forces encountered from the flow of urine. The helical pilus rod provides an additional mechanism to withstand hydrodynamic forces in the urinary tract; the helical rod is able to uncoil under stress to an extended linear fiber, thereby acting as a spring or shock absorber to prevent breakage of the pilus and extend the lifetime of pilus-receptor interactions (29, 30, 32, 61).

1.3.4 The pilus adhesin. The receptor-binding activity of pili is conferred by the pilus adhesin. For composite pili such as type 1 and P pili, the adhesin is located in single copy at the distal end of the tip fiber (Fig. 1.2). Such pili have been termed monoadhesive pili (26). In contrast, for pili lacking a district tip structure, the main structural subunit that builds the pilus fiber may also contain receptor-binding sites along exposed surfaces and thus the entire pilus may function in adhesion (57, 62-64). Such fibers are termed polyadhesive pili.

Crystal structures have been solved for several adhesins from monoadhesive pili (52, 65-70). In contrast to other pilus subunits, the adhesins are two domain proteins, containing an N-

terminal receptor-binding or adhesin domain (in place of the Nte) and a C-terminal pilin domain. The pilin domain mediates incorporation of the adhesin into the pilus fiber and is an incomplete Ig-like fold as found for all CU pilins. Adhesin domains also have Ig-like folds, but the folds are complete (not lacking the terminal ß-strand) and structurally distinct from the pilin domain. Despite their common architecture, adhesins vary greatly in sequence and employ distinct receptor binding mechanisms, reflecting their specific functions within the host (71). The FimH adhesin from type 1 pili folds as an elongated 11-stranded ß-barrel with a jelly roll-like topology (52, 66). The binding site for the mannose ligand is located at the tip of the adhesin domain and is formed by a deep, negatively-charged pocket surrounded by a hydrophobic ridge (Fig. 1.2B). In comparison, the adhesin domain of the P pilus adhesin PapG adopts a structure with two sub regions; one region having a ß-barrel fold similar to FimH and the other region having a unique, largely ß-sheet structure that contains the binding site for the globoside receptor (65, 67). In contrast to FimH, the receptor-binding site of PapG is located in a shallow groove along the side of the adhesin (Fig. 1.2B).

Pilus adhesins such as FimH exhibit the property of shear-enhanced binding, which enables tighter binding under conditions of shear stress such as encountered during bacterial colonization of the urinary tract (31). The application of shear stress causes FimH to switch from a low-affinity to a high-affinity binding state. This greater affinity presumably allows the bacteria to avoid being washed away by the flow of urine, and may also provide a mechanism for the bacteria to discriminate between surface-located and soluble receptors, as binding to the latter will not result in force generation on the pilus and FimH will stay in the low-affinity state. Moreover, the physical properties of both the type 1 pilus tip fiber and the helical pilus rod appear to be designed to optimize the shear-enhanced behavior of FimH, and the

flexibility of the pilus tip likely provides FimH maximum opportunity to find its target receptors (72, 73).

1.4 Pilus Assembly by the Chaperone/Usher Pathway

1.4.1 Formation of chaperone-subunit complexes in the periplasm. Pilus subunits are synthesized with an N-terminal signal sequence that directs them to the Sec general secretory pathway for translocation to the periplasm (74). The signal sequence is cleaved in the periplasm, and the subunits form stable, binary complexes with the periplasmic chaperone (Fig. 1.2A). The chaperone enables proper folding of the pilus subunits, prevents premature subunit-subunit interactions, and maintains the subunits in an assembly-competent state (52-55). In the absence of the chaperone, pilus subunits misfold and form aggregates that are degraded by the DegP periplasmic protease (75, 76).

The structure of the PapD chaperone and subsequent structures of chaperone-subunit complexes revealed the molecular basis for chaperone function in pilus biogenesis (52-54, 77-79). As described above, pilins have an incomplete Ig fold, lacking the C-terminal G ß-strand. The chaperone contains two Ig-like domains oriented in an L or boomerang shape. The binding site for subunits resides in the cleft between the two domains and extends out along the chaperone's N-terminal domain (domain 1). The chaperone functions by a mechanism termed donor strand complementation, in which the chaperone inserts its G1 ß-strand and a portion of its F1-G1 loop into the groove caused by the missing G strand of the subunit, completing the Ig fold of the pilin domain (Fig. 1.2A) (52, 53, 79, 80).

The groove in the pilin domain caused by the missing ß-strand contains a series of binding pockets, termed P1-5 (54). The G1 ß-strand donated by the chaperone contains a

conserved motif of alternating hydrophobic residues, and during donor strand exchange these residues insert into the P1-4 pockets of the subunit, forming a ß-zipper interaction (55, 81). The chaperone G1 ß-strand is inserted parallel to the F strand of the subunit, forming a non-canonical Ig fold. This, together with the large size of the residues inserted by the chaperone maintains pilins in an open, "activated" state, which enables subsequent assembly into the pilus fiber (54, 55, 82). The groove of the pilin domain is also the site of subunit-subunit interactions, which are mediated by the donor strand exchange reaction as described above for the pilus fiber (54, 55). Thus, donor strand complementation by the chaperone couples the folding of pilins with the simultaneous capping of their interactive surfaces, preventing premature fiber assembly in the periplasm. Recent studies have shown that chaperones also perform a quality control function during the initial binding of pilus subunits and that formation of chaperone-subunit complexes results in an allosteric change in the chaperone that permits binding to the outer membrane usher assembly platform (83, 84).

1.4.2 Assembly of the pilus fiber at the outer membrane. Chaperone-subunit complexes must interact with the outer membrane usher for release of the chaperone, assembly of subunits into the pilus fiber, and secretion of the fiber to the cell surface through the usher channel (56, 85). The usher acts as a pilus assembly catalyst, accelerating the rate of subunit incorporation into the pilus fiber (86). Subunit-subunit interactions form at the periplasmic face of the usher via the donor strand exchange mechanism (54, 55). The donated subunit Nte contains a conserved motif of alternating hydrophobic residues, similar to the chaperone G1 ß-strand (87, 88). At the usher, the hydrophobic residues of the Nte from an incoming chaperone-subunit complex insert into the subunit groove of the preceding chaperone-subunit complex

bound at the usher, displacing the donated G1 ß-strand of the chaperone from the preceding subunit by a concerted strand displacement mechanism that initiates at the P5 pocket (54, 55, 81, 89, 90). In contrast to the donated chaperone ß-strand, the Nte is inserted anti-parallel to the F strand of the preceding subunit and inserts smaller-sized residues into the subunit groove, thus completing the Ig fold of the pilin domain in a canonical fashion and allowing the subunit to adopt a highly stable final state (54, 55, 60, 82). ATP is not available in the periplasm and pilus biogenesis at the outer membrane usher does not require input from other energy sources (91, 92). The canonical Ig fold formed by donor strand exchange represents a more compact, lower energy state compared to the non-canonical Ig fold formed by donor strand complementation with the chaperone (54, 55, 82). This topological transition from the higher-energy chaperone-subunit complex to the lower-energy subunit-subunit interaction provides the driving force for fiber formation and secretion at the usher (93).

Pili are assembled in a top-down order, with the adhesin incorporated first, followed by the rest of the pilus tip and finally the rod. Each subunit specifically interacts with its appropriate neighbor subunit in the pilus, with the specificity of binding determined by the donor strand exchange reaction (94-96). In addition, the usher ensures ordered and complete pilus assembly by differentially recognizing chaperone-subunit complexes according to their final position in the pilus; i.e., chaperone-adhesin complexes have highest affinity for the usher, whereas chaperone-rod subunit complexes have low affinity (97-99). The usher channel is only wide enough to allow secretion of a linear fiber of folded pilus subunits (85). Therefore, the pilus rod is constrained to a linear fiber as it passes through the usher and only converts to its final helical form upon reaching the bacterial surface.

1.4.3 The pilus usher. Ushers are large, integral outer membrane proteins containing five domains: a central transmembrane ß-barrel domain that forms the secretion channel, a middle domain located within the ß-barrel region that forms a channel gate (the plug domain), a periplasmic N- terminal domain (NTD), and two periplasmic C-terminal domains (CTD1 and CTD2) (Fig. 1.3) (56, 85, 100-104). The NTD provides the initial binding site for chaperone-subunit complexes and functions in the recruitment of periplasmic complexes to the usher (100, 105). The CTDs provide a second binding site for chaperone-subunit complexes and anchor the growing pilus fiber (56). The usher is present as a oligomeric complex in the OM, but only one channel is used for secretion of the pilus fiber and the function of the usher oligimer remains to be determined, particularly since the usher monomer appears to be sufficient for pilus assembly (56, 85, 101, 106-108).

The structure of the type 1 pilus usher FimD bound to the FimC-FimH chaperone-adhesin complex was recently solved, revealing the usher pilus assembly machine in action (Fig. 1.3) (56). The usher channel is formed by a 24-stranded ß-barrel that is occluded by an internal plug domain (56, 85). The binding of the FimH adhesin to FimD activates the usher for pilus biogenesis (86, 98, 108, 109), resulting in displacement of the plug to the periplasm and insertion of the FimH adhesin domain inside the usher channel. The FimH pilin domain remains in complex with the FimC chaperone and bound to the usher CTDs (Fig. 1.3). CU pili extend by step-wise addition of new chaperone-subunit complexes to the base of the fiber. New chaperone-subunit complexes are recruited by binding to the usher NTD, which is unoccupied in the FimD-FimC-FimH structure (56, 100, 105). Modelling studies suggest that binding of a chaperone-subunit complex to the usher NTD would perfectly position the Nte of the newly recruited subunit to initiate donor strand exchange with the P5 pocket of the subunit bound at the usher

CTDs, providing a molecular explanation for the catalytic activity of the usher in pilus assembly (56). Following donor strand exchange, the chaperone is displaced from the subunit bound at the CTDs and released into the periplasm. To reset the usher for another round of subunit incorporation, the newly incorporated chaperone-subunit complex must transfer from the NTD to the CTDs, concomitant with translocation of the pilus fiber through the usher channel toward the cell surface. Repeated iterations of this cycle would then result in assembly and secretion of a complete pilus fiber.

1.5 Functions of Type 1 and P CU Pili Expressed by UPEC

Type 1 pili are expressed by most strains of *E. coli* and mediate binding to a variety of surfaces and host tissues in a mannose-sensitive manner. Type 1 pili are a major virulence factor of UPEC and antibodies to the type 1 pilus adhesin FimH provide protection against urinary tract infection by *E. coli* in both murine and primate models (110, 111). However, a definitive requirement for type 1 pili in human UTIs has remained elusive (112), likely due to the large repertoire of adhesins expressed by uropathogenic strains. UPEC use type 1 pili to bind to α-D-mannosylated proteins present in the bladder, leading to bacterial colonization, bladder epithelial cell invasion, and the development of cystitis (34, 113). In addition to urothelial cells, type 1 pili have been reported to bind to Tamm-Horsfall protein, surface glycoproteins of immune cells, extracellular matrix proteins, and abiotic surfaces (114-117).

Type 1 pili are encoded by the *fim* gene cluster (Fig. 1.1), which is present on the chromosome of pathogenic as well as non-pathogenic and laboratory strains of *E. coli*. Type 1 pili are built from 4 different types of pilins arranged into a rigid helical rod measuring 6.9 nm in diameter, and a short tip fiber measuring 2 nm in diameter and generally 10-19 nm in length

(Fig. 1.1) (118, 119). The type 1 pilus rod is built from greater than 1,000 copies of the FimA major pilin arranged into a right-handed helix (119). Type 1 pilus tips contain a single copy of the FimH adhesin at the distal end, followed by the FimG and FimF adaptor subunits, which are generally present in single copy (Fig. 1.2A) (118-120). The mannose binding site of the FimH adhesin is located in a deep pocket at the tip of the adhesin domain (Fig. 1.2B) (66). This places the receptor-binding site at the most distal end of the type 1 pilus organelle, which presumably facilitates access of the pilus to its receptor.

Studies using the murine urinary tract infection model have revealed many aspects of type 1 pilus function during UPEC pathogenesis. Upon entering the urinary tract, UPEC use their type 1 pili to bind to uroplakins, mannosylated proteins that coat the luminal surface of the bladder, allowing the bacteria to colonize the bladder and avoid being washed out by the flow of urine (34, 121). Type 1 pili not only mediate binding of UPEC to the bladder surface, but also trigger host cell signaling pathways that lead to actin rearrangement in the urothelial cells and invasion of the bacteria inside the cells by a zipper-like mechanism (33, 34, 122). Additionally, bacterial uptake is facilitated by binding of type 1 pili to ß1 and α3 integrins (35). Binding of *E. coli* to the urothelium leads to induction of innate host cell responses, such as upregulation of proinflammatory cytokines and cell death pathways (34, 122, 123). The FimH adhesin acts as a pathogen-associated molecular pattern that is recognized by Toll-like receptor 4 (TLR4), present on bladder epithelial cells as well as macrophages, and stimulates immune signaling pathways through a mechanism independent of LPS (37).

Following uptake inside bladder epithelial cells, UPEC are initially contained within vesicles, which may be routed for exocytosis in a TLR4-and cyclic AMP-dependent mechanism that may be used by the host cells to expel the invading bacteria (124). Bacteria that evade

16

expulsion enter the cytoplasm where they rapidly replicate to form aggregates termed intracellular biofilm-like communities or pods (125, 126). Bacteria within these intracellular communities are protected from host innate immune responses and shielded from antibiotics (127). Type 1 pili, which are known to contribute to the formation of extracellular biofilms (117), are also expressed by the intracellular bacteria and required for formation of the pods, separate from their function in host cell binding and invasion (36, 128). Urothelial cells respond to UPEC invasion by undergoing programmed cell death and exfoliating into the bladder lumen, a host-defense mechanism to wash out the colonizing bacteria (34). However, UPEC counter this by fluxing out of the host cells and undergoing additional rounds of attachment to and invasion of neighboring cells, presumably mediated by type 1 pili as in the initial round of infection (126, 129). During this process, the *E. coli* may gain access to the underlying bladder epithelium, leading to the formation of quiescent bacterial reservoirs from which recurrent infections can be seeded to begin the infection process anew (129, 130). Thus, type 1 pili function at multiple different points during UPEC pathogenesis in the urinary tract and have both extracellular and intracellular roles.

P pili are expressed by UPEC and are strongly associated with the ability of the bacteria to colonize the kidney and cause pyelonephritis (65, 131, 132). P pili bind to Gal(α1-4)Gal moieties present in the globoseries of glycolipids found in kidney epithelial cells. The glycolipid receptor is also part of the P blood group antigen, thus allowing P pilus-mediated agglutination of human erythrocytes (133). P pili are encoded by the chromosomal *pap* (pyelonephritis-associated pili) gene cluster (Fig. 1.1), which is present on pathogenicity islands of UPEC strains, and also found in *E. coli* causing neonatal meningitis and avian pathogenic strains (134). Individual *E. coli* strains may carry more than one *pap* gene cluster, located in different

pathogenicity islands (135, 136).

P pili are built from 6 different structural subunits that form a right-handed helical rod and distal tip fiber, similar to type 1 pili (Fig. 1.1). The P pilus tip fiber is longer and more flexible compared to type 1 pilus tips, measuring ~40 nm in length. The P pilus tip is composed mainly of PapE, which is present at approximately 5-10 copies per pilus. The PapG adhesin is present in single copy at the distal end of the tip and is joined to PapE via the PapF adaptor subunit (137, 138) (Fig. 1.2A). Another adaptor subunit, PapK, links the tip fiber to the pilus rod (138). The helical P pilus rod measures 8.2 nm in diameter and is built from a linear homopolymer of over 1000 copies of the PapA major pilin (139). The P pilus rod is terminated by the PapH minor pilin, which also plays a role in anchoring the pilus fiber in the OM (140, 141).

The glycolipid binding site on the PapG adhesin is formed by a shallow pocket on one side of the adhesin domain (Fig. 1.2B) (65, 67). This is in contrast to the tip-located mannose-binding site of FimH on type 1 pili. P pili have a longer, more flexible tip fiber compared to type 1 pili. The flexibility of the P pilus tip and side-on orientation of the PapG binding site likely function in tandem to facilitate docking of the adhesin onto the globoside moiety of the glycolipid receptor, which is oriented parallel to the membrane surface (65).

Expression of P pili promotes ascending urinary tract infection and facilitates colonization of the kidneys by *E. coli* (132, 142). Consistent with a role in pathogenesis, vaccination with P pili was shown to provide protection against pyelonephritis in both murine and primate models (143, 144). However, studies using P pilus mutants have had variable results in establishing an essential requirement for the pili in kidney infections, likely due to the many different adhesins expressed by UPEC strains (145). As for type 1 pili, P pilus-mediated

adhesion of UPEC to the urothelium stimulates cytokine production and resultant inflammatory responses in the urinary tract, which likely exacerbates kidney damage during acute pyelonephritis (38, 146, 147). Binding of P pili to its glycolipid receptor in kidney epithelial cells causes release of the second messenger ceramide, which forms the membrane anchor portion of the receptor. Ceramide is as an agonist for TLR4, and thus provides a potential link between bacterial adhesion and induction of innate immune pathways (148).

1.6 The ß-barrel Assembly Machinery Complex

The Gram-negative OM is a unique and essential organelle that serves many diverse functions. This asymmetrical OM lipid bilayer consists of an extracellular-facing leaflet composed of lipopolysaccharide (LPS) and a periplasmic-facing phospholipid inner leaflet. The OM plays a critical role in protecting the intracellular contents from environmental insults, providing structural integrity, intra and inter-bacterial communication, and serving as a selective permeability barrier (149).

The majority of proteins in the OM can be divided into two main categories: lipoproteins and outer membrane proteins (OMPs). Lipoproteins are soluble molecules that associate with hydrophobic membranes via a lipidated N terminus. OM lipoproteins play a variety of roles in the cell including sensing of intracellular and extracellular stressors (150, 151), protein transport (152), membrane biogenesis (153), and assisting in the folding and assembly of other proteins (154). When anchored in the OM, lipoproteins can be exposed to either the extracellular milieu or periplasm.

The most distinctive characteristic of OM lipoproteins is the mechanism by which they are distinguished from inner membrane lipoproteins and localized to the OM. Following translation

in the cytoplasm and subsequent translocation across the inner membrane by the Sec system, the lipoprotein N terminus is processed, exposing a sequence motif known as the lipobox. The lipobox directs lipoprotein processing and dictates whether the protein will be retained in the inner member or transported to the OM via the Lol (Lipoprotein outer membrane localization) pathway (155). While localization by the Lol pathway explains how lipoproteins can be localized to the periplasmic face of the OM, little is known regarding the process by which some lipoproteins become exposed to the extracellular environment. Recent evidence suggests that certain lipoproteins can be threaded through the lumen of OMPs, thereby granting them access to the extracellular milieu {Konovalova, 2014 #2312}.

The second category of proteins that make up the OM are the OMPs. OMPs are a class of membrane spanning OM proteins that adopt a characteristic ß-barrel fold consisting of a series of antiparallel ß-strands arranged in a cylindrical conformation (156). Like lipoproteins, OMPs also preform a variety of tasks, including enzymatic functions (157), active and passive transport of small molecules (158) (159), adhesion (160), and secretion (92). The FimD and PapC ushers are examples of OMPs involved in secretion. OMPs also exist in the OMs of mitochondria and chloroplasts, which are believed to be the descendants of endosymbiotic free-living bacteria (161) (162).

ß-barrel proteins are extremely stable structures requiring the addition of heat and/or urea to be fully denatured (105, 163, 164). This stability is in part due to their intrinsic nature to spontaneously fold into lipid bilayers and detergent micelles, in the absence of an energy source (165). One then may ask what prevents ß-barrel proteins from spontaneously, and uncontrollably, folding into both the inner membrane and OM of Gram-negative bacteria? Gram-negative bacteria have evolved a unique system to control such a situation called the ß-barrel

assembly machinery (Bam) complex (154, 166) (Fig. 1.4). Following translation in the cytoplasm, nascent OMPs are translocated across the inner membrane and into the periplasm via the Sec system. Once in the periplasm OMPs are received by a number of specialized chaperone proteins including SurA, Skp, and DegP. DegP possesses chaperoning activity in addition to its proteolytic activity (167). A primary function of these chaperones is to maintain the ß-barrel in an unfolded state, preventing it from spontaneously folding and randomly inserting into the nearest membrane while in the aqueous periplasmic environment (168). The chaperones are also responsible for delivering OMPs to the Bam complex, which facilitates their proper assembly and insertion into the OM (154).

The Bam system is an essential protein complex consisting of five key components: BamA, BamB, BamC, BamD, and BamE (Fig. 1.4). BamA , a 16 stranded integral OM ß-barrel protein with a large N-terminal periplasmic domain, is the central constituent of the complex and a member of the Omp85 protein family, (169). The BamA N terminus is divided into five polypeptide translocation associated (POTRA) domains, which share a high degree of structural homology with each other (170). The POTRA domains also act as the primary interface by which the two of the four accessory Bam lipoproteins, BamB and BamD, interact directly with BamA. BamA is essential for viability and cannot be deleted from the *E. coli* genome (166, 171).

BamB is an eight bladed ß-propeller protein, which is anchored to the periplasmic face of the OM, and has been shown to interact with POTRAs 2-5 of BamA (170, 172). BamB is not essential for viability but *bamB* deletion mutants do display OMP assembly defects including diminished levels of OM porins such as OmpA, OmpC, and OmpF, and increased OM

permeability to certain antibiotics (173, 174). *In vitro* and *in vivo* studies suggest that BamB may contribute to the assembly of nascent BamA in the OM (175, 176).

BamC is the second accessory lipoprotein of the Bam complex. Even though crystal structures are available for this protein (177) little is known about its function or what role it plays in the overall complex. A Δ*bamC* mutant shows no discernable defect in OMP assembly and only minor changes in membrane permeability. However, BamC may be involved in stabilizing the Bam complex since the interaction between BamA and BamD is dampened when *bamC* is deleted from the bacterial chromosome (178). Recent evidence suggests that portions of BamC may actually be exposed to the extracellular surface but the significance of this remains unknown (179).

BamD is the only other essential component of the Bam complex. Like BamB, BamD interacts directly with BamA but only through POTRA 5 (171). The structure of BamD contains five α-helical tetratricopeptide repeat domains, which are common among scaffold proteins (180). In fact, a major function of BamD is to serve as a conduit for BamC and BamE to interact with the rest of the Bam complex since these lipoproteins do not directly interact with BamA. Additionally, like BamB, BamD has also been implicated in the assembly of BamA molecules (175, 176).

The final and smallest member of the Bam complex is BamE. BamE is a ~12 kDa protein whose association with the Bam complex, like BamC, is mediated through BamD (171, 182, 183). A *bamE* deletion mutant displays slightly increased sensitivity to certain antibiotics, SDS, and EDTA, and minor changes to steady-state OMP levels can sometimes be observed (178, 183). However, when paired with deletions of other non essential Bam lipoproteins, BamB and BamC, more dramatic synthetic phenotypes are observed (178). Δ*bamE* Δ*bamC* double mutants

display a temperature-sensitive growth defect at 37°C and significant defects in OMP assembly. A $\Delta bamE$ $\Delta bamB$ mutant is synthetically lethal. Also, like BamC, BamE is important for stabilizing the BamA-BamD interaction. Furthermore, a *bamE* mutant alters the conformational state of BamA, exposing an extracellular loop (loop 6) from the BamA ß-barrel making it accessible to protease cleavage (184). However, this change in conformation must be mediated through BamD since BamE does not interact directly with BamA.

Taken together, the Bam complex can be divided into two subcomplexes, BamACDE and BamAB, where BamB and BamD interact independently with BamA via its POTRA domains and BamC and BamE interact with the rest of the complex through their association with BamD. The necessity of the Bam complex is evident by the sheer number of OMPs which require it for their assembly in the OM. This includes usher proteins such as FimD and PapC, making chaperone/usher pili dependent on this assembly machinery (185, 186). How the members of the Bam complex work in concert to assemble OMPs remains unknown and is an area of intense study.

1.7 Anti-virulence Strategies

UTI diagnoses are one of the leading drivers behind antimicrobial prescriptions in healthcare settings. Fortunately, uncomplicated cystitis and pyelonephritis can be treated with standard antibiotics (187, 188). Recurrent UTIs require more aggressive treatment modalities. Prophylactic antibiotics can be prescribed for female patients experiencing more than three UTIs per year and treatment times can last for 6-12 months. However, these means of care do not come without caveats. With increasing rates in antibiotic resistance seen in strains of UPEC and other uropathogens, second and third line antimicrobials are often employed to tackle hard to

treat infections. These therapies have also been shown to further promote the development of resistance and may have other adverse effects on the patient. Additionally, long-term prophylactic treatments not only carry with them the potential to enhance resistance, but also can cause considerable damage to the normal gut microbial flora, potentially leading to severe complications. It is for these reasons that new and effective therapeutics are needed to successfully treat this disease (189).

Pilus mediated adhesion is crucial at early stages of infection, and thus represents an attractive target for therapeutic intervention. Advances in understanding the structure and assembly of bacterial adhesins will be critical for the development of effective vaccines and antimicrobial agents that target adhesion. Pilus-based vaccines have shown promise in preventing UTIs, although none have reached clinical use. Studies using purified P pili or recombinant PapG adhesin purified in complex with its PapD chaperone demonstrated protection against pyelonephritis in primates (143, 190). Similarly, vaccination with the type 1 pilus adhesin FimH, purified in complex with its FimC chaperone, provided protection in primates against challenge with a UPEC cystitis isolate (110).

An alternative approach to vaccination is to disrupt bacterial adhesion to host cells through the use of small molecule competitive inhibitors of adhesin-receptor interactions. Examples include the use of galabiose- and mannose-based inhibitors to interfere with adhesion mediated by P and type 1 pili, respectively, with the goal of preventing UPEC colonization of the urinary tract (191-194). Another alternative approach is to develop small molecule inhibitors that disrupt the machinery used for adhesin biogenesis, thereby preventing assembly of the adhesins on the bacterial surface. Once such class of small molecules, termed pilicides, interferes with the CU assembly pathway and blocks expression of both P and type 1 pili by *E. coli* (195). Pilicides

described to date target the periplasmic chaperone and appear to disrupt pilus assembly by interfering with binding of chaperone-subunit complexes to the outer membrane usher. Other pilicides have been developed to inhibit the assembly of stable chaperone-subunits complexes in the periplasm (196). Treatment of UPEC with one of these inhibitors blocked assembly of type 1 pili, reduced biofilm formation, and attenuated bacterial colonization in the murine urinary tract infection model (197). Small molecules that disrupt polymerization of the pilus fiber as well as effect pilus gene expression have also been identified (198, 199). These compounds highlight the potential for a new class of anti-infective agents that target virulence factor secretion systems and the assembly of virulence-associated surface structures, rather than disrupting essential biological processes as for conventional antibiotics (200, 201). Such anti-virulence molecules should place less pressure on the bacteria and thus may be less prone to the development of resistance mechanisms. This strategy may also allow the selective targeting of pathogenic bacteria, avoiding detrimental side effects of broad-spectrum antibiotics on the normal bacterial flora.

1.8 Nitazoxanide

One initiative to combat the development of antimicrobial resistance and develop new therapeutics is the rescreening and repurposing of Food and Drug Administration (FDA) approved pharmacotherapies. Such an effort aims at identifying novel targets or mechanisms of action for drugs that are already in clinical use, with proven safety records, allowing them to be fast-tracked through the FDA approval process for new disease indications. Additionally, identified molecules can be used as scaffolds for the design of new compounds with increased potency and/or stability (202).

Nitazoxanide (NTZ) is an FDA-approved synthetic nitrothiazolyl-salicylamide compound discovered at the Pasture Institute in the 1970s (Fig. 1.5). It was found to have anti-parasitic activity and was licensed in the United States in 2002 under the brand name Alinia for the treatment of intestinal infections caused by *Giardia* and *Cryptosporidia* (203). Today, NTZ is prescribed orally with a typical dose being 500 mg twice daily for a 3-day period in adults. Peak plasma concentrations of the drug can reach ~30 µM with this standard regimen or ~60 µM if the dosage is increased to 1 g (204).

Since its discovery NTZ has been the focus of intense study to identify its mechanism of action as well as other potential activities it may possess. In addition to *Giardia* and *Cryptosporidia*, NTZ has been shown to have broad spectrum activity against a number of viral pathogens and is currently undergoing clinical trials to treat infections due to influenza and hepatitis C (205, 206). NTZ is also being explored as a chemotherapeutic to treat cancer based on its observed activity against a number of tumorigenic cell lines (207). However, the mechanism(s) by which it elicits these activities is poorly understood.

In addition to viruses and cancer, NTZ also displays antibacterial activity against a range of Gram-positive and Gram-negative anaerobic bacteria, including *Clostridium diffcile* and *Helicobacter pylori* (208-210). Pyruvate:ferridoxin oxidoreductase (PFOR), an essential anaerobic metabolic enzyme present in many bacteria and protozoa, has been identified as a direct target of the drug allowing for its antimicrobial activity. These findings have also allowed NTZ to serve as a scaffold molecule for the development of analogues with increased potency and stability against PFOR such as amixicile (211). Unlike anaerobes though, enterobacteriaceae are considered generally resistant to the drug due to the lack of PFOR in these organisms (210, 212).

Though NTZ displays pleotropic effects against a wide range of organisms, enterobacteriaceae are unaffected by the antibacterial effects of the drug. Interestingly, Shamir *et al.* (213) observed that NTZ inhibited the ability of enteroaggregative *E. coli* (EAEC) to form biofilms in *vitro*. EAEC is an intestinal pathogen and a leading cause of acute and persistent diarrhea globally (214). Shamir *et al.* demonstrated that NTZ mediated inhibition of biofilm formation was dose dependent at non-toxic and physiological concentrations (~30-60 µM) of the drug. Biofilm formation by EAEC is dependent on the presence of aggregative adherence fimbriae (AAF) on the bacterial surface, which are assembled by the CU pathway (215). Shamir *et al.* also observed an NTZ dependent loss of pilus function as measured by the ability of EAEC expressing AAF pili to agglutinate erythrocytes (213). This phenotype was also extended to type 1 pili, which EAEC also expresses. This loss of biofilm formation and pilus function was the result of decreased AAF fimbriae on the bacterial surface, suggesting that NTZ may inhibit pilus assembly. This possibility was further supported by qRT-PCR studies showing that the loss of pilus subunits was not the result of transcriptional down regulation of the pilus genes. Additionally, no effect of NTZ was observed on flagellar-based motility, which requires the formation of disulfide bonds by the DsbA and DsbB oxidoredocutases. Disulfide homeostasis is also a requirement for pilus assembly (213). Taken together Shamir *et al.* were able to conclude that NTZ inhibits pilus assembly in EAEC without effecting pilus gene transcription or disulfide maintenance. Additionally, *in vivo* studies using a weaned mouse model of EAEC infection showed that treatment with NTZ decreased bacterial stool shedding, tissue burdens, and changes in body weight, pointing to the potential therapeutic value of the drug to treat these infections (216).

To further unlock its potential, identifying the mechanism by which NTZ inhibits pilus

assembly and its role as a possible pilicide would be critically important to its development as a possible anti-virulence therapeutic agent. It is the elucidation of this mechanism that became the focus of this thesis work.

1.9 Figures

FIGURE 1.1. Representative CU gene clusters and pili. Gene clusters coding for P (pap), type 1 (fim) and Dr/Afa pili are depicted, with the functions of the genes indicated. Electron micrographs are shown for (A) an E. coli bacterium expressing type 1 pili, (B) a P pilus fiber, and (C) a type 1 pilus fiber. Scale bars equal 700 nm (A), 100 nm (B), and 20 nm (C). The images in panels A-C are reprinted from references (119), (137), and (118), respectively, with permission of the publishers.

FIGURE 1.1
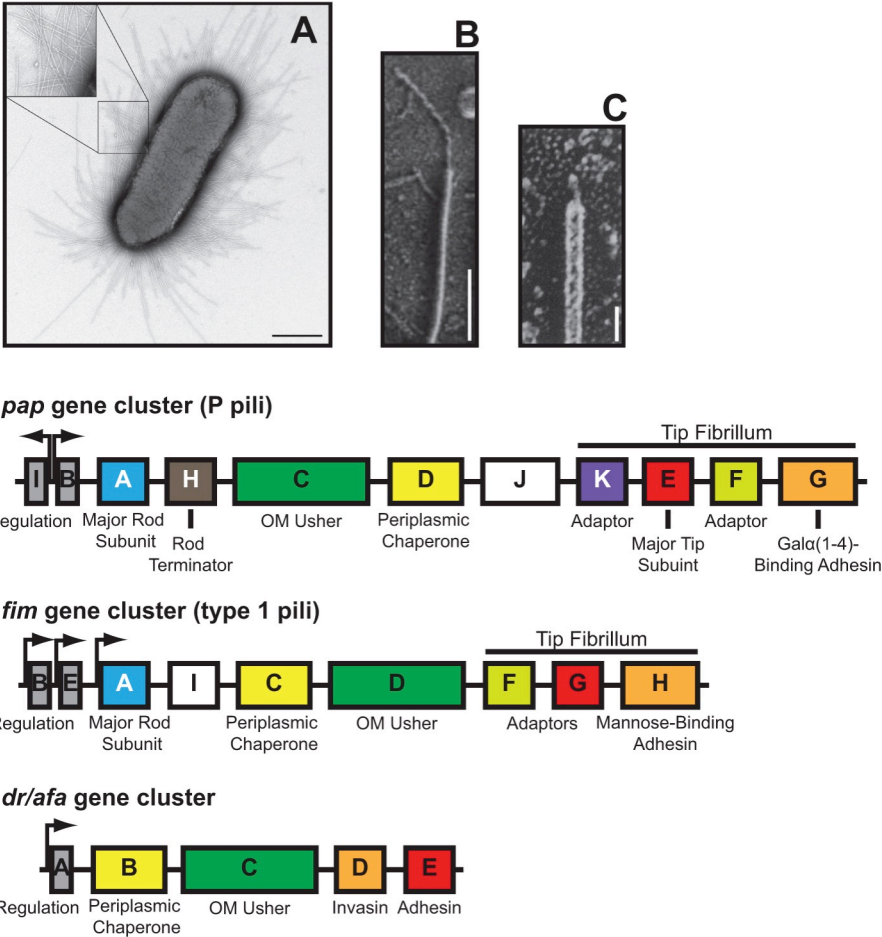
FIGURE 1.2. The chaperone/usher pathway. (A) Model for pilus biogenesis by the CU pathway. Pilus subunits enter the periplasm as unfolded polypeptides via the Sec system. Subunits fold upon forming binary complexes with the periplasmic chaperone (yellow). The crystal structure in the lower right depicts the chaperone-subunit donor strand exchange reaction (PapD-PapA; PDB ID: 2UY6), with the chaperone donor strand indicated in red. Pilus assembly takes place at the outer membrane usher, which catalyzes the exchange of chaperone-subunit for subunit-subunit interactions. Models for assembled P, type 1 and Afa/Dr pilus fibers are shown. The crystal structure in the upper left depicts the subunit-subunit donor strand exchange reaction that occurs in the pilus fiber (PapA-PapA; PDB ID: 2UY6), with the Nte donor strand indicated. (B) Crystal structures of the PapG (P pili; PDB ID: 1J8R) and FimH (type 1 pili; PDB ID: 1KLF) adhesin domains with bound globoside and mannose, respectively. The sugars are depicted as dark gray spheres.

FIGURE 1.2
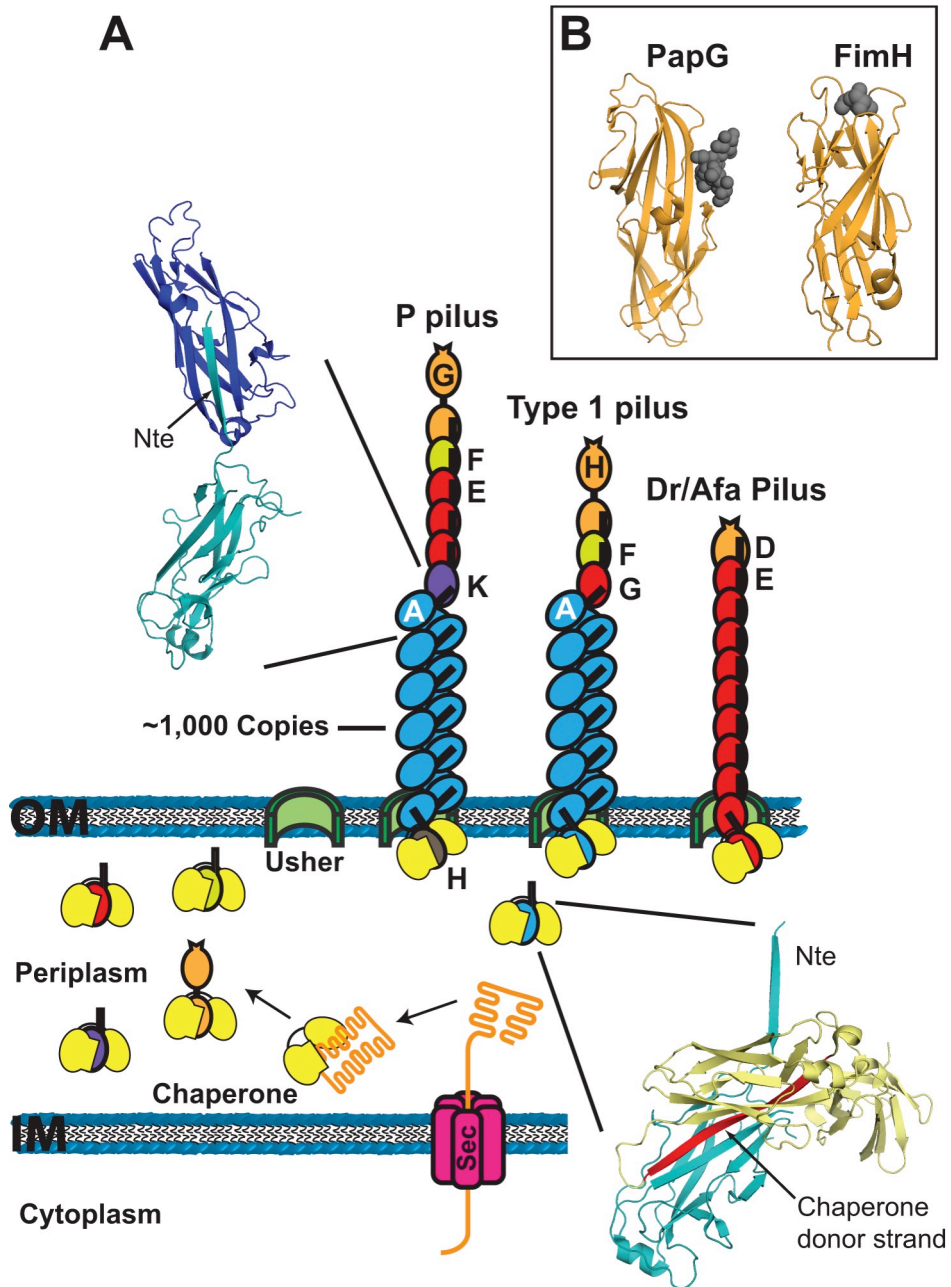
FIGURE 1.3. Crystal structure of the FimD-FimC-FimH type 1 pilus assembly intermediate (PDB ID: 3RFZ). The Usher NTD, plug, ß-barrel channel, and CTD domains are indicated. The FimH adhesin domain (FimH$_A$) is inserted inside the usher channel, and the FimH pilin domain (FimH$_P$) and bound FimC chaperone are located at the usher CTDs.

FIGURE 1.3
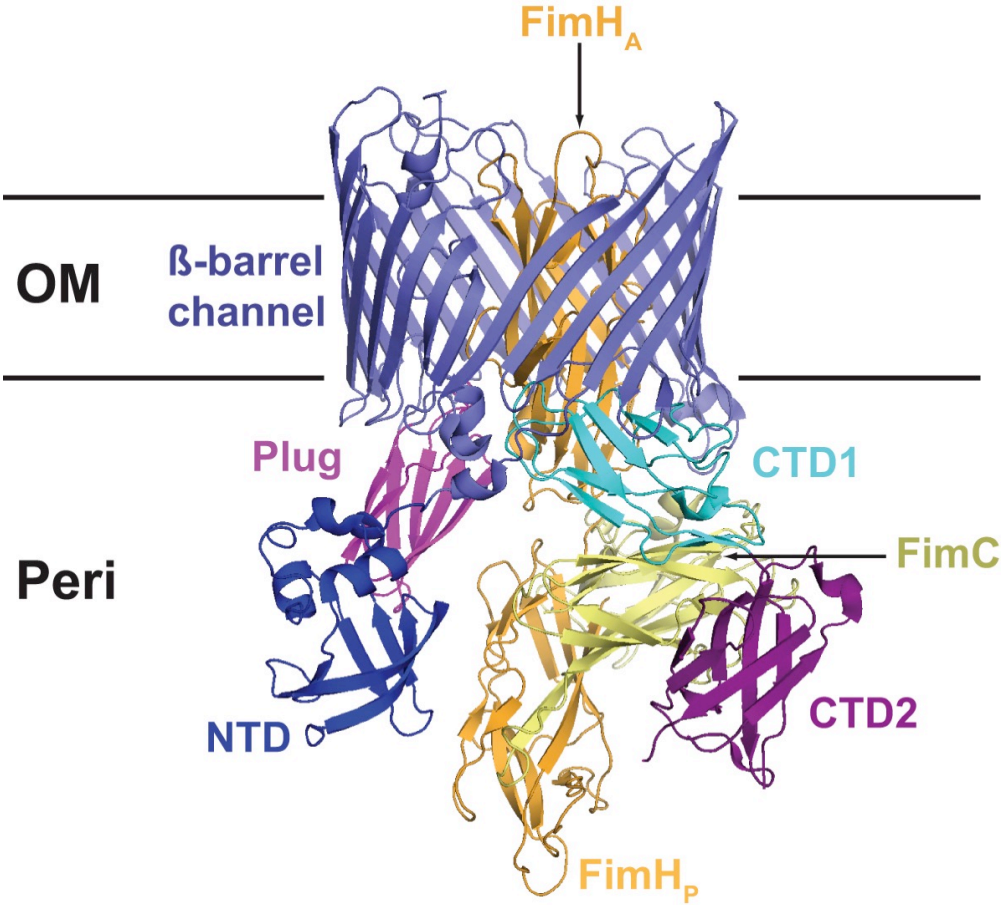
FIGURE 1.4 Biogenesis of outer membrane proteins (OMPs) and schematic of the ß-barrel assembly machinery (Bam) complex. The Bam complex consists of five main components. BamA is a large OM ß-barrel protein which possesses a large N-terminal periplasmic domain divided into five polypeptide translocation associated (POTRA) domains (P1-P5). BamB is a lipoprotein that interacts directly with the POTRA domains of BamA. BamD is also a lipoprotein that interacts directly with POTRA 5 of BamA and serves as a scaffold for two other accessory lipoproteins BamC and BamE. OMPs are first translated in the cytoplasm (i) and translocated across the inner membrane via the Sec pathway into the periplasm (ii). Once in the periplasm OMPs are received by chaperones such as SurA, Skp, and DegP (not shown), which transport the unfolded protein to the Bam complex (iii). The Bam complex then facilitates the proper assembly and insertion of the protein into the OM (iv).
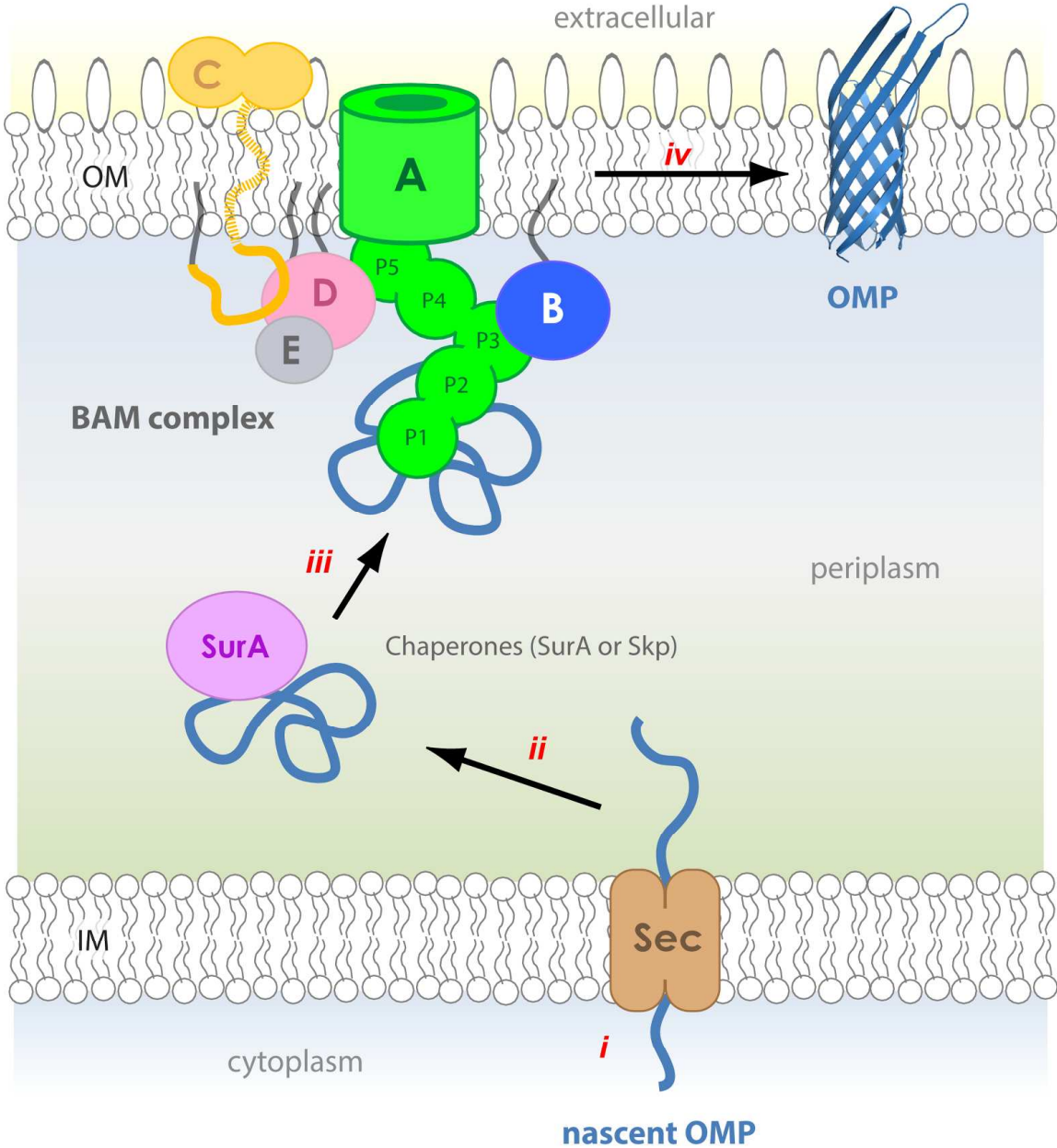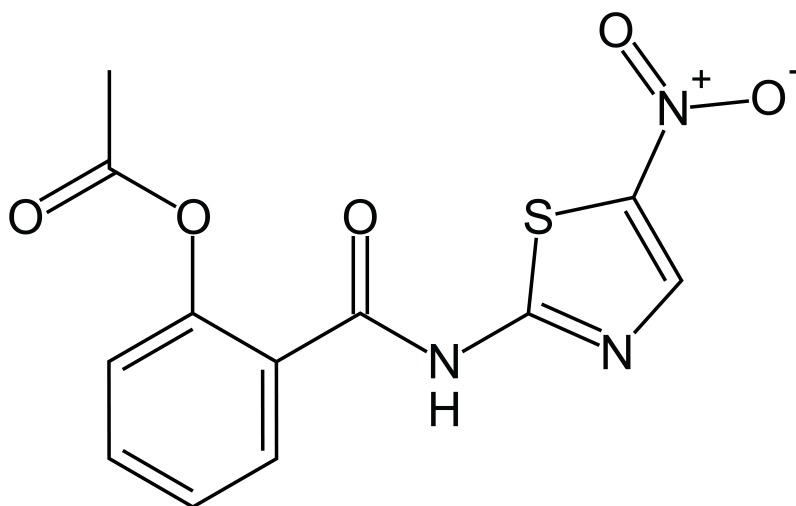
FIGURE 1.4

FIGURE 1.5

FIGURE 1.5 Chemical structure of nitazoxanide.

CHAPTER 2

Material and Methods

Nitazoxanide preparation. NTZ powder (Waterstone Technology) was dissolved in dimethyl sulfoxide (DMSO) to give a stock concentration of 10 mg/ml. A final concentration range of 0–20 µg/ml NTZ was used, as previous studies indicated that NTZ is inhibitory to growth at higher concentrations (213).

Strains, plasmids, and growth conditions. All *E. coli* strains, plasmids used in this study are listed in Table 2.1. All primer used in this study are listed in Table 2.2. Host strain BW25113Δ*ompT* was obtained from the Keio collection (217, 218) and cured of its kanamycin resistance cassette by introduction of Flp recombinase on the temperature sensitive plasmid pCP20 (219). Strain BW25113Δ*degP* was generated by P1 transduction (220) using donor strain KS474 (221). Plasmid pBamB was generated by digesting pBAD18::*bamB* (gift from Thomas Silhavy Princeton University) with EcoRI and HindIII and ligating the *bamB* fragment into pTRYC (36). Plasmid pBamE was generated by amplifying the *bamE-His8* fragment from pBamE-His (gift from Thomas Silhavy) using a forward primer containing a EcoRI site and a reverse primer with a HindIII site. The fragment was then ligated into pTRYC. Plasmids pBamABCDE and pBamA were generated by subcloning into pTRYC-NdeI the desired Bam genes from plasmid pJH114 (gift from Harris Bernstein at the National Institutes of Health), which encodes all the Bam complex genes in pTRC99a (222). The *bamE* gene in this sequence also contains a C-terminal His tag. To do this forward and reverse primers were generated to introduce an NdeI site into the multiple cloning site of pTRYC using a QuikChange XL mutagenesis protocol (Stratagene) to generate pTRYC-NdeI. The desired Bam gene fragment (BamABCDE$_{His8}$ or BamA) was then amplified from pJH114 using a forward primer containing a NdeI site and a reverse primer with an XmaI site. Fragments were digested with the named

restriction enzymes and ligated into pTRYC-NdeI. All BW25113 Bam deletion mutants were obtained from the Keio collection and verified by PCR using forward and reverse primers (Table 2.2) designed to the upstream and downstream genes surrounding the mutant gene of interest. Fragments generated from the mutant strains were compared to the WT strain to determine if the kanamycin cassette was in the correct location.

Unless otherwise stated, *E. coli* overnight cultures were diluted 1:100 into fresh LB medium containing appropriate antibiotics (ampicillin 100 µg/ml, kanamycin 50 µg/ml, tetracycline 15 µg/ml) and 0–20 µg/ml NTZ as indicated. For 0 µg/ml NTZ, a final concentration of 0.2% DMSO was added as a vehicle-only control, and 0.2% DMSO final concentration was maintained for all NTZ concentrations. Cultures were grown at 37ºC with aeration. When the cultures reached OD_{600} of 0.3, the expression of plasmid-encoded genes was induced for 1 h by addition of the appropriate inducing agent (50 or 100 µM isopropyl-ß-D-thiogalactopyranoside (IPTG), 0.1% arabinose).

Hemmagglutination assay. Hemmagglutination (HA) assays were conducted as previously described (59) by serial dilution in microtiter plates. *E. coli* strain AAEC185 (223) transformed with pFJ29 (91) or pETS9 (224) were used to test P and type 1 pilus functionality, respectively. Plasmids pACYC184 and pETS11 served as negative controls for pFJ29 and pETS9, respectively.. Following growth in 0–20 µg/ml NTZ and induction with 50 µM IPTG, bacteria were harvested and washed with phosphate buffered saline (PBS), before being resuspended and normalized to an OD_{540} of 1.0. Following serial dilution of the bacteria in microtiter plates, either human or guinea pig (Colorado Serum Company) erythrocytes were added, and agglutination titers were determined visually as the highest dilution of bacteria able to

maintain agglutination. To test HA in the Bam mutant backgrounds pFJ29 was transformed into BW25113, BW25113Δ*bamB*, BW25113Δ*bamC*, and BW25113Δ*bamE* obtained from the Keio collection, grown in the presence of DMSO only and induced for P pili expression as described. Plasmid pACYC184 was also transformed into these strains as a negative control. For each assay, three independent experiments were performed and each experiment contained three replicates.

Pilus isolation from the bacterial surface. Using a previously established pilus isolation protocol (225), P pili were purified from host strain AAEC185/pFJ29 by heat extraction and $MgCl_2$ precipitation. Strain AAEC185/pACYC184 served as a vector-only control. Following growth in 0–20 µg/ml NTZ and induction with 50 µM IPTG, bacteria were harvested and washed with 5 mM Tris-HCl (pH 8.0), 75 mM NaCl. Cultures were then normalized to OD_{600} 1.5 in the same buffer to ensure equal bacterial numbers. Pili were dissociated from the bacterial surface by heating equal sample volumes at 65ºC for 30 min, and precipitated from supernatant fractions by addition of $MgCl_2$. Pelleted protein precipitate was resuspended in 1 mM Tris-HCl (pH 8.0) with 2X SDS sample buffer containing 4 M urea and analyzed by SDS-PAGE. PapA was visualized by Coomassie blue staining and bands were quantified by gel densitometry using a LI-COR Odyssey CLx Imager. The pilus tip adhesion PapG was detected by Immunoblotting with primary anti-PapD-PapG antibody (1:50,000) and visualized with secondary LI-COR IRDye 800CW goat anti-rabbit infrared conjugated antibody (1:15,000) (LI-COR Biosciences) using the LI-COR Odyssey CLx Imager.

Periplasm isolation. Periplasmic fractions were isolated from *E. coli* strain BW25113

(226) transformed with plasmid pPAP58 (227) or pMMB91 as a vector control. Following growth in 0–20 µg/ml NTZ and induction with 100 µM IPTG, bacteria were harvested, washed, and normalized to OD_{600} 2.0 using 20 mM Tris-HCl (pH 8.0). Equal sample volumes were processed to isolate the periplasm fractions as described (105). The periplasm fractions were analyzed by SDS-PAGE and PapD-PapG was detected by immunoblotting, as described for the pilus isolation. Alternatively, the PapE pilus tip subunit was detected by immunoblotting with a primary anti-P pilus tips antibody (1:1000), followed by an anti-rabbit alkaline phosphatase-conjugated secondary antibody. The blot was developed by treatment with BCIP (5-bromo-4-chloro-3-indolyl phosphate)-nitro blue tetrazolium (NBT) substrate (KPL).

Chaperone-subunit complex co-purification with the usher. A previously described co-purification method (59, 101) was used to isolate P pilus usher-chaperone-subunit complexes from the OM. Host strain BW25113Δ*ompT* was transformed with plasmids pMJ3 (228) and pPAP58. Following growth in 0–20 µg/ml NTZ and induction with 0.1% L-arabinose and 100 µM IPTG, bacteria were harvested, washed, and normalized to OD_{600} 2.0 in 20 mM Tris-HCl (pH 8.0) containing 1X Complete Protease Inhibitor cocktail (Roche). OM fractions were isolated and solubilized with n-dodecly-ß-D-maltoside (DDM) (Anatrace), as described (59). The His_6- tagged PapC usher, together with stably bound pilus assembly intermediates, was purified by nickel affinity chromatography using an AKTA chromatography system (GE Life Sciences). Fractions eluted from the column using imidazole were analyzed for the presence of PapC a by SDS-PAGE and Coomassie blue staining. Corresponding peak fractions were then pooled and treated with a final concentration of 9% trichloroacetic acid (TCA) for 1 h on ice to precipitate chaperone-subunit-usher complexes. Samples were centrifuged (5 min, 16,100 x g,

4ºC), supernatants were carefully removed and protein pellets were washed 3X with 1 ml cold acetone. Protein pellets were left to air dry to remove access acetone and then resuspended in 1X SDS sample buffer for SDS-PAGE. P pilus tip proteins were detected by Immunoblotting with anti-P pilus tips antibody as described for the periplasm isolation.

OM isolation and analysis of the usher. OM fractions were isolated from *E. coli* strains BW25113, BW25113Δ*degP*, BW25113Δ*bamB*, BW25113Δ*bamC*, and BW25113Δ*bamE*. Strain BW25113 was transformed with PapC plasmids pMJ3, pDG2ΔN2ΔC640 (85), or pNH281 (102), or the FimD plasmid pETS4 (98). Plasmids pMON6235Δcat and pMMB66 served as vector controls for the PapC and FimD plasmids, respectively. Strains BW25113Δ*degP*, BW25113Δ*bamB*, BW25113Δ*bamC*, and BW25113Δ*bamE* were transformed with pMJ3. Bacteria were grown in the presence of 0–20 µg/ml NTZ and induced with 0.1% L-arabinose for the PapC plasmids or 100 µM IPTG for FimD. Bacteria were harvested, washed, resuspended, and normalized to OD$_{600}$ 1.5 in 20 mM Tris-HCl (pH 8.0) + 1X Complete Protease Inhibitor cocktail, and OM fractions were isolated as previously described (105). For all strains except BW25113/pETS4, OM pellets were resuspended in 20 mM Tris-HCl, 0.3 M NaCl, followed by the addition of SDS sample buffer. For BW25113/pETS4, to remove any inclusion bodies, OM pellets were resuspended in 20 mM Tris-HCl, 0.3 M NaCl, 1% DDM and rocked overnight at 4°C. The next day, samples were centrifuged (30 min, 16,100 x g, 4°C) and supernatant fractions were collected, to which SDS sample buffer was added. The OM samples were incubated at 25ºC or heated to 95ºC for 10 min. Samples were analyzed by SDS-PAGE and immunoblotted with a primary anti-His$_6$ (1:1000) antibody (Covance) followed by a secondary IRDye 680 goat anti-mouse conjugated infrared antibody (1:40:000) (LI-COR Biosciences). Blots were

visualized and band densitometry was performed using a LI-COR Odyssey CLx Imager.

Overlay assay. Overlay assays were performed as described (101). OM fractions were obtained as described above from strain BW25113 transformed with PapC plasmids pFJ20 (229) or pTN1Δ2-11 (T. Ng and D.G.T., unpublished), or pMON6235Δcat as vector control. The bacteria were grown without the addition of DMSO or NTZ. OM fractions were subjected to SDS-PAGE and either stained with Coomassie blue or transferred to polyvinylidene difluoride (PVDF) membrane (Osmonic Inc). Separately, periplasm fractions were extracted from BW25113/pPAP58 as described above. The bacteria were grown without the addition of DMSO or NTZ. NTZ (0–20 μg/ml) was then added to the isolated periplasm fractions and these samples were incubated with the PVDF membranes containing the immobilized OM for 1 h with shaking. The PVDF membranes were washed with Tris buffered saline, 0.05% Tween-20, 0.02% sodium-azide (TBST), and probed with an anti-PapD (1:10,000) primary antibody. Secondary anti-rabbit alkaline phosphatase antibody followed by incubation with BCIP-NBT substrate was used to visualize chaperone-subunits complexes bound to the usher.

Over- and under-expression of the Bam complex. To over-express the Bam complex, strain BW25113 was co-transformed with plasmids pMJ3 and pBamABCDE. Plasmid pMON6235Δcat served as a vector control for PapC. Over night bacteria were diluted 1:100 in LB media containing 100 μM IPTG to induce pBamABCDE and OM fractions were isolated and analyzed as described above. Anti-BamA (1:30,000) (gift from Thomas Silhavy) primary antibody was used to determine relative BamA levels. To under-express the Bam complex strains MC4100 and MC4100*bamA101* were obtained from the Silhavy laboratory and transformed with

pMJ3. Complementation and over-expression of BamA was achieved by co-transforming MC4100*bamA101*and MC4100 with both pMJ3 and pBamA. All MC4100 based strains were grown and OM fractions were isolated and analyzed as described above. Leaky constitutive expression of pBamA was sufficient for protein expression.

Post NTZ treatment of OM fractions and purified PapC: OM isolations were obtained as described above using host strain BW25113/pMJ3. Cultures however were not grown in the presence of DMSO or NTZ. Insoluble OM pellets were resuspended in 1 ml 20 mM Tris-HCl (pH 8.0) and a final concentration of 10 μg/ml NTZ, 20 μg/ml NTZ, or 0.2% DMSO was added to the samples and incubated for 1 h at 37$^{\text{o}}$C with gentle shaking. Samples we then centrifuged (30 min, 16,100 x g, 4$^{\text{o}}$C), OM pellets were resuspended in 100 µl 20 mM Tris-HCl + 0.3 M NaCl and 33.3 µl of 4X SDS sample buffer was added. Samples were left at 25$^{\text{o}}$C, analyzed by SDS-PAGE, and blotted with anti-His antibody with IR680 secondary as mentioned to determine usher ß-barrel mobility.

To identify any effect of NTZ on purified usher, PapC was purified as previously described (230). 20 µl of purified PapC elutant was added to 20 µl of 20 mM Tris-HCl (pH 8.0) containing 0.4% DMSO, 20 µg/ml NTZ, or 40 µg/ml NTZ bringing the final mixtures to 0.2% DMSO, 10 µg/ml NTZ and 20 µg/ml NTZ in 20 mM Tris-HCl (pH 8.0) + 0.25M NaCl + 2.5 mM Lauryldimethylamine-oxide (LDAO). Samples were incubated at 37$^{\text{o}}$C with gentle shaking followed by the addition of 13.3 µl of 4x SDS sample buffer. Samples were then immediately analyzed by SDS-PAGE and Coomassie blue staining.

Statistical analysis. Densitometry analysis of protein bands was performed using a LI-COR Odyssey CLx Imager on samples from three independent experiments. Statistical significance was calculated by one-way analysis of variance and Bonferroni's multiple-comparison posttest using Prism 6 (GraphPad Software). For comparison of folded versus unfolded PapC usher levels, a two-way analysis of variance was used. P values < 0.05 were considered significant.

TABLE 2.1 Strains and plasmids used in this study

Strain or plasmid	Relevant characteristic(s)	Reference or source
Strains[a]		
AAEC185	MM294 λ- F- *supE44 hsdRI7 mcrA mcrB endAl* thi-l Δ*fimB-fimH* Δ*recA*	(223)
BW25113	*LacI^q rrnB* Δ*lacZ hsdR514* Δ*araBAD* Δ*rhaBAD*	(226)
BW25113Δ*ompT*	BW25113 Δ*ompT*	This study
BW25113Δ*degP*	BW25113 *degP::kan*	This study
BW25113Δ*bamB*	BW25113 *bamB::kan*	(217)
BW25113Δ*bamC*	BW25113 *bamC::kan*	(217)
BW25113Δ*bamE*	BW25113 *bamE::kan*	(217)
MC4100	MC4100 *ara*^r/-	(149)
MC4100*bamA101*	MC4100 *ara*^r/- *bamA101*	(181)
Plasmids		
pCP20	Encodes FLP recombinase	(219)
pACYC184	Cloning vector, P*trc*, Clm^r, Tet^r	(231)
pMMB66	Cloning vector, P*tac*, Amp^r	(232)
pMMB91	Cloning vector, P*tac*, Kan^r	(97)
pMON6235Δcat	Cloning vector, P*ara*, Amp^r	(233)
pFJ29	pACYC184 derivative encoding the whole *pap* operon	(91)

pTRYC	Cloning vector, P$_{trc}$, Clm^r	(36)
pTRYC-NdeI		This study
pETS4	pMMB66 derivative encoding His-tagged FimD	(98)
pETS9	pMMB66 derivative encoding the whole *fim* operon	(224)
pETS11	pMMB66 derivative encoding a Δ*fimD fim* operon	(224)
pPAP58	pMMB91 derivative encoding PapDJKEFG	(227)
pFJ20	pMON6235Δcat derivative encoding PapC	(91)
pTN1Δ2-11	pMON6235Δcat derivative encoding PapC$_{Δ2-11}$	(T. Ng and D.G.T., unpublished)
pMJ3	pMON6235Δcat derivative encoding His-tagged PapC	(228)
pDG2ΔN2ΔC640	pMON6235Δcat derivative encoding His-tagged PapC$_{129-640}$, deleted for the N and C-terminal periplasmic domains	(85)
pNH281	pMON6235Δcat derivative encoding His-tagged PapC$_{Δ252-333, R251G}$, deleted for the plug domain	(102)
pJH114	pTRC99a/NdeI derivative encoding BamABCDE-His	(222)
pBAD18::*bamB*	pBAD18 derivative encoding BamB	(166)
pBamE-His	pET22-42 derivative encoding BamE-His	(183)
pBamABCDE	pTRYC derivative encoding BamABCDE-His	This study
pBamA	pTRYC derivative encoding BamA	This study
pBamB	pTRYC derivative encoding BamB	This study

| pBamE | pTRYC derivative encoding BamE-His | This study |

TABLE 2.2 Oligonucleotides used in this study

Primer name	Sequence (5'-3')
Bam mutant verification primers	
bamBUPForward	5'-CTGAAAACCCTTGATACCAT-3'
bamBDOWNReverse	5'-ATAAATCATCAGACAACGC-3'
bamCUPForward	5'-GCCATTACACAACAAACTAT-3'
bamCDOWNReverse	5'-GTTTGCGTATCATATCAGAA-3'
bamEUPForward	5'-AAGTCACACGTAATACACT-3'
bamEDOWNReverse	5'-AGCGAATAAATAACAGACAG-3'
Cloning primers	
bamE-HisForward	5'-GCGCGCGAATTCATGCGCTGTAAAACGCTGACTGC-3'
bamE-HisReverse	5'-GCGCGCAAGCTTTTAGTGGTGGTGGTGGTGGTG-3'
pTRYC/NdeIFwd	5'-CACACAGGAAACAGCATATGGAATTCGAGCTCGG-3'
pTRYC/NdeIRev	5'-CCGAGCTCGAATTCCATATGCTGTTTCCTGTGTG-3'
bamFwd	5'-GATATACATATGGTTAGGAAGAACGCATAATAACG-3'
bamRev	5'-TATATACCCGGGTTAGTGGTGATGATGGTGTGATGAT-3'
BamAREVXmaI	5'-CTTATTACCCGGGCACTTACCAGGTTTTACGATG-3'

CHAPTER 3

Mechanism of Chaperone/Usher Pilus Inhibition by Nitazoxanide

3.1 Chapter overview

Adhesive surface structures termed pili or fimbriae are key virulence factors for many bacterial pathogens (21, 28, 234). Pili are hair-like fibers composed of multiple different subunit proteins, one or more of which function as adhesins that confer binding to receptor molecules on host cells. Pilus-mediated adhesion is critical for early stages of infection, allowing invading bacteria to establish a foothold within the host. Following bacterial attachment, pili may also function to modulate host cell signaling pathways, promote or inhibit invasion inside host cells, and facilitate bacterial-bacterial interactions leading to the formation of community structures such as biofilms. Pili thus function both to initiate and sustain infection, and therefore represent attractive therapeutic targets (235, 236).

The chaperone/usher (CU) pathway is a conserved secretion system dedicated to the biogenesis of pili in Gram-negative bacteria (28) (25, 26, 237), including pathogens such as *Klebsiella pneumoniae*, *Pseudomonas aeruginosa*, *Proteus mirabilis*, *Yersinia pestis*, *Acinetobacter baumannii*, and intestinal and extra-intestinal pathogenic *Escherichia coli* (34, 43, 132, 238-242). Pilus biogenesis by the CU pathway requires two specialized assembly components: a periplasmic chaperone and an integral outer membrane (OM) assembly and secretion platform termed the usher. The chaperone allows proper folding of pilus subunits in the periplasm, maintains subunits in an assembly-competent state, and prevents premature subunit-subunit interactions (52, 53). The usher catalyzes the exchange of chaperone-subunit for subunit-subunit interactions, promotes ordered polymerization of the pilus fiber, and provides the channel for secretion of the pilus fiber to the cell surface (56, 85, 86, 108).

The type 1 and P pili expressed by uropathogenic *Escherichia coli* (UPEC) are prototypical pili assembled by the CU pathway. UPEC is the primary causative agent of urinary

tract infections (UTIs), and is responsible for ~85% of all uncomplicated and catheter-associated forms of the disease (18). Type 1 and P pili are key UPEC virulence factors, mediating adhesion to and colonization of the bladder and kidney, respectively (21, 28, 34, 132). Type 1 and P pili have composite architectures, consisting of a helical rod segment that extends from the bacterial surface and a distal tip fiber that contains the adhesin (118, 119, 137). The type 1 pilus adhesin FimH binds to a variety of surfaces and host tissues in a mannose-sensitive manner (113). UPEC use type 1 pili to bind to mannosylated proteins present in the bladder, leading to bacterial colonization, bladder epithelial cell invasion, and the development of cystitis (34). The P pilus adhesin PapG binds to di-galactose moieties present in the globoseries of glycolipids found in kidney epithelial cells (131). The expression of P pili by UPEC is strongly associated with the ability of the bacteria to colonize the kidney and cause pyelonephritis (65, 132). The glycolipid receptor is also part of the P blood group antigen, thus allowing P pilus-mediated agglutination of human erythrocytes (133).

UTIs are one of the most commonly acquired infections of the human body, afflicting greater than 50% of women and accounting for 40% of all hospital-acquired infections (8, 9). UTIs lead to over 7 million office visits per year at a cost of more than $3.5 billion annually in the United States alone (9) (10). Although standard antibiotic treatment is often successful in clearing UTIs, high rates of recurrence are associated with the disease. In addition, with the increasing prevalence of antibiotic resistance among UPEC and other pathogenic bacteria, there is an urgent need for the development of new and alternative therapeutics (6). Pili assembled by the CU pathway represent a promising target for clinical intervention and a number of approaches have been taken to develop anti-pilus therapeutics, including vaccines against pilus proteins, competitive inhibitors of pilus-mediated adhesion, and small molecules that disrupt

pilus biogenesis (48, 110, 190, 193-195, 197, 198). An example of the latter is a class of small molecules termed pilicides, which interfere with the CU pathway and block assembly of both P and type 1 pili by UPEC (195, 197).

Nitazoxanide (NTZ) is a synthetic nitrothiazolyl-salicylamide therapeutic used to treat intestinal parasitic diseases such as *giardiasis* and *cryptosporidiosis* (243, 244). NTZ also exhibits broad-spectrum activity *in vitro* against strictly anaerobic bacteria (245), including *Clostridium difficile*, and against members of the epsilon proteobacteria, including *Helicobacter pylori* and *Campylobacter jejuni*, by inhibition of pyruvate ferredoxin oxidoreductase in these organisms (209, 211). In contrast, bacteria such as the Enterobacteriacae lack this drug target and are generally insensitive to the drug(210, 212). Although NTZ does not exhibit bactericidal activity against *E. coli*, previous work demonstrated that NTZ inhibits biofilm formation by enteroaggregative *E. coli* (EAEC), a leading cause of acute and persistent diarrhea(213). NTZ inhibited the assembly of aggregative adherence fimbriae (AAF), which are assembled by the CU pathway and are responsible for both biofilm formation and attachment of bacteria to intestinal epithelial cells. The loss of AAF assembly in response to NTZ was not due to repression of pilus gene expression or interference with disulfide bond formation. In addition to inhibition of AAF-mediated biofilm formation, treatment of EAEC with NTZ also inhibited AAF- and type 1 pilus-mediated hemagglutination (HA) activity of the bacteria(213). Consistent with a loss of pilus-mediated colonization, subsequent modeling studies in mice demonstrated that treatment of EAEC-infected animals with NTZ shortened the duration of infection by causing washout of the bacteria(216).

In this study we demonstrate that NTZ inhibits biogenesis of the UPEC type 1 and P pili, suggesting that NTZ is broadly active against CU pathways. Furthermore, we have determined

that pilus inhibition by NTZ is due to a specific interference with proper maturation of the usher protein in the bacterial OM. These findings point to a novel mechanism of action for NTZ that is distinct from current pilicides.

3.2 Results

3.2.1 NTZ has inhibitory activity against both type 1 and P pili. Previous work by Shamir *et al*. (213) demonstrated that treatment of EAEC with NTZ ablated the assembly of AAF on the bacterial surface, and inhibited HA activity mediated by AAF as well as type 1 pili. Both AAF and type 1 pili are assembled by the CU pathway. To extend this observation to other strains of *E. coli* and to other types of pili assembled by the CU pathway, we examined the effect of NTZ on the type 1 and P pili expressed by UPEC.

To examine pilus assembly and function separate from any effects that NTZ might have on pilus gene expression, we recombinantly expressed the type 1 (*fim*) or P (*pap*) operons from UPEC strain J96 (246) under control of an inducible promoter in the *E. coli* K-12 background. We first assessed the assembly of functional type 1 pili on the bacterial surface by measuring agglutination of guinea pig erythrocytes, using a HA assay. Bacteria (AAEC185/pETS9) were grown in the presence of DMSO (as a vehicle only control) or increasing concentrations of NTZ, and induced for expression of type 1 pili. As shown in Table 3.1, growth in the presence of 10 or 20 µg/ml (30 or 60 µM) NTZ caused a dose-dependent decrease in HA activity. This confirms the previous observation of Shamir *et al*. (213) that NTZ inhibits type 1 pilus function, and demonstrates that NTZ is effective against type 1 pili expressed by different strains of *E. coli*.

We next determined the effect of NTZ on P pili. Bacteria (AAEC185/pFJ29) grown in the presence of 0–20 µg/ml NTZ were induced for expression of P pili, and then used to

agglutinate human erythrocytes. As observed for type 1 pili, growth in the presence of NTZ caused a dose- dependent decrease in HA titer, with concentrations greater than 10 µg/ml inhibiting P pilus function completely (Table 3.1). To determine if the decrease in HA activity correlated with a loss of pilus assembly on the bacterial surface, we isolated P pili from bacteria grown in the absence or presence of NTZ. Analysis of the purified pili by gel electrophoresis revealed that yields of both the major pilus rod subunit PapA (~1000 copies per pilus) and tip-located adhesin PapG (1 copy per pilus) decreased in a dose-dependent manner in response to NTZ treatment of the bacteria (Fig. 3.1A). Quantitation of the PapA band by densitometry showed that growth in the presence of 10 µg/ml NTZ caused an ~50% decrease in pilus levels compared to the vehicle only control, while 20 µg/ml NTZ caused an ~80% decrease in pilus assembly (Fig. 3.1B). Together with the previous findings of Shamir *et al*. (213), these results indicate that NTZ is active against genetically distinct CU pilus systems, and that NTZ functions by interfering with pilus assembly on the bacterial surface.

3.2.2 NTZ inhibits pilus biogenesis by decreasing levels of the usher protein in the OM. Pilus biogenesis by the CU pathway is a well characterized, multi-step assembly process (237). Upon entry into the periplasm, nascent pilus subunits must interact with the periplasmic chaperone (PapD for P pili) for proper folding (52, 53). If complex formation between pilus subunits and the chaperone is disrupted, the subunits will misfold and be degraded by periplasmic proteases(229, 233). To determine if NTZ decreases pilus biogenesis by interfering with formation of chaperone-subunit complexes, we analyzed periplasm fractions isolated from bacteria (BW25113/pPAP58) grown in the absence or presence of NTZ and induced for expression of PapD and P pilus tip subunits. Immunoblotting with anti-PapD-PapG or anti-P pilus tip antibodies showed no change in levels of the PapD chaperone, PapG adhesin, or PapE

major pilus tip subunit in response to the addition of 10 or 20 µg/ml NTZ (Fig. 3.2). Therefore, NTZ does not interfere with chaperone-subunit interactions. Note that PapD contains an essential disulfide bond, which is catalyzed by the oxidoreductases DsbA and DsbB (229). Failure to form this disulfide bond leads to the degradation of PapD by periplasmic proteases. Therefore, our results confirm that NTZ does not interfere with disulfide bond formation in the periplasm, as previously suggested (213). Additionally, since levels of the P pilus proteins in the periplasm were unchanged by drug treatment, these results confirm that NTZ does not alter transcription or translation of the pilus genes in our recombinant system.

The second step of P pilus biogenesis requires that periplasmic chaperone-subunit complexes bind to the usher protein PapC, which functions as the pilus assembly and secretion platform in the OM. The N-terminal periplasmic domain of PapC is the initial binding site for chaperone-subunit complexes (105). To determine if NTZ interferes with this step of pilus biogenesis, we used an *in vitro* overlay assay, which measures binding of chaperone-subunit complexes to the usher N-terminal domain (105). OM fractions from *E. coli* expressing the full-length PapC usher or a mutant lacking residues 2-11 of the N-terminal domain as a negative control were isolated and transferred to a PVDF membrane. Separately, periplasm fractions were isolated from *E. coli* expressing PapD and the P pilus tip subunits. NTZ (0, 10, or 20 µg/ml) was added to the isolated periplasm fractions, and the supplemented fractions were then incubated with the PVDF membrane to allow binding of chaperone-subunit complexes to the usher. Binding was detected by immunoblotting with anti-PapD antibody. As shown in Fig. 3.3, equivalent binding for each of the periplasm fractions was detected to the full-length PapC, whereas no binding was detected to the PapC Δ2-11 negative control. These results indicate that

NTZ does not interfere with the initial binding of chaperone-subunit complexes to the usher N-terminal domain.

We next used a co-purification assay to examine the effect of NTZ on the formation of stable usher-pilus assembly intermediates *in vivo* (59). Bacteria were grown in the absence or presence of NTZ, and induced for expression of P pilus tip subunits and His-tagged PapC usher. OM fractions were isolated and the His-tagged usher was purified by affinity chromatography. Coomassie staining was used to detect the purified PapC usher, and immunoblotting was performed to detect co-purifying pilus complexes. If NTZ interfered with the formation of pilus assembly intermediates at the usher, we would expect levels of the purified usher protein to remain constant, but yields of co-purifying pilus subunits to decrease in response to increasing concentrations of NTZ. Instead, we observed a parallel decrease in both the usher and co-purifying subunits (Fig. 3.4). The corresponding decrease in both the usher and bound subunits suggests that NTZ does not interfere with the formation of usher-chaperone-subunit interactions in bacteria. Instead, we hypothesized that NTZ might act by reducing levels of the usher protein in the OM.

To directly test the effect of NTZ on usher levels, bacteria (BW25113/pMJ3) were grown in the absence or presence of NTZ and induced for expression of His-tagged PapC alone. Analysis of OM fractions isolated from these bacteria revealed that PapC levels decreased in a dose-dependent manner in response to NTZ (Fig. 3.5A). Densitometry analysis of PapC, as detected by immunoblotting with anti-His-tag antibody, revealed that 10 µg/ml NTZ caused an ~40% decrease in OM usher levels compared to the vehicle only control, while 20 µg/ml NTZ caused an ~80% decrease in usher levels (Fig. 3.5B). This closely matches the decrease observed for pilus assembly on the bacterial surface in response to NTZ (Fig. 1.1B). Notably,

analysis of the OM fraction by Coomassie staining revealed little to no effect of NTZ on levels of other OM proteins, including the major porins (OmpA, OmpC, and OmpF) (Fig. 3.5A). Moreover, immunoblotting for the OM LPS transporter LptD also revealed no changes in response to NTZ (Fig. 3.5A). To extend these results to the type 1 pilus system, OM fractions were isolated from bacteria (BW25113/pETS4) grown in the absence or presence of NTZ and induced for expression of the His-tagged FimD usher. Analysis of the OM fractions revealed that FimD levels decreased in a dose-dependent manner in response to NTZ (Fig. 3.6), as found for the P pilus usher PapC. Thus, NTZ treatment leads to a decrease in usher protein levels in the OM, and this effect appears to be specific for usher proteins.

3.2.3 NTZ prevents proper folding of the usher ß-barrel domain in the OM. Ushers are integral OM proteins comprising five distinct domains; a transmembrane ß-barrel channel that resides in the OM, a plug domain that functions as a channel gate, a periplasmic N-terminal domain, and two periplasmic C-terminal domains (56, 85, 100). To localize the effect of NTZ to a specific region of the usher, we examined different domain deletion mutants of PapC. A PapC mutant lacking the N- and C-terminal periplasmic domains (PapCΔNΔC) displayed the same sensitivity to NTZ as found for the full-length PapC usher (Fig. 3.7A and B). OM levels of a PapC mutant lacking the plug domain (PapCΔplug) also decreased in response to NTZ (Fig. 7A). Note that deletion of the plug domain destabilizes the usher, resulting in low levels of PapCΔplug in the OM even in the absence of drug. However, addition of NTZ caused a further decrease in the usher below levels detectable by immunoblot (Fig. 3.7A). Taken together, the sensitivity of both the PapCΔNΔC and PapCΔplug mutants to NTZ suggests that the effect of NTZ is specific to the usher ß-barrel domain.

To test if NTZ interferes with proper folding of the usher ß-barrel domain, we took advantage of the characteristic resistance of OM ß-barrel proteins, including the usher, to denaturation by SDS (105, 163). This resistance results in heat-modifiable mobility on SDS-PAGE, in which a fraction of the usher remains folded in the absence of heating and migrates with faster mobility when compared to fully denatured protein. OM isolated from bacteria (BW25113/pMJ3) grown in the absence or presence of NTZ was incubated at 25ºC in SDS sample buffer prior to analysis by SDS-PAGE. Levels of both the folded and unfolded PapC species decreased similarly in response to increasing concentrations of NTZ (Fig. 3.8A). One interpretation for this result is that NTZ causes misfolding of the usher, and the improperly folded usher is then subject to degradation. DegP, which functions as both a chaperone and protease in the periplasm, is known to target misfolded OM proteins such as the usher for degradation (167, 186, 247). We therefore reasoned that analysis of PapC levels in a strain lacking DegP would result in retention of misfolded usher, and allow discrimination between the effects of NTZ on usher folding and usher degradation. Indeed, repetition of the experiment in a Δ*degP* mutant background revealed that whereas levels of the folded usher species decreased almost completely in response to NTZ, levels of the unfolded species decreased only slightly (Fig. 3.8B). Taken together, these results demonstrate that treatment of bacteria with NTZ interferes with proper folding of the usher in the OM, with DegP then largely responsible for degrading the misfolded protein.

3.3 Discussion

The CU pathway is a conserved and widespread secretion system responsible for biogenesis of virulence-associated surface structures by Gram-negative bacteria. Adhesive pili

or fimbriae assembled by the CU pathway mediate binding to host cells and colonization of host tissues, and thus perform key roles in the ability of bacterial pathogens to establish and maintain infection. In this study, we demonstrate that the small molecule drug NTZ inhibits type 1 and P pili expressed by UPEC by interfering with pilus assembly on the bacterial surface. Through analysis of different steps of the CU pathway, we show that NTZ interferes with pilus biogenesis by preventing proper folding of the usher protein in the bacterial OM. Together with previous results showing that NTZ inhibits AAF and type 1 pili expressed by EAEC (213), our findings confirm that NTZ is a pilicide with activity against different CU pathways. Furthermore, compared to previously characterized pilicides, we demonstrate that NTZ has a novel mechanism of action and is inhibitory in the low μM range typical for most antibiotics.

We found that growth of bacteria in the presence of NTZ inhibited type 1 and P pilus-mediated agglutination of red blood cells in a dose-dependent manner, with inhibition observed beginning at ~10 µg/ml (30 µM) NTZ. This is below growth-inhibitory concentrations of NTZ (213) and within the range achievable in human plasma (204). Our further analysis of P pilus assembly revealed a dose-dependent decrease in the levels of pili on the bacterial surface in response to NTZ, corresponding with the decrease in HA activity. This agrees with the previous analysis of AAF assembly on the surface of EAEC (213), and demonstrates that the anti-pilus activity of NTZ is due to disruption of pilus biogenesis on the bacterial surface. A difference between the current and previous studies is that we expressed our CU pilus genes recombinantly under an artificial promoter, rather than from the native chromosomal loci. Although Shamir *et al*. (213) did not detect changes in *aaf* transcript levels in EAEC in response to NTZ, our experimental setup allowed us to examine pilus assembly separate from any potential regulatory effects on pilus gene expression. In agreement with a lack of NTZ effect on transcription and

61

translation of the pilus genes, we detected no changes in periplasmic levels of P pilus proteins in response to NTZ (Fig. 2).

We took advantage of the detailed understanding of the CU secretion pathway to gain insight into the mechanism by which NTZ inhibits pilus assembly. Using the P pilus system, we found no evidence that NTZ interferes with the formation of chaperone-subunit complexes or the stability of pilus proteins in the periplasm. NTZ did not affect PapD chaperone function in stabilizing pilus subunits (229), which is dependent on disulfide bonding catalyzed by DsbA (248). Therefore, our studies and those of Shamir *et al*. (213) formally rule out DsbA as a target of NTZ action. Periplasmic chaperone-subunit complexes must dock at the OM usher for exchange of chaperone-subunit for subunit-subunit interactions, leading to polymerization of the pilus fiber and secretion through the usher to the bacterial surface. Using both overlay and co-purification assays, we found no evidence that NTZ disrupts the formation of usher-chaperone-subunit interactions. However, the co-purification assay did reveal a dose-dependent decrease in both levels of the PapC usher and bound pilus subunits in response to NTZ (Fig. 4), suggesting that the drug might be acting to reduce levels of available usher protein in the OM. This would explain the loss in pilus assembly on the bacterial surface in response to NTZ, as the usher is the rate-limiting component for pilus biogenesis (85, 86, 249). Indeed, analysis of bacteria expressing the PapC or FimD ushers in the absence of any other pilus proteins showed that usher protein levels in the OM decreased in a dose-dependent manner in response to NTZ. This decrease in usher protein levels closely paralleled the decreases in HA activity and the loss of pilus fibers on the bacterial surface in response to NTZ, consistent with the amount of functional ushers dictating the number of pili assembled.

Using domain deletion mutants of PapC, we were further able to localize the effect of NTZ to the usher's transmembrane ß-barrel channel domain. The majority of integral bacterial OM proteins adopt a ß-barrel fold (250). The usher has a more complicated architecture compared to major OM proteins such as the porins, but other OM proteins, such as the LPS transporter LptD, have similarly complicated architectures (251, 252). Therefore, a surprising and interesting finding from our studies is the apparent of specificity of NTZ for the usher, as we did not observe changes in the general OM protein profile or in levels of LptD in response to NTZ (Fig. 3.5A). This specificity demonstrates that the pilicide activity of NTZ is not due to broad physiological or pleiotropic effects on the bacterial envelope. An important clue for how NTZ affects the usher was obtained by using heat-modifiable mobility to monitor folding of the usher in the OM. Comparison of folded and unfolded usher species in WT and Δ*degP E. coli* strain backgrounds revealed that growth in the presence of NTZ causes a loss of properly folded ushers in the OM. The misfolded ushers are then subject to degradation by DegP, explaining the decrease in usher protein levels observed in the OM in response to NTZ.

How could treatment of bacteria with NTZ lead to misfolding of the usher? We envision several possibilities. First, the drug could directly bind to a conserved region of usher molecules, either preventing proper folding or destabilizing already-folded ushers. In studies to date, we have not observed a direct effect of NTZ on purified usher protein or isolated OM fractions (see Chapter 4). Second, the drug could interfere with a periplasmic chaperone, such as SurA, Skp or DegP, which are required for proper passage of nascent ß-barrel proteins to the OM (253). Maturation of the PapC and FimD ushers is known to involve SurA (185, 186, 254). However, this might be unlikely since these chaperones are involved in the delivery of porins and other proteins to the OM, whereas we observe a specific effect on the usher. Third, the drug could

interfere with proper insertion of nascent usher molecules into the OM. As for the majority of integral OM proteins, insertion of the usher occurs via the ß-barrel assembly machinery (Bam) complex (154, 186). Since the usher appears to have distinct requirements for insertion into the OM compared to other proteins such as the porins (186), the Bam machinery is a possible target of NTZ. In this regard, NTZ might serve as a useful chemical tool to interrogate the complex interactions of the Bam system in assembly of usher proteins into the OM.

Rates of antibiotic resistance among pathogenic bacteria have risen to alarming levels (6). The development of anti-virulence therapeutics such as pilicides represents an alternative to traditional antibiotics that may limit the development of drug resistance and avoid the detrimental side effects of conventional antibiotics (255). The anti-pilus activity of NTZ is distinct from that of previously characterized pilicides. Previous pilicides were shown to target the periplasmic chaperone and disrupt pilus biogenesis by interfering with binding of chaperone-subunit complexes to the usher or by inhibiting chaperone-subunit interactions (195, 196). Small molecules have also been identified that disrupt polymerization of the pilus fiber, and effects of pilicides on pilus expression have also been observed (198, 199). In contrast, we show here that NTZ disrupts pilus biogenesis by decreasing the number of usher molecules in the OM, which is a novel mechanism of action. The usher functions as an essential pilus assembly and secretion platform, making it an excellent target for therapeutic development. Moreover, our results together with those of Shamir *et al.* (213) demonstrate that NTZ has activity against diverse CU pili, suggesting a target common to all CU systems. Further investigation is required to determine both the range of CU pathways affected by NTZ and whether the drug interferes with a common requirement for usher folding in the OM such as the Bam system. NTZ holds promise as a novel pilicide with broad therapeutic potential against Gram-negative pathogens.

64

3.4 Table and Figures
TABLE 3.1

Effect of NTZ on pilus-mediated hemagglutination.

| Pili expressed	NTZ (μg/ml)[a]	HA titer[b]
Type 1 pili		
–	0	0
+	0	121
+	10	46
+	20	16
P pili		
–	0	0
+	0	256
+	5	213
+	10	60
+	15	0
+	20	0

[a]Strain AAEC185 was grown in the presence of the indicated concentrations of NTZ and induced for expression of type 1 (pETS9) or P pili (pFJ29).

[b]Hemagglutination (HA) titer is the maximum fold dilution of bacteria able to agglutinate guinea pig (type 1 pili) or human (P pili) red blood cells.

FIGURE 3.1 Effect of NTZ on P pilus assembly on the bacterial surface. (A) Strain AAEC185/pJF29 was grown in the presence of increasing concentrations of NTZ and induced for expression of P pili. Pili isolated from the bacterial surface were separated by SDS-PAGE and blotted with anti- PapD-PapG antibody to visualize the PapG adhesin (top panel) or stained with Coomassie blue to visualize the major pilus subunit PapA (middle panel). The bottom panel shows the Coomassie-stained whole bacteria used for pilus isolation as a loading control. *E. coli* containing vector only (pACYC184) served as a negative control for pilus isolation. (B) Quantitation of PapA levels in the isolated pili. PapA levels were measured by densitometry of the middle panel in (A), and percent PapA levels were calculated relative to 0 μg/ml NTZ. Bars represent means ± standard errors of the means (SEM) from three independent experiments. ***, $P < 0.001$; ****, $P < 0.0001$ for comparison with 0 μg/ml NTZ.
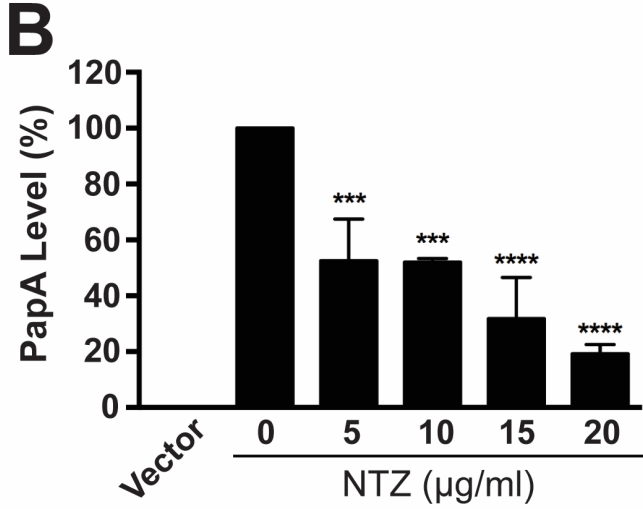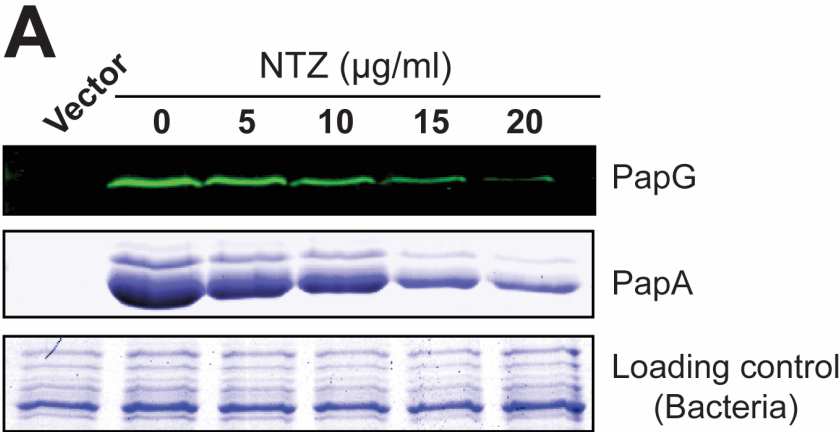
FIGURE 3.1

FIGURE 3.2 Effect of NTZ on chaperone-subunit interactions in the periplasm. Strain BW25113/pPAP58 was grown in the presence of increasing concentrations of NTZ and induced for expression of the PapD chaperone and P pilus tip subunits (PapG, E, F, and K). Periplasm fractions isolated from the bacteria were separated by SDS-PAGE and blotted with anti-PapD-PapG antibody (top panel) to visualize the chaperone and adhesin, or anti-P pilus tips antibody to visualize the PapE major tip subunit (middle panel). The bottom panel shows the periplasm fractions stained with Coomassie blue as a loading control.

FIGURE 3.2
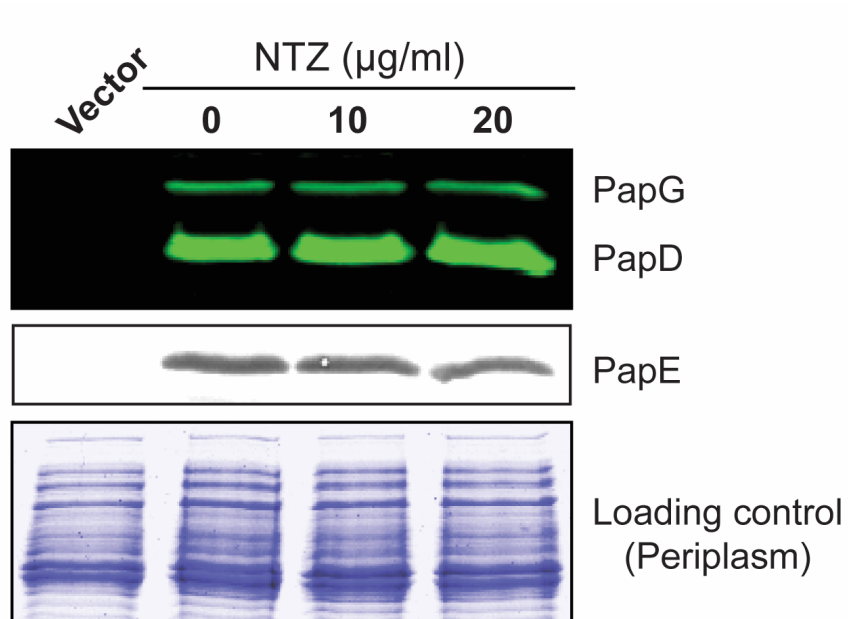
FIGURE 3.3 *In vitro* **analysis of chaperone-subunit binding to the usher.** (A) OM fractions were isolated from strain BW25113 expressing either WT PapC usher (pFJ20), PapC Δ2-11 (pTN1Δ2-11), or vector only (pMON6235Δcat). The OM fractions were separated by SDS-PAGE and stained with Coomassie blue. (B) The OM fractions from (A) were transferred to PVDF membrane and incubated with periplasm fractions isolated from strain BW25113/pPAP58, expressing the PapD chaperone and P pilus tip subunits. The isolated periplasm fractions were supplemented with NTZ at the indicated concentrations. Binding of PapD-subunit complexes to PapC on the PVDF membrane was visualized by blotting with anti-PapD antibody.

FIGURE 3.3
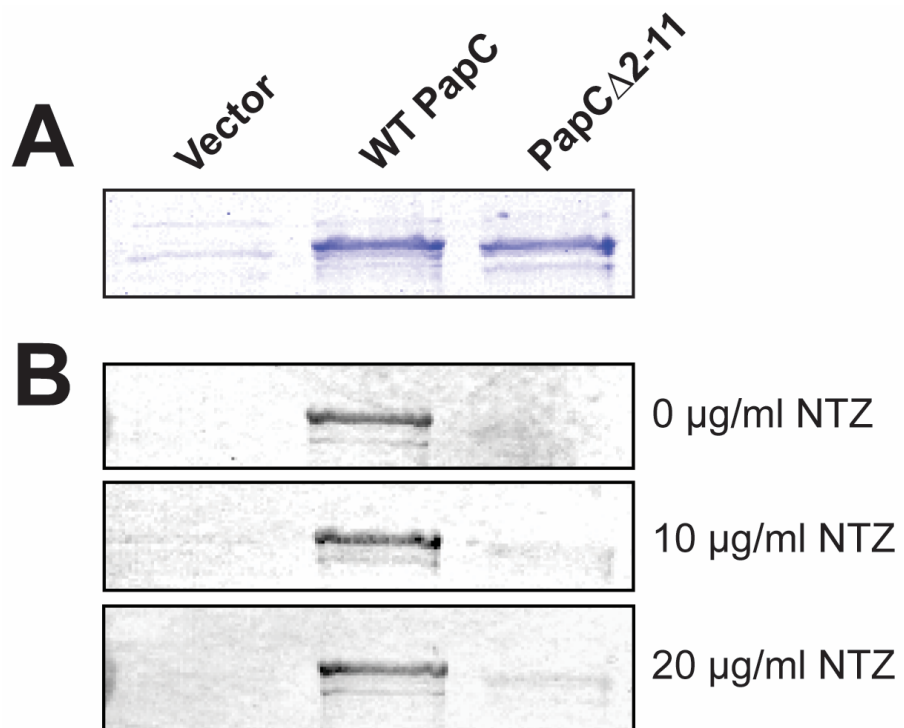
FIGURE 3.4 Effect of NTZ on formation of usher-chaperone-subunit complexes in bacteria. Strain BW25113Δ*ompT* was grown in the presence of increasing concentrations of NTZ and induced for expression of the His-tagged PapC usher (pMJ3), along with the PapD chaperone and P pilus tip subunits (pPAP58). PapC-His, together with any stably bound pilus assembly complexes, was purified from solubilized OM fractions by nickel affinity chromatography and separated by SDS-PAGE. The purified PapC was visualized by Coomassie blue staining (top panel). Co-purifying pilus tips subunits were visualized by blotting with anti-P pilus tips antibody to detect the PapG, PapE and PapF tip subunits (middle panels). The bottom panel shows the solubilized OM fractions stained with Coomassie blue as a loading control.
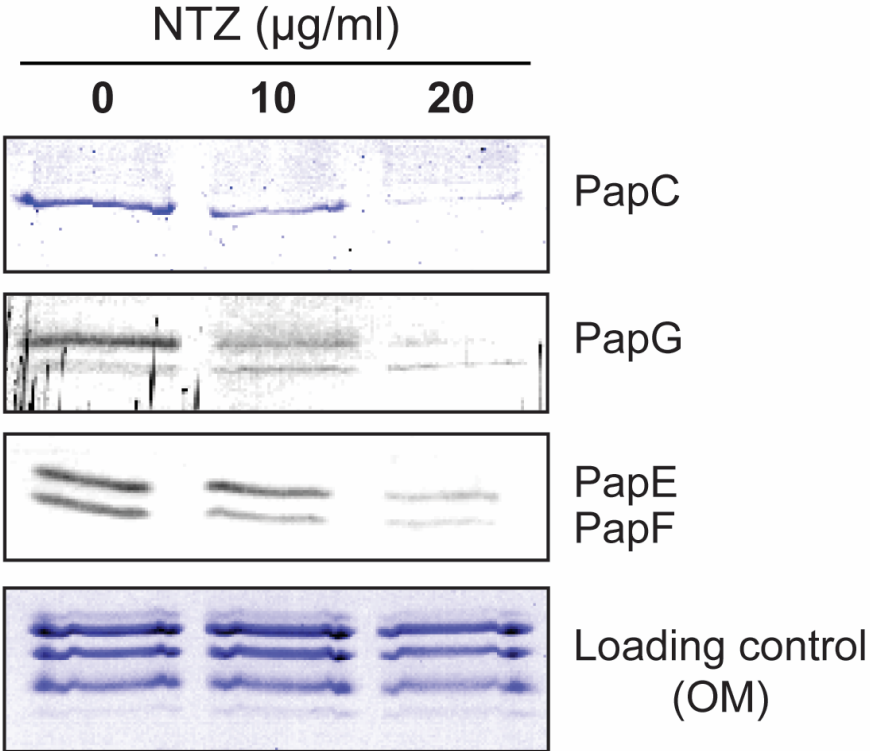
FIGURE 3.4

FIGURE 3.5 Effect of NTZ on levels of the PapC usher in the OM. (A) Strain BW25113/pMJ3 was grown in the presence of increasing concentrations of NTZ and induced for expression of the His-tagged PapC usher. OM fractions isolated from the bacteria were subjected to SDS-PAGE and Coomassie staining to observe PapC and the major OM protein constituents (top panel). Samples were also probed with anti-His antibody to visualize PapC (middle panel), or anti-LptD antibody to visualize the LPS transporter LptD (bottom panel). *E. coli* containing vector only (pMON6235Δcat) served as a negative control for PapC expression. (B) Quantitation of PapC levels in the OM. PapC levels were measured by densitometry of the anti-His blot in (A), and percent PapC levels were calculated relative to 0 μg/ml NTZ. Bars represent means ± SEM from three independent experiments. *, $P < 0.05$; **, $P < 0.01$ for comparison with 0 μg/ml NTZ.
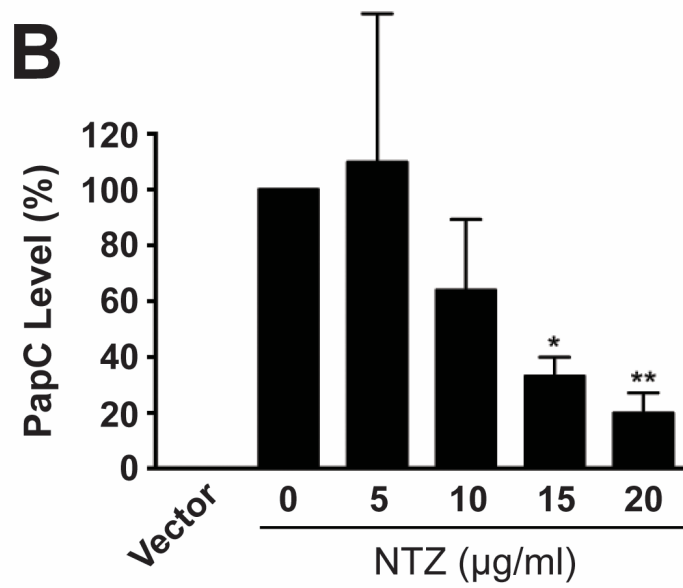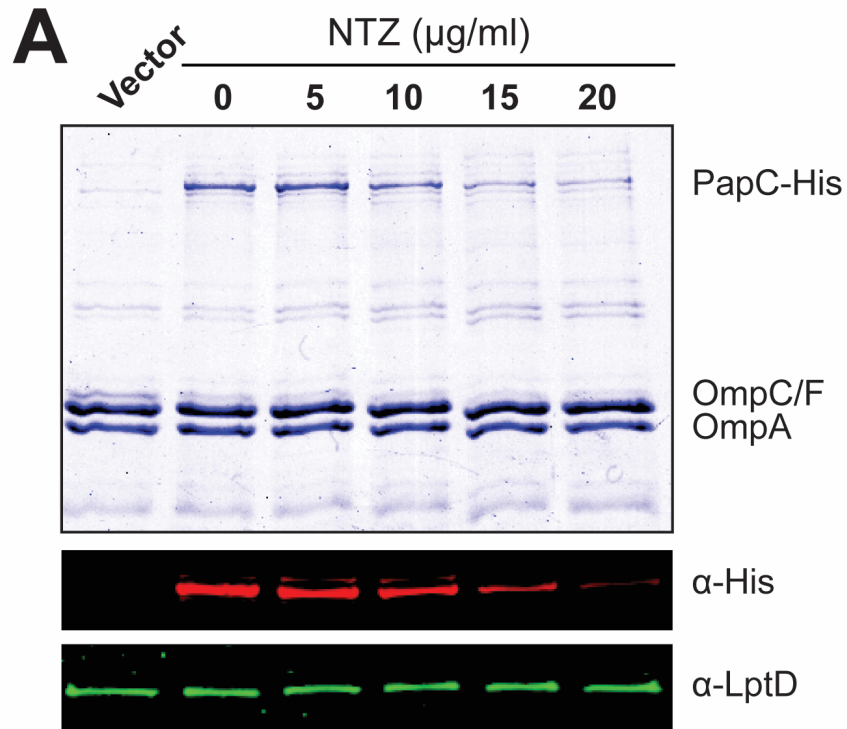
FIGURE 3.5

FIGURE 3.6 Effect of NTZ on levels of the FimD usher in the OM. (A) Strain BW25113/pETS4 was grown in the presence of increasing concentrations of NTZ and induced for expression of the His-tagged FimD usher. OM fractions isolated from the bacteria were subjected to SDS-PAGE and blotted with anti-His antibody to visualize FimD (top panel). The bottom panel shows the OM fractions stained with Coomassie blue as a loading control. *E. coli* containing vector only (pMMB66) served as a negative control for FimD expression. (B) Quantitation of FimD levels in the OM. FimD levels were measured by densitometry of the anti-His blot in (A), and percent FimD levels were calculated relative to 0 μg/ml NTZ. Bars represent means ± SEM from three independent experiments. ****, $P < 0.0001$ for comparison with 0 μg/ml NTZ.

FIGURE 3.6

FIGURE 3.7 Analysis of domain deletion mutants of the PapC usher. (A) Strain BW25113 transformed with plasmid pDG2ΔN2ΔC640 or pNH281 was grown in the presence of increasing NTZ concentrations and induced for expression of PapC lacking the N- and C-terminal periplasmic domains (ΔNΔC) or the plug domain (Δplug), respectively. OM fractions isolated from the bacteria were subjected to SDS-PAGE and blotted with anti-His antibody to visualize PapC ΔNΔC (upper panel) or PapC Δplug (lower panel). *E. coli* containing vector only (pMON6235Δcat) served as a negative control for PapC expression. (B) Quantitation of PapC ΔNΔC levels in the OM. PapC levels were measured by densitometry of the upper panel in (A), and percent PapC levels were calculated relative to 0 μg/ml NTZ. Bars represent means ± SEM from three independent experiments. ***, $P < 0.001$; ****, $P < 0.0001$ for comparison with 0 μg/ml NTZ.

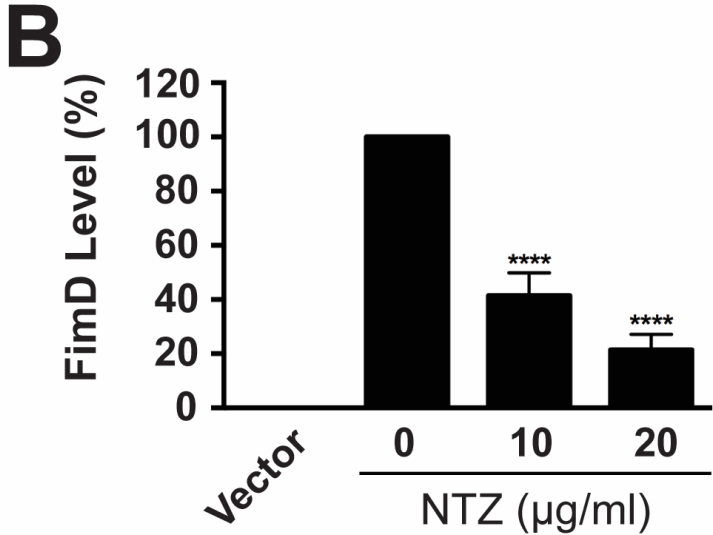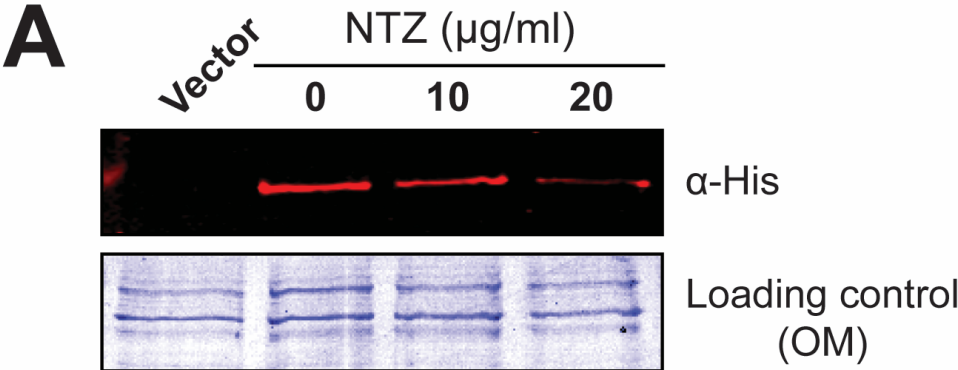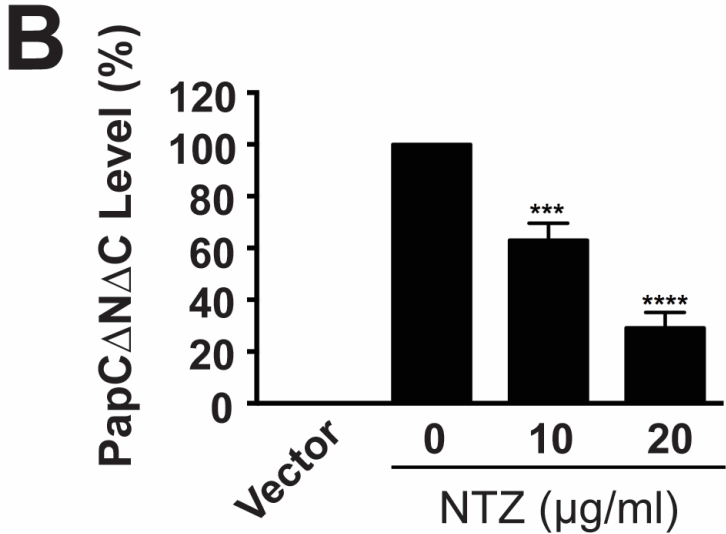**FIGURE 3.7**
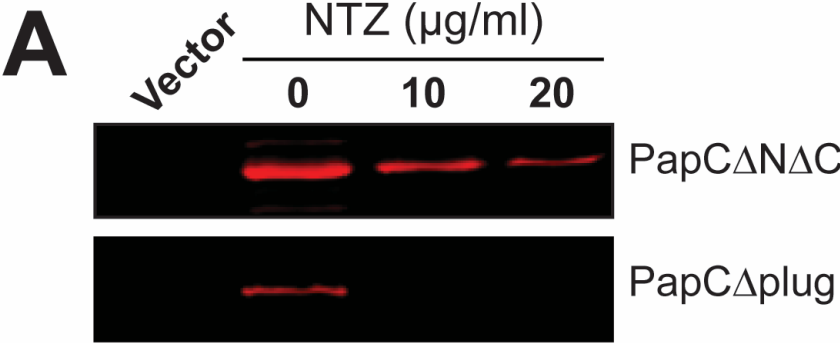
FIG 3.8 Analysis of usher folding in the OM. Strains BW25113 (A) or BW25113Δ*degP* (B) transformed with pMJ3 were grown in the presence of increasing concentrations of NTZ and induced for expression of the His-tagged PapC usher. OM fractions isolated from the bacteria were incubated in SDS sample buffer at 25°C, subjected to SDS-PAGE, and probed with anti-His antibody to visualize PapC. Positions of the folded (F) and unfolded (U) PapC species are indicated on the left of each gel image. *E. coli* containing vector only (pMON6235Δcat) served as a negative control for PapC expression. Quantitation of the folded and unfolded PapC bands is presented below each gel image. The PapC levels were measured by densitometry of the anti-His blots, and percent PapC levels were calculated relative to the respective folded or unfolded species present at 0 μg/ml NTZ. Bars represent means ± SEM from three independent experiments. *, $P < 0.05$; **, $P < 0.01$; ***, $P < 0.001$ for comparison of folded to unfolded PapC at each NTZ concentration.

FIGURE 3.8
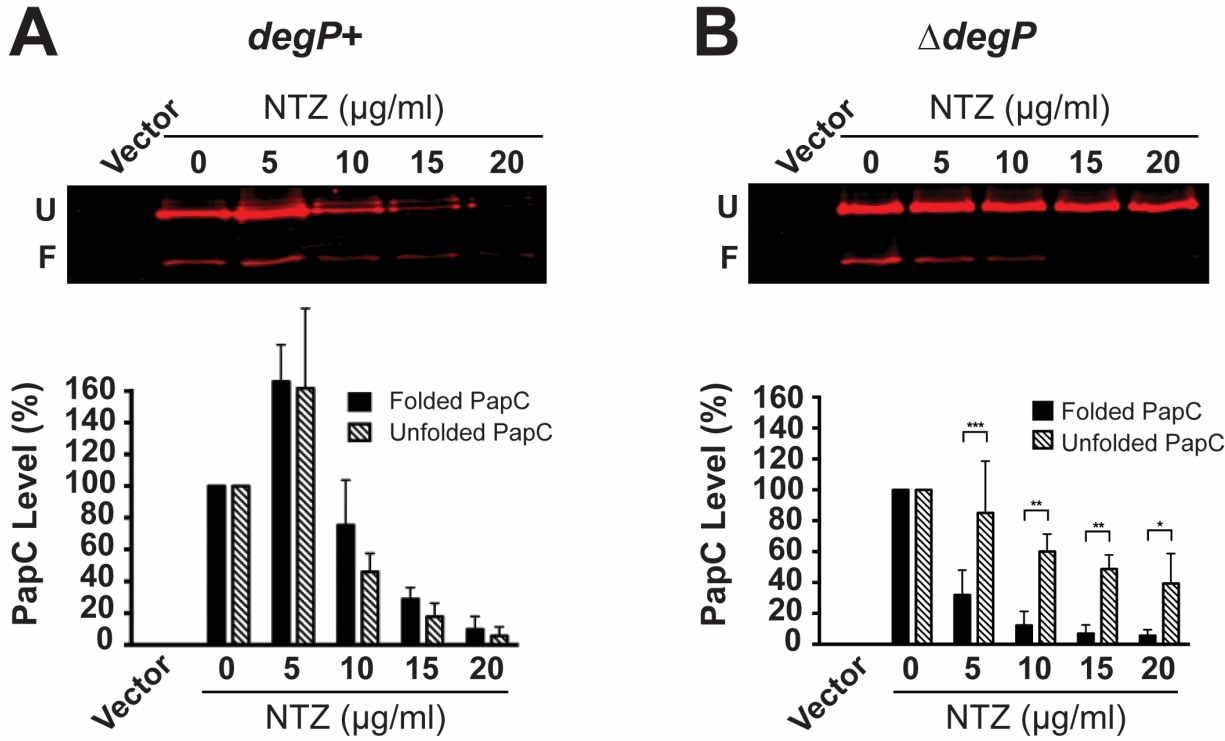
CHAPTER 4

Role of the ß-barrel Assembly Machinery in the Effect of NTZ on Usher

Folding

4.1 Chapter overview

The experiments described in previous chapter provide evidence that NTZ-mediated loss of CU pili from the bacterial surface is due to a reduction of the usher protein in the OM. Moreover, loss of the usher is not due to transcriptional or translational defects but rather an inability of the usher to assemble properly in the OM, leading to its proteolytic degradation. This is the first described instance of a pilicide that inhibits pilus assembly via this mechanism and, to our knowledge, the first pharmacotherapy-mediated effect on the assembly of an OM ß-barrel protein.

While the evidence in chapter 3 provides a mechanism for pilus loss, it does not explain how NTZ causes the usher to misassemble in the OM or what the direct target of the drug is. Some clues on how to approach these questions can be found in the data. The experiments utilizing usher domain deletions clearly indicate that the effect of NTZ is isolated to the large transmembrane ß-barrel domain of the usher. Additionally, the Δ*degP* experiment demonstrates that NTZ affects the folding status of the usher's ß-barrel domain. This evidence is relevant given that, within the last ten years, the Bam complex has been identified as the major assembly machinery required to assemble ß-barrel proteins in the OM. Based on the conclusion that NTZ inhibits pilus biogenesis by specifically preventing proper maturation of the usher ß-barrel domain in the OM, I sought to test the following hypothesis: *NTZ inhibits pilus biogenesis by targeting the machinery required for assembly of the usher protein in the OM.*

Previous studies have revealed some details about the pathway for usher assembly in the OM. Early work by Hunstad *et al.* (256) showed that clinical UPEC isolates suppressed bladder epithelial cell immuno-stimulatory cytokine responses *in vitro*. This suppression was abolished when insertional mutations were introduced into *surA* and a number of LPS biosynthetic genes.

Later work demonstrated that a *surA* mutant had significantly diminished levels of type 1 and P pili on the surface of UPEC due to decreased levels of the ushers FimD or PapC in the OM (185, 254). Loss of SurA also prevented UPEC from persisting in the urinary tract of mice and inhibited the bacterium's ability to properly form intracellular communities required for its pathogenesis (257).

Knowing that SurA is a major chaperone responsible for shuttling nascent OMPs to the Bam complex (258), more recent work has focused of determining which Bam components are critical for usher biogenesis. In 2011 Palomino *et al.* (186) verified that SurA is important for assembly of FimD and that loss of FimD in a Δ*surA* mutant is due to proteolytic degradation of the unfolded protein by DegP. Using a conditional *bamA* mutant, Palomino *et al.* also showed that BamA is important for FimD assembly, implicating the Bam complex in the folding of the usher (186). Taking this one step further, they observed the effect of various Bam lipoprotein deletions on FimD levels. A Δ*bamB* mutant showed diminished levels of both folded and unfolded FimD, as was the case for Δ*bamC* Δ*bamB* and Δ*bamC* Δ*bamE* double mutants. An increase in unfolded FimD was also observed in Δ*bamC* and Δb*amE* mutants alone. These data provided further evidence that the Bam complex is responsible for folding the usher.

The work described in this chapter suggests that NTZ interferes with the functionality of the Bam complex, as it relates to usher folding, and that one or more components of the complex is the likely target of the drug. Furthermore, I provide evidence for the utility of NTZ not only as a potential anti-virulence therapeutic agent but also as a tool to study the Bam system.

4.2 Results

4.2.1 Effect of NTZ on folded usher. The results described in chapter 3 indicate that NTZ's effect is directed towards the folding status of the usher ß-barrel domain. To test the possibility that NTZ could be acting directly on the usher, and destabilizing it in the OM, I expressed His-tagged PapC in *E. coli* grown in the absence of drug and isolated the OM fraction. OM pellets were then resuspended in buffer containing increasing concentrations of NTZ and incubated at 37°C for one hour. To distinguish the folded from the unfolded usher species samples were left unboiled and analyzed by immunoblotting. As shown in Fig. 4.1A the presence of NTZ did not effect the ability of the usher to maintain a folded conformation in the OM. This experiment was repeated, but with PapC that had been purified from the OM before being incubated with NTZ. Analysis of the usher by SDS-PAGE and Coomassie blue staining (Fig 4.1B) again showed that the drug had no effect on the stability of the of the usher ß-barrel, indicating that the folded usher is likely not the direct target of the drug.

4.2.2 Effect of Bam mutants on usher folding and sensitivity to NTZ. Having previously shown (Chapter 3) that NTZ prevented proper maturation of the usher in the OM, leading to its degradation by DegP, coupled with published evidence that the Bam machinery is required for usher folding (186), I wanted to determine if Bam complex mutants could alter the usher's sensitivity to the drug. Δ*bamB*, Δ*bamC*, and Δ*bamE* mutants were obtained from the Keio collection (217) (background strain BW25113), PCR verified, and transformed with plasmid pMJ3, which recombinantly expresses His-tagged PapC under the control of an arabinose inducible promoter. BW25113 transformed with pMON6235Δcat was used as the vector only control. Strains were grown in the presence and absence of NTZ, OM fractions were isolated, and relative usher levels were analyzed by Coomassie blue staining and

immunoblotting. A WT strain expressing PapC was also grown along side each Bam mutant, in the absence of NTZ, to discern any effect the Bam mutant strain on overall usher levels irrespective of the drug.

I first examined the effect of NTZ on PapC levels in a Δ*bamB* mutant background (Fig. 4.2). As had been reported previously (173) (174), the Δ*bamB* strain had diminished levels of the OM porins OmpA, OmpC, and OmpF when compared to the WT strain. Unexpectedly though, PapC levels were ~2-3X higher in the mutant background compared to WT (Fig. 4.2A). When the Δ*bamB* mutant was grown in the presence of increasing concentrations of NTZ another interesting phenotype was observed. Unlike the result in Figure 3.5, where usher levels decreased in a dose dependent manner in response to NTZ, there was no significant decrease in PapC levels regardless of drug concentration in the Δ*bamB* mutant (Fig. 4.2A and B).

I next examined that ability of the usher to fold in the OM in the Δ*bamB* mutant background. To distinguish between the folded and unfold species of the usher, I again utilized the intrinsic resistance ß-barrel proteins have to SDS treatment (Fig. 4.3). An OM sample from WT *E. coli* expressing PapC in the absence of NTZ was used as a positive control and compared to the Δ*bamB* mutant expressing usher in the presence or absence of drug. All samples were incubated at 25°C for 10 min in SDS sample buffer and then analyzed by immunblotting. Interestingly, unlike the WT strain, the Δ*bamB* mutant was unable to produce any folded usher regardless of the presence of NTZ, as indicated by the loss of the folded usher band (Fig. 4.3A). Additionally, the unfolded band remained present in the OM with no evidence of loss due to degradation. Complementation of the Δ*bamB* mutant with a plasmid expressing the *bamB* gene restored usher folding in the OM back to WT levels (Fig. 4.3B). This verifies the specificity of the Δ*bamB* mutant strain. Taken together, these data highlight the importance of BamB for

proper folding of the usher in the OM and suggests that BamB could play a role in meditating the effect of NTZ.

The effect of NTZ on PapC OM levels was next investigated in a ΔbamC mutant. Unlike the ΔbamB mutant, the ΔbamC strain displayed no noticeable defect in porin assembly and PapC levels remained unchanged when compared to WT (Fig. 4.4A). Additionally, in the presence of increasing concentrations of NTZ, PapC levels were diminished in a dose dependent manner similar to what was observed in the WT strain (Fig. 4.4A and B). Since no altered phenotype was observed in this strain background, BamC likely does not play a role in the activity of NTZ.

The last of the non-essential Bam proteins tested was BamE. When analyzed, the OM of the ΔbamE mutant showed no changes in porin or PapC levels (Fig. 4.5A), similar to what was observed for the ΔbamC mutant. However, unlike the ΔbamC strain, the addition of increasing concentrations of NTZ caused no significant decrease in PapC levels (Fig. 4.5A and B). I next wanted to determine if the ΔbamE mutant was able to properly fold the usher into the OM. As described for the ΔbamB mutant, ΔbamE OM samples were obtained from bacteria grown in the presence and absence of NTZ, incubated at 25°C, and analyzed by immunoblot to visualize the folded and unfolded usher species. BW25113/pMJ3 grown in the absence of drug again served as a positive control (Fig. 4.6A). The WT strain produced PapC bands corresponding to both folded and unfolded usher, while the folded band was significantly diminished in the ΔbamE mutant irrespective of the drug. Complementation of the ΔbamE mutant with a plasmid expressing the bamE gene restored usher folding in the OM back to WT levels (Fig. 4.6B). This verifies the specificity of the ΔbamE mutant strain. These data suggest that in addition to BamB, BamE plays a role in usher folding and is implicated in the activity of NTZ.

4.2.3 ΔbamB and ΔbamE mutants differentially affect pilus function. The ability of

the Bam complex to facilitate proper maturation of the usher into the OM has only been

measured by examining the sensitivity of the usher ß-barrel to SDS (this work and (186)). While

this is a useful tool to examine the stability of the usher, it provides no means of discerning ß-

barrel conformational stability from function. In studies from our laboratory we have found that

usher mutants can be generated that are fully capable of assembling pili, and thus must be

properly folded in the OM, but when analyzed by SDS-PAGE appear to be sensitive to SDS

treatment even when incubated at $25^{\circ}C$ (Henderson and Thanassi, unpublished data). With this in

mind, it could be possible that the ΔbamB or ΔbamE mutant is capable of folding the usher, even

though the usher appears to be more sensitive to SDS (Figs. 4.3 and 4.6). To test this, plasmid

pFJ29, which encodes the entire *pap* operon under the control of an IPTG inducible promoter,

was transformed into WT BW25113, BW25113ΔbamB, BW25113ΔbamC, and

BW25113ΔbamE. BW25113/pACYC184 was used as a vector only control. Bacteria were

grown and induced for the expression of P pili, harvested, and submitted to hemagglutination

(HA) analysis using human red blood cells to determine if functional P pili could be assembled

on the bacterial surface (Table. 4.1). HA titers indicated that the WT strain produced a robust

score of 128, while the ΔbamB mutant abolished agglutination completely as indicated by an HA

score of 0. This result confirms that the lack of folded usher seen in the ΔbamB strain was indeed

due to the inability of this mutant to fold the usher. The HA titer of a ΔbamC mutant was

identical to WT. This was expected given that the ΔbamC strain showed no alteration in usher

sensitivity to NTZ and confirms that folded and functional usher is produced in this background.

The most intriguing result was observed for the ΔbamE mutant, which produced an HA titer of

512, four times greater than what was observed for the WT strain. This result was striking for

two reasons: i) there was no observed increase in OM usher levels in the $\Delta bamE$ mutant compared to WT, and ii) the mutant strain greatly diminished the levels of folded usher in the presence of SDS. Based on these observations I can conclude that BamB is essential for usher assembly in the OM, while BamE promotes usher ß-barrel conformational stability. Additionally, these data highlight that sensitivity to denaturation by SDS, as determined by heat modifiability, does not necessarily reflect the usher's conformational state *in vivo*. Therefore, the terminology "folded" and "unfolded" in this dissertation should only be understood to describe the usher as it is observed by SDS-PAGE analysis, not necessarily its *in vivo* state.

4.2.4 Modulation of Bam complex expression alters sensitivity to NTZ. My results thus far support the hypothesis that NTZ may act on the Bam complex to affect usher folding in the OM. If the Bam complex is the direct target of NTZ then over-expression of Bam proteins should provide resistance to NTZ. To test this, an expression plasmid containing all five genes of the Bam complex (*bamABCDE*) was obtained from Harris Bernstein's laboratory at the National Institutes of Health (222). I then subcloned the *bam* genes into a vector that that places the complex under the control of an IPTG inducible promoter (pBamABCDE). This plasmid is also compatible with the PapC-His construct (pMJ3), allowing expression of the Bam complex and the usher to be controlled independently. First, BW25113/pMJ3 was grown in the presence and absence of NTZ, and OM fractions were re-analyzed by immunoblot to serve as a baseline control for WT usher sensitivity to the drug (Fig. 4.7A). BW25113 was then transformed with both pMJ3 and pBamABCDE, grown in the presence and absence of NTZ, and its OM fractions were also analyzed by immunoblot (Fig. 4.7B). For each experiment, samples were analyzed at both 95°C and 25°C to determine if Bam complex over-expression had any influence on PapC

folding. Samples from BW25113/pMJ3 and BW25113/pMJ3 + pBamABCDE grown in the absence of NTZ were also run side by side to identify any affect over-expression of the Bam complex might have on total OM PapC levels.

As was observed previously, in the condition where PapC was expressed alone, usher levels decreased by ~50% at the 10 µg/ml concentration of NTZ and by ~70% at the 20 µg/ml concentration (Fig. 4.7A and C). There was also no observable defect in porin levels and the folded and unfolded usher bands diminished in the standard does dependent manner (Fig. 4.7A). When the Bam complex was over-expressed along with the usher a number of altered phenotypes were apparent (Fig. 4.7B). First, when Bam complex expression was measured using an anti-BamA antibody, BamA levels were ~4-5X higher when compared to the WT levels. Usher levels also remained unchanged between the two conditions and Bam over-expression had no effect on usher folding. Interestingly though, when usher levels in the presence of NTZ were quantified, only an ~25% decrease in usher levels was achievable at the 10 µg/ml concentration of NTZ and a ~55% decrease at 20 µg/ml (Fig. 4.7B and C). This result indicates that Bam over-expression generates a significant level of resistance to NTZ.

In contrast to over-expression, under-expression of a drug target should increase sensitivity to the drug. To test this for the Bam system, a *bamA* mutant strain, MC4100*bamA101*, was obtained from Thomas Silhavy's laboratory at Princeton University. This strain contains a transposon insertion in the upstream promoter region of the *bamA*, which results in at least a ~10 fold decrease in BamA expression (181). This *bamA101* mutant displays defects in porin assembly but retains enough BamA to maintain cell viability. Additionally, this mutant does not effect expression of BamD; however no analysis has been done on the other Bam lipoproteins (259). Since BamA is the central component of the Bam complex, reduced BamA levels would

result in less overall complex formation. Strains MC4100 and MC4100*bamA101* were transformed with pMJ3, grown in the presence and absence of NTZ, and OM fractions were analyzed by immunoblot to determine the relative usher levels (Fig. 4.8A). An anti-BamA antibody was used to determine BamA expression levels in the WT and mutant strains. Samples were analyzed at both 95°C and 25°C to determine if *bamA101* had any influence on usher folding.

Similar to what was observed in strain BW25113, PapC levels decreased by ~40% at the 10 µg/ml concentration of NTZ and by ~65% at the 20 µg/ml concentration in strain MC4100 (Fig. 4.8A and C). The response of folded and unfolded usher was also similar between MC4100 and BW25113. When the usher was expressed in the *bamA101* strain, more dramatic phenotypes were visible. When compared to WT MC4100, the *bamA101* strain displayed significantly diminished levels of OmpA, OmpC, and OmpF, which had been described previously (181, 259). Interestingly though, total usher levels remained unchanged between the two strains. BamA levels were also significantly decreased in the *bamA101* strain as expected (Fig. 4.8B). Notably, the usher was significantly more sensitive to NTZ in the *bamA101* strain, showing a ~70% decrease at 10 µg/ml and a ~95% decrease at 20 µg/ml of drug (Fig. 4.8B and C). Compared to the WT strain, the *bam101* mutant showed a noticeable increase in the unfolded PapC species while folded usher was dramatically reduced (Fig. 4.8B). An increase in unfolded PapC degradation products was also present in the mutant. Additionally, levels of the unfolded usher species greatly diminished in response to the addition of NTZ.

To test if the *bamA101* mutant could be complemented by expressing *bamA* in trans, *bamA* was cloned into an expression vector under the control of an IPTG inducible promoter (pBamA). MC4100*bamA101* was then transformed with both pBamA and pMJ3 to allow for

individual control of both BamA and PapC expression. Strains were again grown in the presence

or absence of NTZ, and OM fractions were isolated and analyzed by immunoblot. Over-

expression of BamA in the *bamA101* background led to a 40X increased in the protein in the OM

(Fig. 4.9B). The excess BamA rescued the porin assembly defect that was present in the mutant

(Fig. 4.9A and B). When usher levels were examined it became clear that BamA over-expression

to alleviated PapC's sensitivity to NTZ from what was seen in the *bam101* mutant alone. PapC

levels were now decreased by ~55% and ~25% at the 10 µg/ml and 20 µg/ml NTZ respectively

(Fig. 4.9C). These values are similar to what was observed in the WT MC4100 strain. Lastly,

BamA over-expression in the *bamA101* mutant was also able to restore normal folding of the

usher as indicated by the presence of the folded usher band when compared to the mutant alone

(Fig. 4.9B). These experiments, examining usher sensitivity to NTZ in the *bamA101* strain and

complementation with pBamA, provide evidence that modulation of Bam complex levels can

alter sensitivity to the drug, suggesting that one or more proteins of the complex may be the

direct target of NTZ.

4.3 Discussion

The Bam system is a conserved protein complex found in the OM of all Gram-negative

bacteria and is the primary machinery responsible for assembly of ß-barrel proteins into the OM.

Its physical location in the bacterial cell and essential role in the biogenesis of OM proteins

makes it an attractive target for therapeutic development. Previous work investigating the

importance of the Bam complex in biogenesis of usher proteins demonstrated that ushers are i)

highly dependent on the SurA chaperone for transport across the periplasm to the Bam complex,

ii) are more dependent on BamB for their assembly compared to other ß-barrel proteins, and iii)

are degraded by the periplasmic protease DegP if they cannot be assembled properly (185, 186, 254). Given the findings from the preceding chapter that NTZ inhibits the assembly of CU pili by preventing proper maturation of the usher ß-barrel domain in the OM, leading to its degradation, exploration of the Bam complex posed as a logical approach to identify the direct target of NTZ.

The availability of deletion mutants for the non-essential components of the Bam complex (BamB, BamC, and BamE) served as a good starting point to examine the potential role for the complex in NTZ's activity. One caveat of using these mutants is that some, like Δ*bamB*, have been shown to activate stress responses such as the σ^E pathway, which alter gene expression (260). A previous analysis of the role of the Bam complex in usher biogenesis relied on chromosomal expression of endogenous usher genes (186), and thus usher expression could have been altered by any induced stress responses. To eliminate this possibility, usher expression was artificial induced from a recombinant plasmid for this study.

Analysis of the Δ*bamB* mutant revealed an increase in PapC levels compared to the WT strain. However, the usher appeared to be unfolded as tested by heat modifiability, and non-functional when HA was used as a measure of P pilus assembly. Strikingly, PapC was insensitive to NTZ in the Δ*bamB* strain, showing no significant decrease as the drug concentration increased. Additionally, while a Δ*bamB* mutant was reported to have diminished levels in porins and increased membrane permeability (173, 174), the folding defect seen in the mutant appears to be specific to the usher (this study and (186)). To our knowledge, these are the most prominent Δ*bamB* phenotypes to be observed thus far and validate the importance of BamB in folding the usher.

Two questions now become apparent, how does a ΔbamB mutant generate insensitivity to NTZ and why is the unfolded usher not degraded? One possibility to explain the first question could be that when BamB is missing the complex is no longer competent to initiate folding of the usher. In other words, it is possible that while a complex of BamACDE is capable of folding other ß-barrels, it cannot actively fold the usher. We postulate that the effect of NTZ only occurs when the usher is in the process of being folded. Therefore, if usher folding cannot be initiated in the ΔbamB mutant, NTZ will have no effect. One possibility to explain the second question is that the usher in the ΔbamB mutant is still bound by chaperone molecules such as SurA, protecting it from degradation. Another possibility could be that the usher is somehow inserted into the membrane or bound by the Bam complex in a manner that prevents it from being accessible to proteases. Additional work needs to be done to answer these questions.

The ΔbamC mutant displayed no altered phenotype in the sensitivity of PapC to NTZ or the ability of the usher to assemble P pili. This was not unexpected considering that a significant phenotype has yet to be identified for this mutant. I conclude from these experiments that BamC is unlikely to be the target or implicated in the activity of NTZ.

The ΔbamE mutant had a surprising and interesting phenotype. Overall PapC levels were unaffected in the mutant; however, similar to the ΔbamB mutant, insensitivity to NTZ was observed. When PapC folding was analyzed, the folded species was greatly diminished in the mutant background but the usher was still able to assemble functional P pili, producing an HA titer that was four times greater than that obtained for the WT strain. Given that the usher must be folded to assemble pili, one explanation is that's the folded usher in the ΔbamE mutant is altered such that it is sensitive to SDS and denatured at 25°C. Such a phenotype has been observed by others showing what appears to be an unfolded ß-barrel on an SDS-PAGE gel but

retaining functionality *in vivo* (261). In the context of the Bam complex, this would suggest that loss of BamE prevents the complex from assembling a conformationally stable usher. This alteration in Bam functionality and usher folding in the Δ*bamE* strain could explain the usher's insensitivity to NTZ. Previously described phenotypes for a Δ*bamE* mutant include minor changes in OM permeability to certain antibiotics, little to no deficiency in porin assembly, and induced conformational changes in BamA (178, 181, 184). To our knowledge, we describe here the first distinctive phenotype for a Δ*bamE* mutant on a ß-barrel protein other than BamA.

My analysis of the *bam* deletion mutants suggests that the Bam complex could be the target of NTZ. If true, then over-expression of the complex should result in decreased sensitivity to the drug. To test this, an expression plasmid encoding all five components of the Bam complex was co-expressed with PapC in a WT *E. coli* strain. Bam over-expression had no effect on steady state PapC levels; however, increased resistance to NTZ was observed as indicated by elevated PapC levels at the tested NTZ concentrations compared to a strain without Bam over-expression. This result is consistent with the Bam complex as a target of NTZ.

Knowing that over-expression of the Bam complex generated insensitivity to NTZ, then a logical hypothesis would be that under-expression of the complex should increase sensitivity to the drug. A *bamA* promoter mutant, *bamA101*, was obtained that significantly reduces BamA expression but retains enough BamA to sustain bacterial viability. Additionally, the Bam complex components do not exist in an operon, so only BamA levels are effected by this mutant (259). When PapC expression was checked in this background there was no change in steady state usher levels; however, the unfolded PapC species was far more prevalent than the folded species in the *bamA101* mutant compared to the WT strain. When PapC sensitivity to NTZ was tested, the mutant was also significantly more sensitive to the drug than the WT strain. This is

again consistent with the Bam complex being targeted by the drug. An interesting phenotype of the *bamA101* mutant is that the abundant unfolded usher is not degraded in the absence of drug. Further work needs to be done explain this observation and to determine if the usher is functional in this strain. One distinction to be made is that insensitivity to NTZ was generated when the unfolded usher was observed as the predominant species in the Δ*bamB* and Δ*bamE* mutants. Conversely, though unfolded usher is the major species in the *bamA101* mutant, the heightened sensitivity to NTZ may indicate that the remaining complex is functional and accessible to the drug. Finally, complementation of the *bamA101* mutant with BamA expressed *in trans* returned sensitivity to NTZ to near WT levels and restored the general OMP assembly defects that were observed in the *bamA101* strain alone. This experiment, together with the data collected from both the over and under-expression experiments, provides strong genetic evidence for one or more components of the Bam complex as the possible target of NTZ.

4.4 Table and Figures

TABLE 4.1 Effect of Bam complex mutants on pilus-mediated hemagglutination.

P pili	Strain^a	HA titer^b
–	WT/vector	0
+	WT/pFJ29	128
+	Δ*bamB*/pFJ29	0
+	Δ*bamC*/pFJ29	128
+	Δ*bamE*/pFJ29	512

^{a}Indicated WT or *bam* mutants of strain BW25113 were grown and induced for expression of P

pili using pFJ29, which recombinantly expresses the entire *pap* operon.

^{b}Hemagglutination (HA) titer is the maximum fold dilution of bacteria able to agglutinate human

red blood cells.

FIGURE 4.1 Effect of NTZ on folded PapC usher. (A) *E. coli* stain BW25113 transformed with pMJ3 was grown in the absence of NTZ and induced for expression of His-tagged PapC usher. OM fractions isolated from the bacteria were resuspended in either DMSO or increasing concentrations of NTZ and incubated at 37°C for one hour. Following incubation samples were left unboiled and subjected to SDS-PAGE and probed with anti-His antibody to visualize PapC. Positions of the folded (F) and unfolded (U) PapC species are indicated on the left of each gel image. (B) Purified PapC usher was obtained and incubated with DMSO or increasing conrentrations of NTZ at 37°C for one hour. Samples were left unboiled and PapC was visualized by SDS-PAGE stained with Coomassie. One untreated PapC sample was heated for 10 min at 95°C to serve as an indicator of unfolded PapC usher.

FIGURE 4.1

A

Empty Vector

0   10   20   NTZ µg/ml

U

F

Loading control

B

0   0   10   20   NTZ µg/ml

U

F

+   –   –   –   95°C
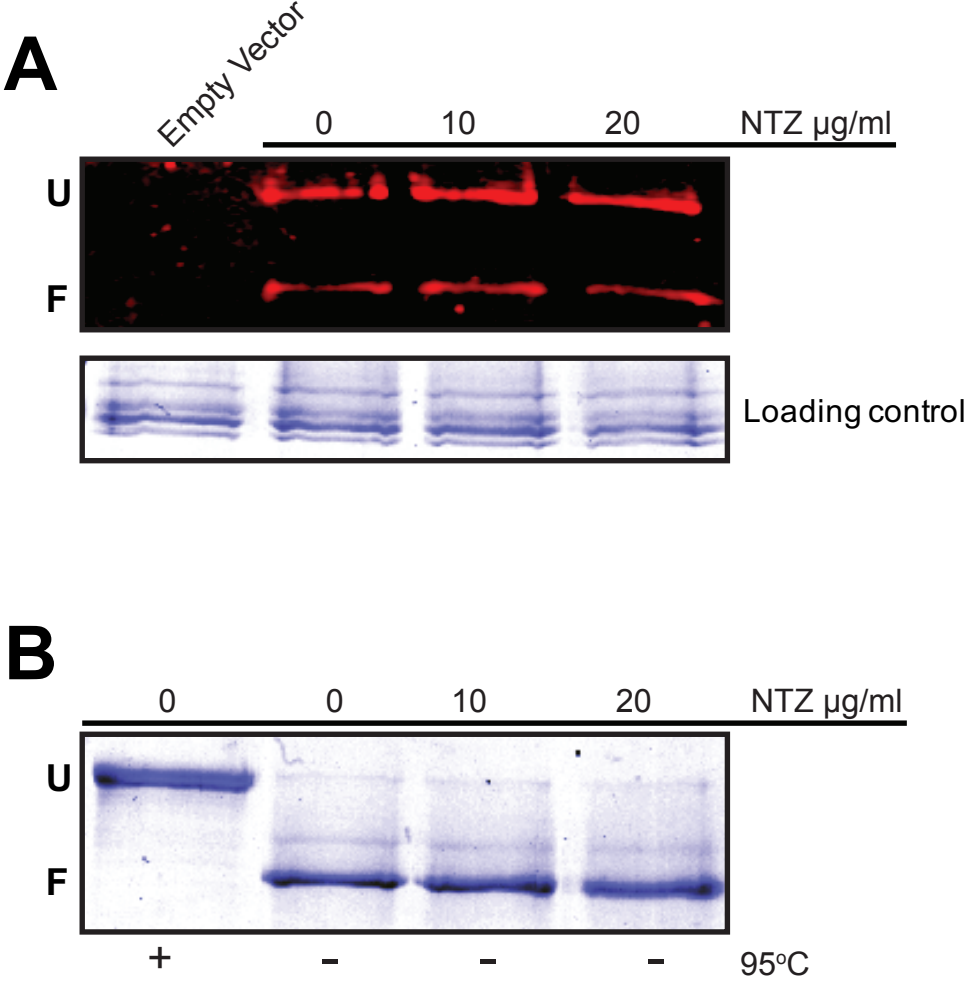
FIGURE 4.2 Effect of NTZ on OM PapC usher levels in a Δ*bamB* mutant. (A) Strain BW25113Δ*bamB*/pMJ3 was grown in the presence of increasing concentrations of NTZ and induced for expression of His-tagged PapC usher. OM fractions isolated from the bacteria were subjected to denaturing SDS-PAGE and Coomassie staining to observe PapC and the major OM protein constituents (top panel). Samples were also probed with anti-His antibody to visualize PapC (bottom panel). WT BW25113 containing vector only (pMON6235Δcat) or PapC (pMJ3) served as negative and positive controls for PapC expression respectively. (B) Quantitation of PapC levels in the OM of the BW25113Δ*bamB* mutant. PapC levels were measured by densitometry of the anti-His blot in (A), and percent PapC levels were calculated relative to 0 μg/ml NTZ. Bars represent means ± SEM from three independent experiments.

FIGURE 4.2

FIGURE 4.3 Analysis of PapC usher folding in the OM of a Δ*bamB* mutant. (A) Strains BW25113/pMJ3 and BW25113Δ*bamB*/pMJ3 were grown in the presence of increasing concentrations of NTZ and induced for expression of the His-tagged PapC usher. OM fractions isolated from the bacteria were incubated in SDS sample buffer at 25°C, subjected to SDS-PAGE, and probed with anti-His antibody to visualize PapC. Positions of the folded (F) and unfolded (U) PapC species are indicated on the right of each gel image. (B) Comparison of PapC folding in OM fractions isolated from strains BW25113/pMJ3, BW25113Δ*bamB*/pMJ3, and BW25113Δ*bamB*/pMJ3 complemented with pBamB. The bacteria were grown in the absence of NTZ (vehicle only control).

FIGURE 4.3

A

WT   ΔbamB

0   0   10   20   NTZ µg/ml

25°C   U   F

B

WT   ΔbamB   ΔbamB + pBamB

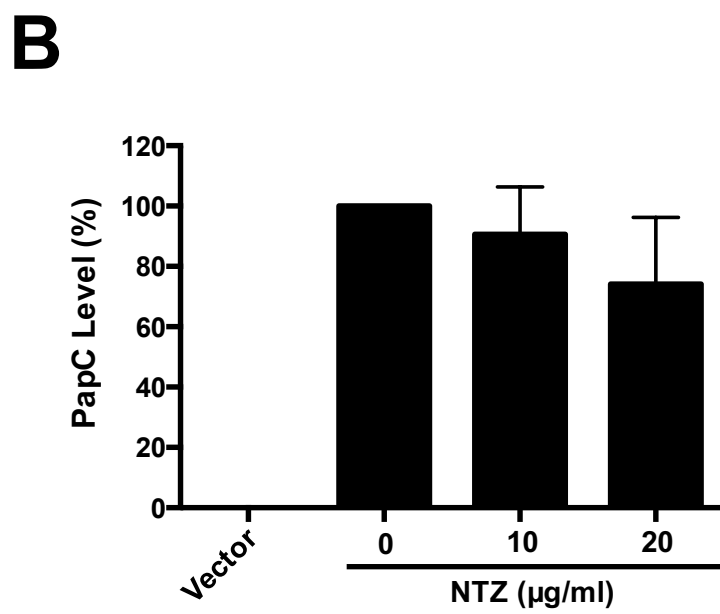25°C   U   F
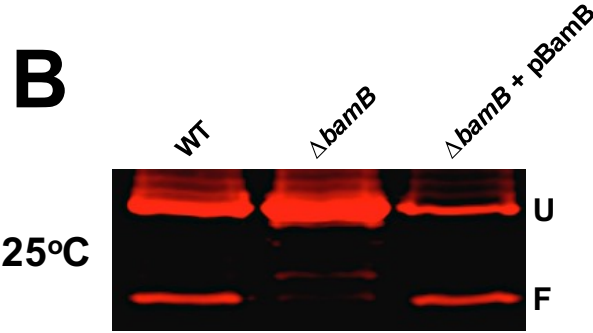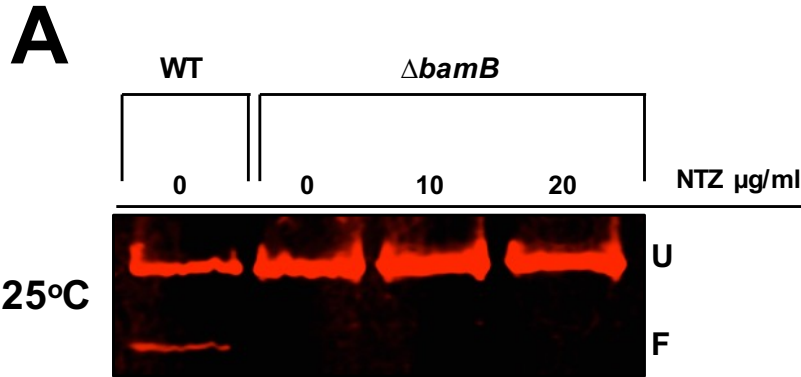
FIGURE 4.4 Effect of NTZ on OM PapC usher levels in a Δ*bamC* mutant. (A) Strain BW25113Δ*bamC*/pMJ3 was grown in the presence of increasing concentrations of NTZ and induced for expression of His-tagged PapC usher. OM fractions isolated from the bacteria were subjected to denaturing SDS-PAGE and Coomassie staining to observe PapC and the major OM protein constituents (top panel). Samples were also probed with anti-His antibody to visualize PapC (bottom panel). WT BW25113 containing vector only (pMON6235Δcat) or PapC (pMJ3) served as negative and positive controls for PapC expression respectively. (B) Quantitation of PapC levels in the OM of the BW25113Δ*bamC* mutant. PapC levels were measured by densitometry of the anti-His blot in (A), and percent PapC levels were calculated relative to 0 μg/ml NTZ. Bars represent means ± SEM from three independent experiments. ****, $P < 0.0001$ for comparison with 0 μg/ml NTZ.
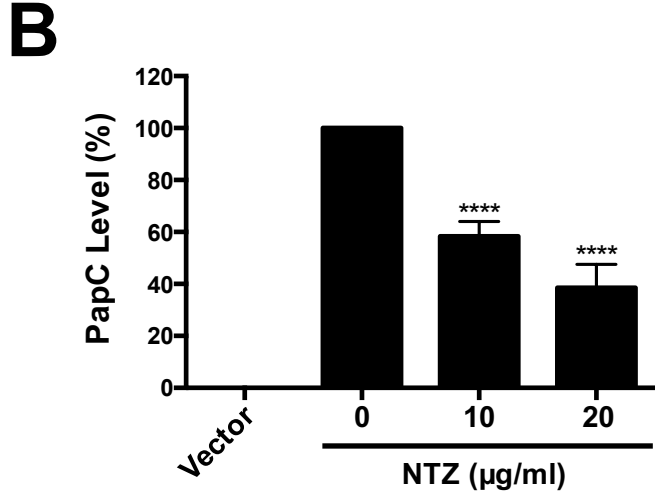
FIGURE 4.4

FIGURE 4.5 Effect of NTZ on OM PapC usher levels in a Δ*bamE* mutant. (A) Strain BW25113Δ*bamE*/pMJ3 was grown in the presence of increasing concentrations of NTZ and induced for expression of His-tagged PapC usher. OM fractions isolated from the bacteria were subjected to denaturing SDS-PAGE and Coomassie staining to observe PapC and the major OM protein constituents (top panel). Samples were also probed with anti-His antibody to visualize PapC (bottom panel). WT BW25113 containing vector only (pMON6235Δcat) or PapC (pMJ3) served as negative and positive controls for PapC expression respectively. (B) Quantitation of PapC levels in the OM of the BW25113Δ*bamE* mutant. PapC levels were measured by densitometry of the anti-His blot in (A), and percent PapC levels were calculated relative to 0 μg/ml NTZ. Bars represent means ± SEM from three independent experiments.
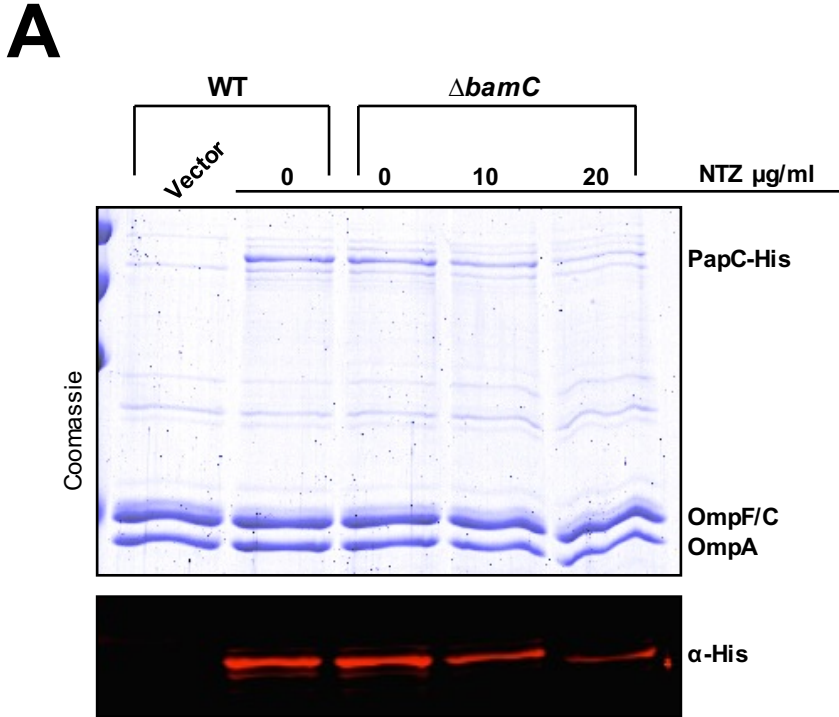
FIGURE 4.5

FIGURE 4.6 Analysis of PapC usher folding in the OM of a Δ*bamE* mutant. (A) Strains BW25113/pMJ3 and BW25113Δ*bamE*/pMJ3 were grown in the presence of increasing concentrations of NTZ and induced for expression of the His-tagged PapC usher. OM fractions isolated from the bacteria were incubated in SDS sample buffer at 25°C, subjected to SDS-PAGE, and probed with anti-His antibody to visualize PapC. Positions of the folded (F) and unfolded (U) PapC species are indicated on the right of each gel image. (B) Comparison of PapC folding in OM fractions isolated from strains BW25113/pMJ3, BW25113Δ*bamE*/pMJ3, and BW25113Δ*bamE*/pMJ3 complemented with pBamE. The bacteria were grown in the absence of NTZ (vehicle only control).

FIGURE 4.6

FIGURE 4.7 Effect of NTZ on OM PapC usher levels when the Bam complex is over-expressed. Strain BW25113 transformed with pMJ3 (A), or both pMJ3 and pBamABCDE (B), was grown in the presence of increasing concentrations of NTZ and induced for expression of the His-tagged PapC usher. Expression of the Bam complex was also induced in (B). OM fractions isolated from the bacteria were subjected to SDS-PAGE and Coomassie staining to observe PapC and the major OM protein constituents (top panels). Samples were also probed with anti-His antibody to visualize PapC (middle panels) and anti-BamA antibody to visualize BamA (middle panel B). Samples were also incubated in SDS sample buffer at 25°C, subjected to SDS-PAGE, and probed with anti-His antibody to visualize the folding status of PapC (bottom panels). Positions of the folded (F) and unfolded (U) PapC species are indicated on the right of each gel image. *E. coli* containing vector only (pMON6235Δcat) served as a negative control for PapC expression in (A) while *E. coli* transformed with the pMON6235Δcat or pMJ3 only served as negative and positive controls respectively in (B). (C) Quantitation of PapC levels in the OM. PapC levels were measured by densitometry of the anti-His blot found in the middle panels of both (A and B), and percent PapC levels were calculated relative to 0 μg/ml NTZ. Bars represent means ± SEM from three independent expe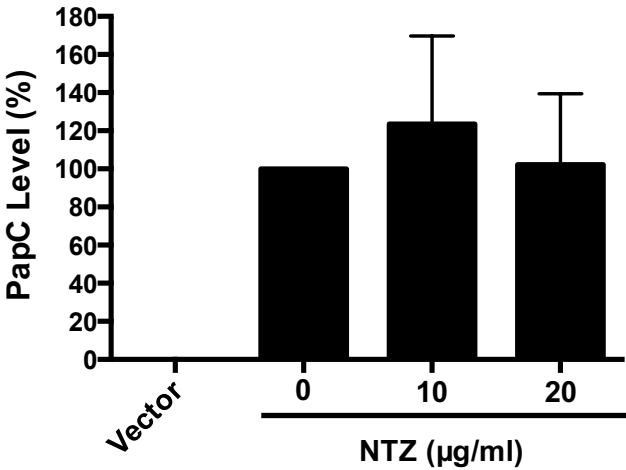riments. *, $P < 0.05$; ***, $P < 0.001$ for comparison of PapC in (A) to PapC co-expressed with the Bam complex in (B) at each NTZ concentration.
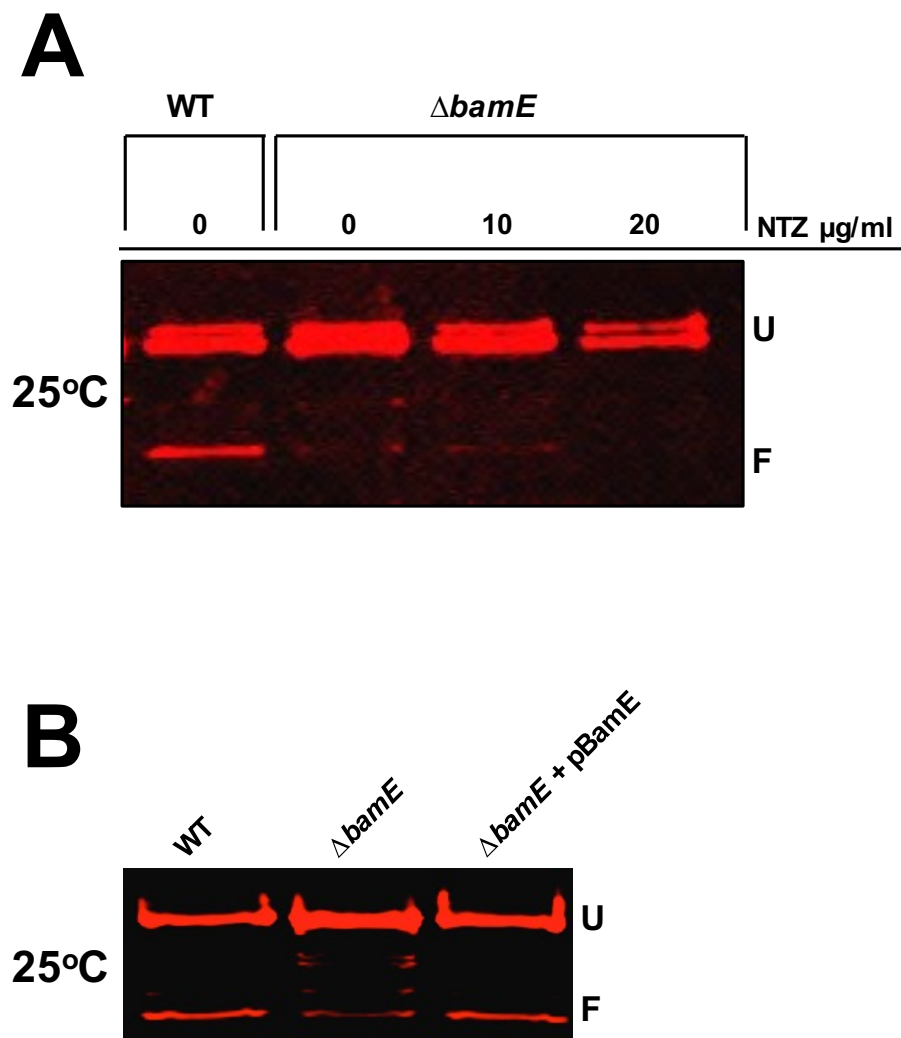
FIGURE 4.7
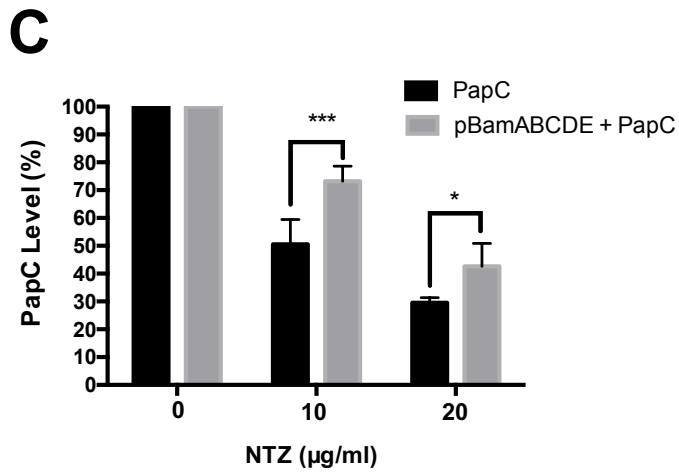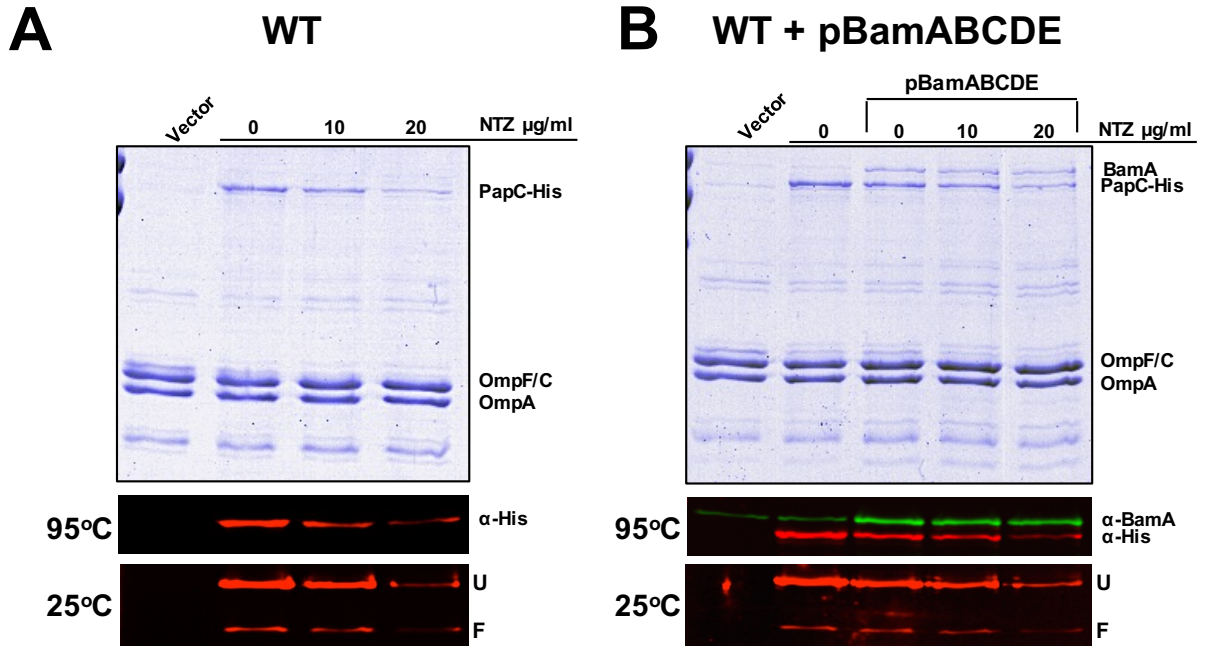
FIGURE 4.8 Effect of NTZ on OM PapC usher levels in a *bamA101* mutant. Strains MC4100 (A) and MC4100*bamA101* (B) transformed with pMJ3 were grown in the presence of increasing concentrations of NTZ and induced for expression of the His-tagged PapC usher. OM fractions isolated from the bacteria were subjected to SDS-PAGE and Coomassie staining to observe PapC and the major OM protein constituents (top panels). Samples were also probed with anti-His antibody to visualize PapC and anti-BamA antibody to visualize BamA (middle panels). Samples were also incubated in SDS sample buffer at 25°C, subjected to SDS-PAGE, and probed with anti-His antibody to visualize the folding status of PapC (bottom panels). Positions of the folded (F) and unfolded (U) PapC species are indicated on the right of each gel image. *E. coli* containing vector only (pMON6235Δcat) served as a negative control for PapC expression in (A) while *E. coli* transformed with the pMON6235Δcat or pMJ3 only served as negative and positive controls respectively in (B). (C) Quantitation of PapC levels in the OM. PapC levels were measured by densitometry of the anti-His blot found in the middle panels of both (A and B), and percent PapC levels were calculated relative to 0 μg/ml NTZ. Bars represent means ± SEM from three independent experiments. *****, $P < 0.001$ for comparison of PapC in (A) to PapC expressed in the MC4100*bamA101* background (B) at each NTZ concentration.

FIGURE 4.8
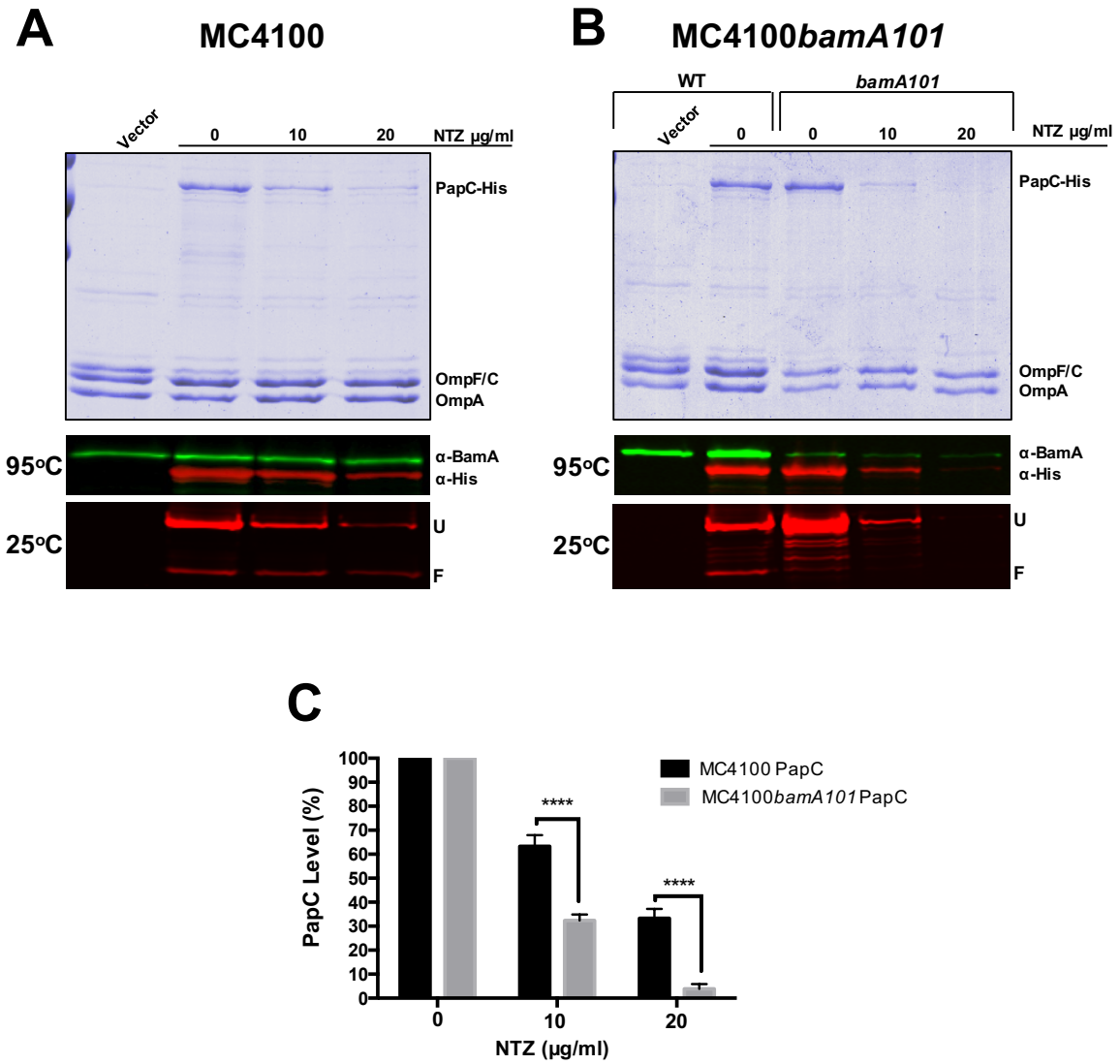
FIGURE 4.9 Effect of NTZ on OM PapC usher levels when *bamA* is complemented in a *bamA101* mutant. (A) Strain MC4100*bamA101* transformed with both pMJ3 and pBamA was grown in the presence of increasing concentrations of NTZ and induced for expression of the His-tagged PapC usher. Leaky expression of plasmid pBamA was used to induce BamA. OM fractions isolated from the bacteria were subjected to SDS-PAGE and Coomassie staining to observe PapC and the major OM protein constituents (top panel). Samples were also probed with anti-His antibody to visualize PapC and anti-BamA antibody to visualize BamA (middle panel). Samples were also incubated in SDS sample buffer at 25°C, subjected to SDS-PAGE, and probed with anti-His antibody to visualize the folding status of PapC (bottom panel). Positions of the folded (F) and unfolded (U) PapC species are indicated on the right of each gel image. *E. coli* transformed with the pMON6235Δcat or pMJ3 only served as negative and positive controls respectively. (B) Quantitation of PapC levels in the OM. PapC levels were measured by densitometry of the anti-His blot found in the middle panel of (A), and percent PapC levels were calculated relative to 0 µg/ml NTZ. PapC levels in the MC4100*bamA101*/pMJ3 + pBamA strain were compared with PapC levels in the MC4100*bamA101*/pMJ3 strain described in figure 4.8A and C. Bars represent means ± SEM from three independent experiments. **, $P < 0.01$; ***, $P < 0.001$ for comparison of the two strains at each NTZ concentration.

FIGURE 4.9

A MC4100*bamA101* + pBamA
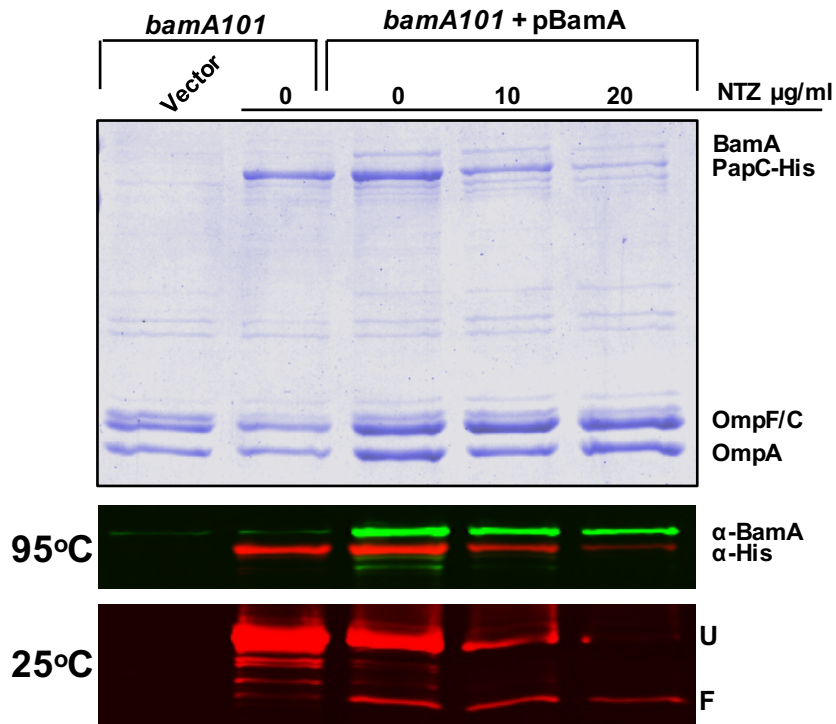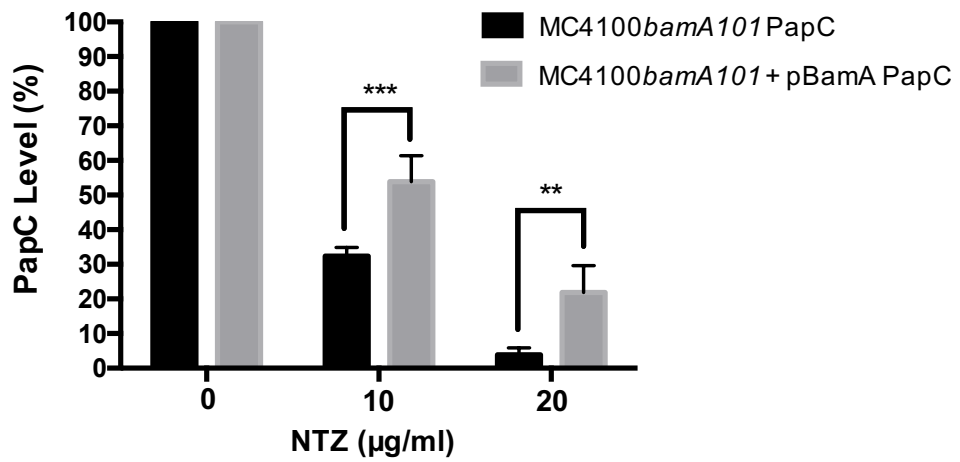
CHAPTER 5

Conclusions and Future Directions

5.1 Conclusions

Increasing rates of antibiotic resistance are challenging the status quo and raising the possibility of a post-antibiotic era, in which even common infections could become life threatening (3). This looming health crisis highlights the immediate need for new and effective therapies, which not only neutralize bacterial pathogens but also limit the development of resistance. A class of therapeutic agents gaining in popularity due to their proposed mechanisms of action are anti-virulence compounds. These molecules selectively target virulence factors utilized by bacterial pathogens to establish disease in the host without interfering with essential processes required for viability. As a result, these compounds are theorized to limit some of the selective pressures that drive the development of resistance (191-195).

Adhesive pili are required by many pathogens to adhere to and colonize host tissues. P and type 1 pili of UPEC are prototypical examples of pili assembled by the CU pathway, and are critical to the establishment of UTIs (13, 92). The key role of pili in promoting pathogenesis has deemed them attractive targets for therapeutic development. While a number of anti-pilus compounds are currently under investigation, including a class of molecules termed pilicides that inhibit the assembly of CU pili, none has entered into clinical development. Moreover, current pilicides are narrow in spectrum, only targeting individual classes of CU pili (195). An effective pilus inhibitor should possess broad spectrum activity and have a proven safety record in humans.

The FDA approved drug nitazoxanide has been widely used for the treatment of intestinal infections caused by *Giardia* and *Cryptosporidium* (203). While NTZ demonstrates pleiotropic effects against a number of organisms, enterobacteriaceae are considered generally resistant to the drug (210, 212). However, studies have identified a potential new use for the compound, as it

117

has been shown to inhibit biofilm formation and prevent the assembly of CU pili on the surface of EAEC (213). It is this potentially novel and uncharacterized mechanism of pilus inhibition that I chose to pursue as the focus of my thesis work.

I first was able to extend the inhibitory effects of NTZ to both P and type 1 pili of UPEC, demonstrating that NTZ is an inhibitor of CU pilus function with activity against a diverse set of CU pilus systems. Next, using a process of elimination, I dissected the various stages of the CU pathway to identify the step at which NTZ exerts its effect. My data shows that chaperone-subunit complex formation in the periplasm, as well as the ability of these complexes to interact with the OM usher protein, are unaffected by the drug. However, there is a specific and dose-dependent loss of the usher protein in the OM when NTZ is present. Analysis of the domains of the usher identified its large transmembrane ß-barrel domain as the site associated with NTZ's activity. Additionally, analysis of a Δ*degP* mutant allowed me to distinguish the effects of the drug on both the folded and unfolded species of the usher, showing a distinct effect on the folded form. These data allow me to conclude that NTZ inhibits CU pilus assembly by preventing maturation of the usher protein in the OM, leading to its degradation and thereby decreasing the pool of available functional ushers to assemble pili. Furthermore, I can now classify NTZ as a pilicide with a novel mechanism of action that is distinct from previously described pilicides.

To develop a more potent inhibitor of pilus biogenesis and to further understand the mechanics of usher folding in the OM, I sought to gain insight into the direct target of NTZ. Previously published work had identified the Bam complex as a necessary component required for usher maturation (186). To determine if NTZ was altering the functionality of the Bam complex, I examined the affect the drug on usher levels, folded state, and functionality in the background of Δ*bamB*, Δ*bamC*, and Δ*bamE* mutations. Two of these mutations, Δ*bamB* and

Δ*bamE*, rendered the usher resistant to NTZ, although both mutant strains appeared to be incapable of properly folding the usher. When the mutants were tested for their ability to assemble functional pili, the Δ*bamB* mutant was unable to agglutinate red blood cells, while the Δ*bamE* mutant retained pilus function. This suggests that the usher in the Δ*bamE* mutant is folded, but in an altered form with decreased stability. The results from these mutant studies assign distinct roles for BamB and BamE in the folding of the usher, with BamB essential for folding and BamE required for optimal folding. To our knowledge, these phenotypes are the most dramatic to be described to date for *bamB* and *bamE* mutants. Additionally, the insensitivity of the usher to NTZ in the *bam* mutant backgrounds provides the first line of evidence that the drug may act by altering the functionality of the Bam complex.

To begin to explore the possibility of one or more components of the Bam complex as the target of NTZ, I employed both over- and under-expression techniques to determine if I could modulate sensitivity to the drug. Using a plasmid that over-expresses the entire Bam complex, I was able to generate decreased sensitivity to the drug, as indicated by increased usher levels in the OM when compared to the WT background. To test under-expression of the Bam complex, I obtained a *bamA* promoter mutant, *bamA101*, which greatly reduces the level of BamA in the cell and thus overall Bam complex formation, without altering expression of the other Bam lipoproteins (181, 259). In the presence of NTZ, usher expressed in the *bamA101* strain displayed dramatically increased sensitivity to the drug when compared to WT. To complement the *bamA*101 mutant, a *bamA* expression plasmid was introduced, which restored usher sensitivity to NTZ back to near WT levels. These experiments provide strong genetic evidence to implicate the Bam complex as the target of NTZ. If the Bam complex is indeed is the target of NTZ, then the drug would then be inhibiting a previously uncharacterized functionality that is

not essential for cell survival but essential for usher biogenesis, thus making it an attractive target for anti-virulence development. Additionally, the study of OM protein biogenesis has proven to be quite difficult given the few genetic, biochemical, and biophysical tools available to explore this aspect of Gram-negative physiology. NTZ would be the first described inhibitor of the Bam complex, providing a chemical means of exploring Bam functionality and the biogenesis of OM proteins. Given that I have yet to obtain any evidence to disprove my original hypothesis, I plan to continue to testing if *NTZ inhibits pilus biogenesis by targeting the machinery required for assembly of the usher protein in the OM.*

5.2 Future directions

The primary goal of this work has been to identify the mechanism of pilus inhibition by NTZ, and to identify the drug's direct target. Having met the first milestone, future experiments will continue to build on the data obtained with the Bam complex to isolate and characterize the direct target as a means to design an inhibitor with enhanced properties. To begin, work is currently under way using over-expression studies of the individual Bam components, as well as sub-complexes of the Bam system, to help narrow target candidates. Once a target is in hand, further genetic studies can be employed, such as suppressor screens, to identify residues that are critical to meditate the effect of the drug.

The use of NTZ as a chemical tool to understand the function of Bam complex as it relates to OM protein biogenesis could provide important new information to broaden our understating of Gram-negative physiology. To understand the mechanistic features of the Bam complex in detail and its interaction with the usher, an *in vitro* system could be employed to examine the complex within an isolated and controlled environment. To achieve this, efforts are

currently underway to reconstitute the Bam complex into lipid nanodiscs. Previously reported work has shown that denatured OMP substrates in combination with SurA can be assembled into the nanodisc bilayer via the reconstituted Bam complex (222). The ability of denatured usher protein to assemble into these nanodiscs would be analyzed in the presence and absence of NTZ and in the context of various Bam complex permutations in which one of more of the components is missing i.e. BamABCD, BamACDE, and BamABD. Additionally, this system could serve as a means to screen NTZ analogues for increase potency. Such an experimental approach will also allow us to study previously uncharacterized aspects of the usher.

To conclusively identify the NTZ target, we need to demonstrate direct binding between the drug and target. Several approaches can be used to measure binding. One technique utilizes a differential radial capillary action of ligand assay (DRaCALA). DRaCALA is a simple and rapid assay to detect binding between a protein and a radiolabeled small molecule, which takes advantage of the ability of protein to be immobilized on a hydrophobic membrane such as nitrocellulose (262). In short, a target candidate would be purified and incubated with a radiolabeled inhibitor. This mixture is then spotted onto a hydrophobic membrane, immobilizing the protein, and the diffusion rate of the inhibitor away from the immobilization site is quantitated. This would also provide a means to assess binding kinetics between the drug and the target. An alternative method could be a spectrophotometric assay that takes advantage of the spectral properties of NTZ. NTZ in solution absorbs at 418 nm and in acidic environments undergoes a shift in absorption to 351 nm (209). Our collaborator, Dr. Paul Hoffman at the University of Virginia, used these spectral properties to measure binding of NTZ to its PFOR target in anaerobic bacteria (209). We can monitor NTZ absorption during titration of increasing amounts of a putative target protein using NTZ-specific shifts in absorption as an indicator of

binding. Once a target is identified, alanine scanning mutagenesis of the target in conjunction with NTZ can be used to identify and characterize the drug's direct binding site. Such studies will be critical to identify the precise mechanism of action for the drug as well as aid in the design of NTZ analogues.

Perhaps the most useful piece of data we could obtain would be a co-crystal structure of NTZ bound to its target. Crystal structures of all the individual Bam components are currently available (169, 177, 180, 182, 263), in addition to complexes of BamD bound to BamC (264) and BamB bound to the POTRA domains of BamA (265). We will attempt to acquire X-ray crystallography data for NTZ bound to its target. As an alternative, *in silico* modeling can be used to identify putative NTZ binding sites. Once a structure is in hand, structure activity relationships can be identified and medicinal chemistry utilized for rational drug design, using NTZ as a scaffold to develop inhibitors with enhanced features. The availability of new and more potent compounds will then allow us to test their effectiveness in murine disease models, such as an ascending UTI model. Given that CU pili are utilized by many Gram-negative bacteria to establish disease, future studies could also investigate the effectiveness of these compounds against other clinically relevant bacteria, including *Klebsiella pneumonia*, *Pseudomonas aeruginosa*, and *Acinetobacter baumannii,* to name a few.

REFERENCES

1. **McDermott W, Rogers DE.** 1982. Social ramifications of control of microbial disease. The Johns Hopkins medical journal **151:**302-312.
2. **Lax E.** 2004. The mold in Dr. Florey's coat : the story of the penicillin miracle, 1st ed. H. Holt, New York.
3. **The Review on Antimicrobial Resistance Chaired by Jim O'Neil.** December 2014. Antimicrobial Resistance: Tackling drug-resistant infections globaly.
4. **World Health Organization.** 2014. Antimcribial resistance: global report on surveillance.
5. **Temkin E, Adler A, Lerner A, Carmeli Y.** 2014. Carbapenem-resistant Enterobacteriaceae: biology, epidemiology, and management. Annals of the New York Academy of Sciences **1323:**22-42.
6. **Centers for Disease Control and Prevention.** 2013. Antibiotic Resistance Threats in the United States, 2013.
7. **Patel G, Huprikar S, Factor SH, Jenkins SG, Calfee DP.** 2008. Outcomes of carbapenem-resistant Klebsiella pneumoniae infection and the impact of antimicrobial and adjunctive therapies. Infection control and hospital epidemiology **29:**1099-1106.
8. **Dielubanza EJ, Schaeffer AJ.** 2011. Urinary tract infections in women. The Medical clinics of North America **95:**27-41.
9. **Foxman B.** 2010. The epidemiology of urinary tract infection. Nature reviews. Urology **7:**653-660.
10. **Foxman B, Barlow R, D'Arcy H, Gillespie B, Sobel JD.** 2000. Urinary tract infection: self-reported incidence and associated costs. Annals of epidemiology **10:**509-515.
11. **Schappert SM, Rechtsteiner EA.** 2011. Ambulatory medical care utilization estimates for 2007. Vital and health statistics. Series 13, Data from the National Health Survey**:**1-38.
12. **Foxman B.** 2014. Urinary tract infection syndromes: occurrence, recurrence, bacteriology, risk factors, and disease burden. Infectious disease clinics of North America **28:**1-13.
13. **Flores-Mireles AL, Walker JN, Caparon M, Hultgren SJ.** 2015. Urinary tract infections: epidemiology, mechanisms of infection and treatment options. Nature reviews. Microbiology **13:**269-284.
14. **Kaper JB, Nataro JP, Mobley HL.** 2004. Pathogenic Escherichia coli. Nature reviews. Microbiology **2:**123-140.
15. **Jacobsen SM, Stickler DJ, Mobley HLT, Shirtliff ME.** 2008. Complicated catheter-associated urinary tract infections due to Escherichia coli and Proteus mirabilis. Clin Microbiol Rev **21:**26-+.
16. **Bent S, Nallamothu BK, Simel DL, Fihn SD, Saint S.** 2002. Does this woman have an acute uncomplicated urinary tract infection? Jama-J Am Med Assoc **287:**2701-2710.
17. **Giesen LGM, Cousins G, Dimitrov BD, van de Laar FA, Fahey T.** 2010. Predicting acute uncomplicated urinary tract infection in women: a systematic review of the diagnostic accuracy of symptoms and signs. Bmc Fam Pract **11**.
18. **Silverman JA, Schreiber HLt, Hooton TM, Hultgren SJ.** 2013. From physiology to pharmacy: developments in the pathogenesis and treatment of recurrent urinary tract infections. Current urology reports **14:**448-456.
19. **Podschun R, Ullmann U.** 1998. Klebsiella spp. as nosocomial pathogens: Epidemiology, taxonomy, typing methods, and pathogenicity factors. Clin Microbiol Rev **11:**589-+.

20. **Pizarro-Cerda J, Cossart P.** 2006. Bacterial adhesion and entry into host cells. Cell **124:**715-727.

21. **Kline KA, Falker S, Dahlberg S, Normark S, Henriques-Normark B.** 2009. Bacterial adhesins in host-microbe interactions. Cell host & microbe **5:**580-592.

22. **Johnson JR.** 1991. Virulence factors in *Escherichia coli* urinary tract infection. Clin. Microbiol. Rev. **4:**80-128.

23. **Hull RA, Gill RE, Hsu P, Minshaw BH, Falkow S.** 1981. Construction and expression of recombinant plasmids encoding type 1 and D-mannose-resistant pili from a urinary tract infection *Escherichia coli* isolate. Infect. Immun. **33:**933-938.

24. **Hacker J, Schmidt G, Hughes C, Knapp S, Marget M, Goebel W.** 1985. Cloning and characterization of genes involved in production of mannose-resistant neuraminidase-susceptible (X) fimbriae from a uropathogenic 06:K15:H31 *Escherichia coli* strain. Infect. Immun. **47:**434-440.

25. **Nuccio SP, Baumler AJ.** 2007. Evolution of the chaperone/usher assembly pathway: fimbrial classification goes Greek. Microbiology and molecular biology reviews : MMBR **71:**551-575.

26. **Zav'yalov V, Zavialov A, Zav'yalova G, Korpela T.** 2010. Adhesive organelles of Gram-negative pathogens assembled with the classical chaperone/usher machinery: structure and function from a clinical standpoint. FEMS microbiology reviews **34:**317-378.

27. **Waksman G, Hultgren SJ.** 2009. Structural biology of the chaperone-usher pathway of pilus biogenesis. Nature reviews. Microbiology **7:**765-774.

28. **Thanassi DG, Bliska JB, Christie PJ.** 2012. Surface organelles assembled by secretion systems of Gram-negative bacteria: diversity in structure and function. FEMS microbiology reviews **36:**1046-1082.

29. **Miller E, Garcia T, Hultgren S, Oberhauser AF.** 2006. The mechanical properties of E. coli type 1 pili measured by atomic force microscopy techniques. Biophys J **91:**3848-3856.

30. **Fallman E, Schedin S, Jass J, Uhlin BE, Axner O.** 2005. The unfolding of the P pili quaternary structure by stretching is reversible, not plastic. Embo Rep **6:**52-56.

31. **Thomas WE, Trintchina E, Forero M, Vogel V, Sokurenko EV.** 2002. Bacterial adhesion to target cells enhanced by shear force. Cell **109:**913-923.

32. **Castelain M, Ehlers S, Klinth J, Lindberg S, Andersson M, Uhlin BE, Axner O.** 2011. Fast uncoiling kinetics of F1C pili expressed by uropathogenic *Escherichia coli* are revealed on a single pilus level using force-measuring optical tweezers. European biophysics journal : EBJ **40:**305-316.

33. **Martinez JJ, Mulvey MA, Schilling JD, Pinkner JS, Hultgren SJ.** 2000. Type 1 pilus-mediated bacterial invasion of bladder epithelial cells. The EMBO journal **19:**2803-2812.

34. **Mulvey MA, Lopez-Boado YS, Wilson CL, Roth R, Parks WC, Heuser J, Hultgren SJ.** 1998. Induction and evasion of host defenses by type 1-piliated uropathogenic Escherichia coli. Science **282:**1494-1497.

35. **Eto DS, Jones TA, Sundsbak JL, Mulvey MA.** 2007. Integrin-mediated host cell invasion by type 1-piliated uropathogenic *Escherichia coli*. PLoS pathogens **3:**e100.

36. **Wright KJ, Seed PC, Hultgren SJ.** 2007. Development of intracellular bacterial communities of uropathogenic *Escherichia coli* depends on type 1 pili. Cell Microbiol **9:**2230-2241.

37. **Mossman KL, Mian MF, Lauzon NM, Gyles CL, Lichty B, Mackenzie R, Gill N, Ashkar AA.** 2008. Cutting edge: FimH adhesin of type 1 fimbriae is a novel TLR4 ligand. J. Immunol. **181:**6702-6706.

38. **Bergsten G, Samuelsson M, Wullt B, Leijonhufvud I, Fischer H, Svanborg C.** 2004. PapG-dependent adherence breaks mucosal inertia and triggers the innate host response. J. Infect. Dis. **189:**1734-1742.

39. **Plancon L, Du Merle L, Le Friec S, Gounon P, Jouve M, Guignot J, Servin A, Le Bouguenec C.** 2003. Recognition of the cellular beta1-chain integrin by the bacterial AfaD invasin is implicated in the internalization of *afa*-expressing pathogenic *Escherichia coli* strains. Cellular microbiology **5:**681-693.

40. **Oelschlaeger TA, Dobrindt U, Hacker J.** 2002. Pathogenicity islands of uropathogenic E. coli and the evolution of virulence. International journal of antimicrobial agents **19:**517-521.

41. **van der Velden AW, Baumler AJ, Tsolis RM, Heffron F.** 1998. Multiple fimbrial adhesins are required for full virulence of *Salmonella typhimurium* in mice. Infection and immunity **66:**2803-2808.

42. **Korea CG, Badouraly R, Prevost MC, Ghigo JM, Beloin C.** 2010. *Escherichia coli* K-12 possesses multiple cryptic but functional chaperone-usher fimbriae with distinct surface specificities. Environ. Microbiol. **12:**1957-1977.

43. **Hatkoff M, Runco LM, Pujol C, Jayatilaka I, Furie MB, Bliska JB, Thanassi DG.** 2012. Roles of chaperone/usher pathways of *Yersinia pestis* in a murine model of plague and adhesion to host cells. Infect. Immun. **80:**3490-3500.

44. **Wurpel DJ, Beatson SA, Totsika M, Petty NK, Schembri MA.** 2013. Chaperone-Usher Fimbriae of *Escherichia coli*. PloS one **8:**e52835.

45. **Blomfield IC.** 2001. The regulation of pap and type 1 fimbriation in Escherichia coli. Adv Microb Physiol **45:**1-49.

46. **van der Woude M, Braaten B, Low D.** 1996. Epigenetic phase variation of the pap operon in Escherichia coli. Trends Microbiol **4:**5-9.

47. **Xia Y, Gally D, Forsman-Semb K, Uhlin BE.** 2000. Regulatory cross-talk between adhesin operons in *Escherichia coli*: inhibition of type 1 fimbriae expression by the PapB operon. EMBO J. **19:**1450-1457.

48. **Totsika M, Kostakioti M, Hannan TJ, Upton M, Beatson SA, Janetka JW, Hultgren SJ, Schembri MA.** 2013. A FimH inhibitor prevents acute bladder infection and treats chronic cystitis caused by multidrug-resistant uropathogenic Escherichia coli ST131. The Journal of infectious diseases **208:**921-928.

49. **Snyder JA, Haugen BJ, Lockatell CV, Maroncle N, Hagan EC, Johnson DE, Welch RA, Mobley HL.** 2005. Coordinate expression of fimbriae in uropathogenic *Escherichia coli*. Infect. Immun. **73:**7588-7596.

50. **Lane MC, Simms AN, Mobley HL.** 2007. complex interplay between type 1 fimbrial expression and flagellum-mediated motility of uropathogenic *Escherichia coli*. J. Bacteriol. **189:**5523-5533.

51. **Servin AL.** 2005. Pathogenesis of Afa/Dr diffusely adhering *Escherichia coli*. Clin. Microbiol. Rev. **18:**264-292.

52. **Choudhury D, Thompson A, Stojanoff V, Langermann S, Pinkner J, Hultgren SJ, Knight SD.** 1999. X-ray structure of the FimC-FimH chaperone-adhesin complex from uropathogenic Escherichia coli. Science **285:**1061-1066.

53. **Sauer FG, Futterer K, Pinkner JS, Dodson KW, Hultgren SJ, Waksman G.** 1999. Structural basis of chaperone function and pilus biogenesis. Science **285:**1058-1061.
54. **Sauer FG, Pinkner JS, Waksman G, Hultgren SJ.** 2002. Chaperone priming of pilus subunits facilitates a topological transition that drives fiber formation. Cell **111:**543-551.
55. **Zavialov AV, Berglund J, Pudney AF, Fooks LJ, Ibrahim TM, MacIntyre S, Knight SD.** 2003. Structure and biogenesis of the capsular F1 antigen from Yersinia pestis: preserved folding energy drives fiber formation. Cell **113:**587-596.
56. **Phan G, Remaut H, Wang T, Allen WJ, Pirker KF, Lebedev A, Henderson NS, Geibel S, Volkan E, Yan J, Kunze MB, Pinkner JS, Ford B, Kay CW, Li H, Hultgren SJ, Thanassi DG, Waksman G.** 2011. Crystal structure of the FimD usher bound to its cognate FimC-FimH substrate. Nature **474:**49-53.
57. **Anderson KL, Billington J, Pettigrew D, Cota E, Simpson P, Roversi P, Chen HA, Urvil P, du Merle L, Barlow PN, Medof ME, Smith RA, Nowicki B, Le Bouguenec C, Lea SM, Matthews S.** 2004. An atomic resolution model for assembly, architecture, and function of the Dr adhesins. Mol Cell **15:**647-657.
58. **Bork P, Holm L, Sander C.** 1994. The immunoglobulin fold. Structural classification, sequence patterns and common core. Journal of molecular biology **242:**309-320.
59. **Henderson NS, Ng TW, Talukder I, Thanassi DG.** 2011. Function of the usher N-terminus in catalysing pilus assembly. Mol Microbiol **79:**954-967.
60. **Puorger C, Eidam O, Capitani G, Erilov D, Grutter MG, Glockshuber R.** 2008. Infinite kinetic stability against dissociation of supramolecular protein complexes through donor strand complementation. Structure **16:**631-642.
61. **Bullitt E, Makowski L.** 1995. Structural polymorphism of bacterial adhesion pili. Nature **373:**164-167.
62. **Pettigrew D, Anderson KL, Billington J, Cota E, Simpson P, Urvil P, Rabuzin F, Roversi P, Nowicki B, du Merle L, Le Bouguenec C, Matthews S, Lea SM.** 2004. High resolution studies of the Afa/Dr adhesin DraE and its interaction with chloramphenicol. J. Biol. Chem. **279:**46851-46857.
63. **Korotkova N, Le Trong I, Samudrala R, Korotkov K, Van Loy CP, Bui AL, Moseley SL, Stenkamp RE.** 2006. Crystal structure and mutational analysis of the DaaE adhesin of *Escherichia coli*. The Journal of biological chemistry **281:**22367-22377.
64. **Zavialov A, Zav'yalova G, Korpela T, Zav'yalov V.** 2007. FGL chaperone-assembled fimbrial polyadhesins: anti-immune armament of Gram-negative bacterial pathogens. FEMS microbiology reviews **31:**478-514.
65. **Dodson KW, Pinkner JS, Rose T, Magnusson G, Hultgren SJ, Waksman G.** 2001. Structural basis of the interaction of the pyelonephritic E. coli adhesin to its human kidney receptor. Cell **105:**733-743.
66. **Hung CS, Bouckaert J, Hung D, Pinkner J, Widberg C, DeFusco A, Auguste CG, Strouse R, Langermann S, Waksman G, Hultgren SJ.** 2002. Structural basis of tropism of Escherichia coli to the bladder during urinary tract infection. Mol. Microbiol. **44:**903-915.
67. **Sung MA, Fleming K, Chen HA, Matthews S.** 2001. The solution structure of PapGII from uropathogenic Escherichia coli and its recognition of glycolipid receptors. Embo Rep **2:**621-627.
68. **Buts L, Bouckaert J, De Genst E, Loris R, Oscarson S, Lahmann M, Messens J, Brosens E, Wyns L, De Greve H.** 2003. The fimbrial adhesin F17-G of enterotoxigenic

Escherichia coli has an immunoglobulin-like lectin domain that binds N-acetylglucosamine. Mol Microbiol **49:**705-715.

69. **Merckel MC, Tanskanen J, Edelman S, Westerlund-Wikstrom B, Korhonen TK, Goldman A.** 2003. The structural basis of receptor-binding by Escherichia coli associated with diarrhea and septicemia. J Mol Biol **331:**897-905.

70. **Li YF, Poole S, Rasulova F, McVeigh AL, Savarino SJ, Xia D.** 2007. A Receptor-binding Site as Revealed by the Crystal Structure of CfaE, the Colonization Factor Antigen I Fimbrial Adhesin of Enterotoxigenic Escherichia coli. The Journal of biological chemistry **282:**23970-23980.

71. **Westerlund-Wikstrom B, Korhonen TK.** 2005. Molecular structure of adhesin domains in Escherichia coli fimbriae. Int J Med Microbiol **295:**479-486.

72. **Forero M, Yakovenko O, Sokurenko EV, Thomas WE, Vogel V.** 2006. Uncoiling mechanics of Escherichia coli type I fimbriae are optimized for catch bonds. PLoS biology **4:**e298.

73. **Aprikian P, Interlandi G, Kidd BA, Le Trong I, Tchesnokova V, Yakovenko O, Whitfield MJ, Bullitt E, Stenkamp RE, Thomas WE, Sokurenko EV.** 2011. The bacterial fimbrial tip acts as a mechanical force sensor. PLoS Biology **9:**e1000617.

74. **Lycklama ANJA, Driessen AJ.** 2012. The bacterial Sec-translocase: structure and mechanism. Philosophical transactions of the Royal Society of London. Series B, Biological sciences **367:**1016-1028.

75. **Jones CH, Dexter P, Evans AK, Liu C, Hultgren SJ, Hruby DE.** 2002. Escherichia coli DegP protease cleaves between paired hydrophobic residues in a natural substrate: the PapA pilin. J Bacteriol **184:**5762-5771.

76. **Slonim LN, Pinkner JS, Branden CI, Hultgren SJ.** 1992. Interactive surface in the PapD chaperone cleft is conserved in pilus chaperone superfamily and essential in subunit recognition and assembly. EMBO J. **11:**4747-4756.

77. **Holmgren A, Brändén C.** 1989. Crystal structure of chaperone protein PapD reveals an immunoglobulin fold. Nature **342:**248-251.

78. **Kuehn MJ, Ogg DJ, Kihlberg J, Slonim LN, Flemmer K, Bergfors T, Hultgren SJ.** 1993. Structural basis of pilus subunit recognition by the PapD chaperone. Science **262:**1234-1241.

79. **Zavialov AV, Kersley J, Korpela T, Zav'yalov VP, MacIntyre S, Knight SD.** 2002. Donor strand complementation mechanism in the biogenesis of non-pilus systems. Mol Microbiol **45:**983-995.

80. **Barnhart MM, Pinkner JS, Soto GE, Sauer FG, Langermann S, Waksman G, Frieden C, Hultgren SJ.** 2000. PapD-like chaperones provide the missing information for folding of pilin proteins. Proc Natl Acad Sci USA **97:**7709-7714.

81. **Remaut H, Rose RJ, Hannan TJ, Hultgren SJ, Radford SE, Ashcroft AE, Waksman G.** 2006. Donor-strand exchange in chaperone-assisted pilus assembly proceeds through a concerted beta strand displacement mechanism. Mol Cell **22:**831-842.

82. **Yu XD, Fooks LJ, Moslehi-Mohebi E, Tischenko VM, Askarieh G, Knight SD, Macintyre S, Zavialov AV.** 2012. Large is fast, small is tight: determinants of speed and affinity in subunit capture by a periplasmic chaperone. Journal of molecular biology **417:**294-308.

83. **Crespo MD, Puorger C, Scharer MA, Eidam O, Grutter MG, Capitani G, Glockshuber R.** 2012. Quality control of disulfide bond formation in pilus subunits by the chaperone FimC. Nat. Chem. Biol. **8:**707-713.

84. **Di Yu X, Dubnovitsky A, Pudney AF, Macintyre S, Knight SD, Zavialov AV.** 2012. Allosteric mechanism controls traffic in the chaperone/usher pathway. Structure **20:**1861-1871.

85. **Remaut H, Tang C, Henderson NS, Pinkner JS, Wang T, Hultgren SJ, Thanassi DG, Waksman G, Li H.** 2008. Fiber formation across the bacterial outer membrane by the chaperone/usher pathway. Cell **133:**640-652.

86. **Nishiyama M, Ishikawa T, Rechsteiner H, Glockshuber R.** 2008. Reconstitution of pilus assembly reveals a bacterial outer membrane catalyst. Science **320:**376-379.

87. **Soto GE, Dodson KW, Ogg D, Liu C, Heuser J, Knight S, Kihlberg J, Jones CH, Hultgren SJ.** 1998. Periplasmic chaperone recognition motif of subunits mediates quaternary interactions in the pilus. The EMBO journal **17:**6155-6167.

88. **Sauer FG, Remaut H, Hultgren SJ, Waksman G.** 2004. Fiber assembly by the chaperone-usher pathway. Biochimica et biophysica acta **1694:**259-267.

89. **Vetsch M, Erilov D, Moliere N, Nishiyama M, Ignatov O, Glockshuber R.** 2006. Mechanism of fibre assembly through the chaperone-usher pathway. Embo Rep **7:**734-738.

90. **Yu J, Kape JB.** 1992. Cloning and characterization of the *eae* gene of enterohaemorrhaic *Escherichia coli* O157:H7. Mol Microbiol **6:**411-417.

91. **Jacob-Dubuisson F, Striker R, Hultgren SJ.** 1994. Chaperone-assisted self-assembly of pili independent of cellular energy. The Journal of biological chemistry **269:**12447-12455.

92. **Thanassi DG, Stathopoulos C, Karkal A, Li H.** 2005. Protein secretion in the absence of ATP: the autotransporter, two-partner secretion, and chaperone/usher pathways of Gram-negative bacteria. Molec Membr Biol **22:**63-72.

93. **Zavialov AV, Tischenko VM, Fooks LJ, Brandsdal BO, Aqvist J, Zav'yalov VP, Macintyre S, Knight SD.** 2005. Resolving the energy paradox of chaperone/usher-mediated fibre assembly. Biochem J **389:**685-694.

94. **Lee YM, Dodson KW, Hultgren SJ.** 2007. Adaptor function of PapF depends on donor strand exchange in P-pilus biogenesis of Escherichia coli. J Bacteriol **189:**5276-5283.

95. **Rose RJ, Verger D, Daviter T, Remaut H, Paci E, Waksman G, Ashcroft AE, Radford SE.** 2008. Unraveling the molecular basis of subunit specificity in P pilus assembly by mass spectrometry. Proceedings of the National Academy of Sciences of the United States of America **105:**12873-12878.

96. **Nishiyama M, Glockshuber R.** 2010. The outer membrane usher guarantees the formation of functional pili by selectively catalyzing donor-strand exchange between subunits that are adjacent in the mature pilus. Journal of molecular biology **396:**1-8.

97. **Dodson KW, Jacob-Dubuisson F, Striker RT, Hultgren SJ.** 1993. Outer membrane PapC usher discriminately recognizes periplasmic chaperone-pilus subunit complexes. Proceedings of the National Academy of Sciences of the United States of America **90:**3670-3674.

98. **Saulino ET, Thanassi DG, Pinkner JS, Hultgren SJ.** 1998. Ramifications of kinetic partitioning on usher-mediated pilus biogenesis. The EMBO journal **17:**2177-2185.

99.	**Li Q, Ng TW, Dodson KW, So SS, Bayle KM, Pinkner JS, Scarlata S, Hultgren SJ, Thanassi DG.** 2010. The differential affinity of the usher for chaperone-subunit complexes is required for assembly of complete pili. Mol Microbiol **76:**159-172.

100.	**Nishiyama M, Horst R, Eidam O, Herrmann T, Ignatov O, Vetsch M, Bettendorff P, Jelesarov I, Grutter MG, Wuthrich K, Glockshuber R, Capitani G.** 2005. Structural basis of chaperone-subunit complex recognition by the type 1 pilus assembly platform FimD. The EMBO journal **24:**2075-2086.

101.	**Shu Kin So S, Thanassi DG.** 2006. Analysis of the requirements for pilus biogenesis at the outer membrane usher and the function of the usher C-terminus. Mol Microbiol **60:**364-375.

102.	**Mapingire OS, Henderson NS, Duret G, Thanassi DG, Delcour AH.** 2009. Modulating effects of the plug, helix, and N- and C-terminal domains on channel properties of the PapC usher. The Journal of biological chemistry **284:**36324-36333.

103.	**Ford B, Rego AT, Ragan TJ, Pinkner J, Dodson K, Driscoll PC, Hultgren S, Waksman G.** 2010. Structural homology between the C-terminal domain of the PapC usher and its plug. J Bacteriol **192:**1824-1831.

104.	**Huang Y, Smith BS, Chen LX, Baxter RH, Deisenhofer J.** 2009. Insights into pilus assembly and secretion from the structure and functional characterization of usher PapC. Proceedings of the National Academy of Sciences of the United States of America **106:**7403-7407.

105.	**Ng TW, Akman L, Osisami M, Thanassi DG.** 2004. The usher N terminus is the initial targeting site for chaperone-subunit complexes and participates in subsequent pilus biogenesis events. J Bacteriol **186:**5321-5331.

106.	**Li H, Qian L, Chen Z, Thahbot D, Liu G, Liu T, Thanassi DG.** 2004. The outer membrane usher forms a twin-pore secretion complex. J Mol Biol **344:**1397-1407.

107.	**Allen WJ, Phan G, Hultgren SJ, Waksman G.** 2013. Dissection of Pilus Tip Assembly by the FimD Usher Monomer. Journal of molecular biology **425:**958-967.

108.	**Werneburg GT, Henderson NS, Portnoy EB, Sarowar S, Hultgren SJ, Li H, Thanassi DG.** 2015. The pilus usher controls protein interactions via domain masking and is functional as an oligomer. Nat Struct Mol Biol **22:**540-546.

109.	**Munera D, Hultgren S, Fernandez LA.** 2007. Recognition of the N-terminal lectin domain of FimH adhesin by the usher FimD is required for type 1 pilus biogenesis. Mol Microbiol **64:**333-346.

110.	**Langermann S, Mollby R, Burlein JE, Palaszynski SR, Auguste CG, DeFusco A, Strouse R, Schenerman MA, Hultgren SJ, Pinkner JS, Winberg J, Guldevall L, Soderhall M, Ishikawa K, Normark S, Koenig S.** 2000. Vaccination with FimH adhesin protects cynomolgus monkeys from colonization and infection by uropathogenic Escherichia coli. The Journal of infectious diseases **181:**774-778.

111.	**Langermann S, Palaszynski S, Barnhart M, Auguste G, Pinkner JS, Burlein J, Barren P, Koenig S, Leath S, Jones CH, Hultgren SJ.** 1997. Prevention of mucosal *Escherichia coli* infection by FimH-adhesin-based systemic vaccination. Science **276:**607-611.

112.	**Hannan TJ, Totsika M, Mansfield KJ, Moore KH, Schembri MA, Hultgren SJ.** 2012. Host-pathogen checkpoints and population bottlenecks in persistent and intracellular uropathogenic *Escherichia coli* bladder infection. FEMS Microbiol. Rev. **36:**616-648.

113. **Abraham SN, Sun D, Dale JB, Beachey EH.** 1988. Conservation of the D-mannose-adhesion protein among type 1 fimbriated members of the family Enterobacteriaceae. Nature **336:**682-684.

114. **Pak J, Pu Y, Zhang ZT, Hasty DL, Wu XR.** 2001. Tamm-Horsfall protein binds to type 1 fimbriated *Escherichia coli* and prevents *E. coli* from binding to uroplakin Ia and Ib receptors. J. Biol. Chem. **276:**9924-9930.

115. **Baorto DM, Gao Z, Malaviya R, Dustin ML, van der Merwe A, Lublin DM, Abraham SN.** 1997. Survival of FimH-expressing enterobacteria in macrophages relies on glycolipid traffic. Nature **389:**636-639.

116. **Kukkonen M, Raunio T, Virkola R, Lahteenmaki K, Makela PH, Klemm P, Clegg S, Korhonen TK.** 1993. Basement membrane carbohydrate as a target for bacterial adhesion: binding of type 1 fimbriae of *Salmonella enterica* and E*scherichia coli* to laminin. Mol. Microbiol. **7:**229-227.

117. **Pratt LA, Kolter R.** 1998. Genetic analysis of *Escherichia coli* biofilm formation: roles of flagella, motility, chemotaxis and type I pili. Mol Microbiol **30:**285-293.

118. **Jones CH, Pinkner JS, Roth R, Heuser J, Nicholoes AV, Abraham SN, Hultgren SJ.** 1995. FimH adhesin of type 1 pili is assembled into a fibrillar tip structure in the *Enterobacteriaceae*. Proc. Natl. Acad. Sci. USA **92:**2081-2085.

119. **Hahn E, Wild P, Hermanns U, Sebbel P, Glockshuber R, Haner M, Taschner N, Burkhard P, Aebi U, Muller SA.** 2002. Exploring the 3D molecular architecture of Escherichia coli type 1 pili. J Mol Biol **323:**845-857.

120. **Le Trong I, Aprikian P, Kidd BA, Forero-Shelton M, Tchesnokova V, Rajagopal P, Rodriguez V, Interlandi G, Klevit R, Vogel V, Stenkamp RE, Sokurenko EV, Thomas WE.** 2010. Structural basis for mechanical force regulation of the adhesin FimH via finger trap-like beta sheet twisting. Cell **141:**645-655.

121. **Zhou G, Mo WJ, Sebbel P, Min G, Neubert TA, Glockshuber R, Wu XR, Sun TT, Kong XP.** 2001. Uroplakin Ia is the urothelial receptor for uropathogenic *Escherichia coli*: evidence from in vitro FimH binding. J Cell Sci **114:**4095-4103.

122. **Thumbikat P, Berry RE, Zhou G, Billips BK, Yaggie RE, Zaichuk T, Sun TT, Schaeffer AJ, Klumpp DJ.** 2009. Bacteria-induced uroplakin signaling mediates bladder response to infection. PLoS Pathog. **5:**e1000415.

123. **Connell H, Agace W, Klemm P, Schembri M, Marild S, Svanborg C.** 1996. Type 1 fimbrial expression enhances Escherichia coli virulence for the urinary tract. Proc Natl Acad Sci USA **93:**9827-9832.

124. **Song J, Bishop BL, Li G, Grady R, Stapleton A, Abraham SN.** 2009. TLR4-mediated expulsion of bacteria from infected bladder epithelial cells. Proc. Natl. Acad. Sci. U S A **106:**14966-14971.

125. **Anderson GG, Palermo JJ, Schilling JD, Roth R, Heuser J, Hultgren SJ.** 2003. Intracellular bacterial biofilm-like pods in urinary tract infections. Science **301:**105-107.

126. **Justice SS, Hung C, Theriot JA, Fletcher DA, Anderson GG, Footer MJ, Hultgren SJ.** 2004. Differentiation and developmental pathways of uropathogenic Escherichia coli in urinary tract pathogenesis. Proceedings of the National Academy of Sciences of the United States of America **101:**1333-1338.

127. **Blango MG, Mulvey MA.** 2010. Persistence of uropathogenic *Escherichia coli* in the face of multiple antibiotics. Antimicrob. Agents Chemother. **54:**1855-1863.

128. **Chen SL, Hung CS, Pinkner JS, Walker JN, Cusumano CK, Li Z, Bouckaert J, Gordon JI, Hultgren SJ.** 2009. Positive selection identifies an in vivo role for FimH during urinary tract infection in addition to mannose binding. Proc Natl Acad Sci USA **106:**22439-22444.

129. **Mulvey MA, Schilling JD, Hultgren SJ.** 2001. Establishment of a persistent Escherichia coli reservoir during the acute phase of a bladder infection. Infection and immunity **69:**4572-4579.

130. **Mysorekar IU, Hultgren SJ.** 2006. Mechanisms of uropathogenic *Escherichia coli* persistence and eradication from the urinary tract. Proc Natl Acad Sci USA **103:**14170-14175.

131. **Bock K, Breimer ME, Brignole A, Hansson GC, Karlsson K-A, Larson G, Leffler H, Samuelsson BE, Strömberg N, Svanborg-Edén C, Thurin J.** 1985. Specificity of binding of a strain of uropathogenic Escherichia coli to Gala(1-4)Gal-containing glycosphingolipids. The Journal of biological chemistry **260:**8545-8551.

132. **Roberts JA, Marklund BI, Ilver D, Haslam D, Kaack MB, Baskin G, Louis M, Mollby R, Winberg J, Normark S.** 1994. The Gal(alpha 1-4)Gal-specific tip adhesin of Escherichia coli P-fimbriae is needed for pyelonephritis to occur in the normal urinary tract. Proceedings of the National Academy of Sciences of the United States of America **91:**11889-11893.

133. **Kallenius G, Mollby R, Svenson SB, Windberg J, Lundblud A, Svenson S, Cedergen B.** 1980. The P[k] antigen as receptor for the haemagglutinin of pyelonephritogenic *Escherichia coli*. FEMS Microbiol. Lett. **7:**297-302.

134. **Ewers C, Li G, Wilking H, Kiessling S, Alt K, Antao EM, Laturnus C, Diehl I, Glodde S, Homeier T, Bohnke U, Steinruck H, Philipp HC, Wieler LH.** 2007. Avian pathogenic, uropathogenic, and newborn meningitis-causing *Escherichia coli*: how closely related are they? International journal of medical microbiology : IJMM **297:**163-176.

135. **Welch RA, Burland V, Plunkett G, 3rd, Redford P, Roesch P, Rasko D, Buckles EL, Liou SR, Boutin A, Hackett J, Stroud D, Mayhew GF, Rose DJ, Zhou S, Schwartz DC, Perna NT, Mobley HL, Donnenberg MS, Blattner FR.** 2002. Extensive mosaic structure revealed by the complete genome sequence of uropathogenic Escherichia coli. Proc. Natl. Acad. Sci. U S A **99:**17020-17024.

136. **Lund B, Marklund BI, Stromberg N, Lindberg F, Karlsson KA, Normark S.** 1988. Uropathogenic *Escherichia coli* Can Express Serologically Identical Pili of Different Receptor-Binding Specificities. Mol. Microbiol. **2:**255-263.

137. **Kuehn MJ, Heuser J, Normark S, Hultgren SJ.** 1992. P pili in uropathogenic *E. coli* are composite fibres with distinct fibrillar adhesive tips. Nature **356:**252-255.

138. **Jacob-Dubuisson F, Heuser J, Dodson K, Normark S, Hultgren SJ.** 1993. Initiation of assembly and association of the structural elements of a bacterial pilus depend on two specialized tip proteins. The EMBO journal **12:**837-847.

139. **Mu XQ, Bullitt E.** 2006. Structure and assembly of P-pili: a protruding hinge region used for assembly of a bacterial adhesion filament. Proceedings of the National Academy of Sciences of the United States of America **103:**9861-9866.

140. **Baga M, Norgren M, Normark S.** 1987. Biogenesis of *E. coli* Pap pili: PapH, a minor pilin subunit involved in cell anchoring and length modulation. Cell **49:**241-251.

141. **Verger D, Miller E, Remaut H, Waksman G, Hultgren S.** 2006. Molecular mechanism of P pilus termination in uropathogenic Escherichia coli. Embo Rep **7:**1228-1232.

142. **Hagberg L, Hull R, Hull S, Falkow S, Freter R, Svanborg Eden C.** 1983. Contribution of adhesion to bacterial persistence in the mouse urinary tract. Infect. Immun. **40:**265-272.

143. **Roberts JA, Hardaway K, Kaack B, Fussell EN, Baskin G.** 1984. Prevention of pyelonephritis by immunization with P-fimbriae. J. Urol. **131:**602-607.

144. **O'Hanley P, Lark D, Falkow S, Schoolnik G.** 1985. Molecular basis of *Escherichia coli* colonizatin of the upper urinary tract in BALB/c mice: Gal-Gal pili immunization prevents *Escherichia coli* pyelonephritis. J. Clin. Invest. **83:**2102-2108.

145. **Lane MC, Mobley HL.** 2007. Role of P-fimbrial-mediated adherence in pyelonephritis and persistence of uropathogenic *Escherichia coli* (UPEC) in the mammalian kidney. Kidney international **72:**19-25.

146. **Hedlund M, Svensson M, Nilsson Å, Duan R-D, Svanborg C.** 1996. Role of the ceramide-signaling pathway in cytokine responses to P-fimbriated *Escherichia coli*. J. Exp. Med. **183:**1037-1044.

147. **Hedlund M, Wachtler C, Johansson E, Hang L, Somerville JE, Darveau RP, Svanborg C.** 1999. P fimbriae-dependent, lipopolysaccharide-independent activation of epithelial cytokine responses. Mol. Microbiol. **33:**693-703.

148. **Fischer H, Ellstrom P, Ekstrom K, Gustafsson L, Gustafsson M, Svanborg C.** 2007. Ceramide as a TLR4 agonist; a putative signalling intermediate between sphingolipid receptors for microbial ligands and TLR4. Cellular microbiology **9:**1239-1251.

149. **Silhavy TJ, Kahne D, Walker S.** 2010. The bacterial cell envelope. Cold Spring Harb Perspect Biol **2:**a000414.

150. **Snyder WB, Davis LJ, Danese PN, Cosma CL, Silhavy TJ.** 1995. Overproduction of NlpE, a new outer membrane lipoprotein, suppresses the toxicity of periplasmic LacZ by activation of the Cpx signal transduction pathway. J Bacteriol **177:**4216-4223.

151. **Majdalani N, Heck M, Stout V, Gottesman S.** 2005. Role of RcsF in signaling to the Rcs phosphorelay pathway in Escherichia coli. J Bacteriol **187:**6770-6778.

152. **Tanaka K, Matsuyama SI, Tokuda H.** 2001. Deletion of lolB, encoding an outer membrane lipoprotein, is lethal for Escherichia coli and causes accumulation of lipoprotein localization intermediates in the periplasm. J Bacteriol **183:**6538-6542.

153. **Malojcic G, Andres D, Grabowicz M, George AH, Ruiz N, Silhavy TJ, Kahne D.** 2014. LptE binds to and alters the physical state of LPS to catalyze its assembly at the cell surface. Proceedings of the National Academy of Sciences of the United States of America **111:**9467-9472.

154. **Ricci DP, Silhavy TJ.** 2012. The Bam machine: a molecular cooper. Biochimica et biophysica acta **1818:**1067-1084.

155. **Chahales P, Thanassi DG.** 2015. A more flexible lipoprotein sorting pathway. J Bacteriol **197:**1702-1704.

156. **Wimley WC.** 2003. The versatile beta-barrel membrane protein. Curr Opin Struct Biol **13:**404-411.

157. **Mangel WF, Toledo DL, Brown MT, Worzalla K, M. L, J. DJ.** 1994. Omptin: an *Escherichia coli* outer membrane proteinase that activates plasminogen. Methods Enzymol. **244:**384-399.

158. **Pratt L, Hsing W, Gibson K, Silhavy T.** 1996. From acids to osmZ: multiple factors influence synthesis of the OmpF and OmpC porins in Escherichia coli. Mol Microbiol **20:**911-917.

159. **Wandersman C, Delepelaire P.** 1990. TolC, an Escherichia coli outer membrane protein required for hemolysin secretion. Proceedings of the National Academy of Sciences of the United States of America **87:**4776-4780.

160. **El Tahir Y, Skurnik M.** 2001. YadA, the multifaceted *Yersinia* adhesin. Int J Med Microbiol **291:**209-218.

161. **Paschen SA, Neupert W, Rapaport D.** 2005. Biogenesis of beta-barrel membrane proteins of mitochondria. Trends in biochemical sciences **30:**575-582.

162. **Hsu SC, Inoue K.** 2009. Two evolutionarily conserved essential beta-barrel proteins in the chloroplast outer envelope membrane. Biosci Trends **3:**168-178.

163. **Sugawara E, Steiert M, Rouhani S, Nikaido H.** 1996. Secondary structure of the outer membrane proteins OmpA of *Escherichia coli* and OprF of *Pseudomonas aeruginosa*. J. Bacteriol. **178:**6067-6069.

164. **Mack D, Heesemann J, Laufs R.** 1994. Characterization of different oligomeric species of the Yersinia enterocolitica outer membrane protein YadA. Med Microbiol Immunol **183:**217-227.

165. **Fleming KG.** 2015. A combined kinetic push and thermodynamic pull as driving forces for outer membrane protein sorting and folding in bacteria. Philosophical transactions of the Royal Society of London. Series B, Biological sciences **370**.

166. **Wu T, Malinverni J, Ruiz N, Kim S, Silhavy TJ, Kahne D.** 2005. Identification of a multicomponent complex required for outer membrane biogenesis in Escherichia coli. Cell **121:**235-245.

167. **Krojer T, Sawa J, Schafer E, Saibil HR, Ehrmann M, Clausen T.** 2008. Structural basis for the regulated protease and chaperone function of DegP. Nature **453:**885-890.

168. **Thoma J, Burmann BM, Hiller S, Muller DJ.** 2015. Impact of holdase chaperones Skp and SurA on the folding of beta-barrel outer-membrane proteins. Nat Struct Mol Biol **22:**795-802.

169. **Albrecht R, Schutz M, Oberhettinger P, Faulstich M, Bermejo I, Rudel T, Diederichs K, Zeth K.** 2014. Structure of BamA, an essential factor in outer membrane protein biogenesis. Acta crystallographica. Section D, Biological crystallography **70:**1779-1789.

170. **Kim S, Malinverni JC, Sliz P, Silhavy TJ, Harrison SC, Kahne D.** 2007. Structure and function of an essential component of the outer membrane protein assembly machine. Science **317:**961-964.

171. **Malinverni JC, Werner J, Kim S, Sklar JG, Kahne D, Misra R, Silhavy TJ.** 2006. YfiO stabilizes the YaeT complex and is essential for outer membrane protein assembly in Escherichia coli. Mol Microbiol **61:**151-164.

172. **Dong C, Yang X, Hou HF, Shen YQ, Dong YH.** 2012. Structure of Escherichia coli BamB and its interaction with POTRA domains of BamA. Acta crystallographica. Section D, Biological crystallography **68:**1134-1139.

173. **Ruiz N, Falcone B, Kahne D, Silhavy TJ.** 2005. Chemical conditionality: a genetic strategy to probe organelle assembly. Cell **121:**307-317.

174. **Charlson ES, Werner JN, Misra R.** 2006. Differential effects of yfgL mutation on Escherichia coli outer membrane proteins and lipopolysaccharide. J Bacteriol **188:**7186-7194.

175. **Misra R, Stikeleather R, Gabriele R.** 2015. In vivo roles of BamA, BamB and BamD in the biogenesis of BamA, a core protein of the beta-barrel assembly machine of Escherichia coli. J Mol Biol **427:**1061-1074.

176. **Hagan CL, Westwood DB, Kahne D.** 2013. bam Lipoproteins Assemble BamA in vitro. Biochemistry **52:**6108-6113.

177. **Kim KH, Aulakh S, Tan W, Paetzel M.** 2011. Crystallographic analysis of the C-terminal domain of the Escherichia coli lipoprotein BamC. Acta crystallographica. Section F, Structural biology and crystallization communications **67:**1350-1358.

178. **Rigel NW, Schwalm J, Ricci DP, Silhavy TJ.** 2012. BamE modulates the Escherichia coli beta-barrel assembly machine component BamA. J Bacteriol **194:**1002-1008.

179. **Webb CT, Selkrig J, Perry AJ, Noinaj N, Buchanan SK, Lithgow T.** 2012. Dynamic association of BAM complex modules includes surface exposure of the lipoprotein BamC. J Mol Biol **422:**545-555.

180. **Sandoval CM, Baker SL, Jansen K, Metzner SI, Sousa MC.** 2011. Crystal structure of BamD: an essential component of the beta-Barrel assembly machinery of gram-negative bacteria. J Mol Biol **409:**348-357.

181. **Ricci DP, Hagan CL, Kahne D, Silhavy TJ.** 2012. Activation of the Escherichia coli beta-barrel assembly machine (Bam) is required for essential components to interact properly with substrate. Proceedings of the National Academy of Sciences of the United States of America **109:**3487-3491.

182. **Knowles TJ, Browning DF, Jeeves M, Maderbocus R, Rajesh S, Sridhar P, Manoli E, Emery D, Sommer U, Spencer A, Leyton DL, Squire D, Chaudhuri RR, Viant MR, Cunningham AF, Henderson IR, Overduin M.** 2011. Structure and function of BamE within the outer membrane and the beta-barrel assembly machine. Embo Rep **12:**123-128.

183. **Sklar JG, Wu T, Gronenberg LS, Malinverni JC, Kahne D, Silhavy TJ.** 2007. Lipoprotein SmpA is a component of the YaeT complex that assembles outer membrane proteins in Escherichia coli. Proceedings of the National Academy of Sciences of the United States of America **104:**6400-6405.

184. **Rigel NW, Ricci DP, Silhavy TJ.** 2013. Conformation-specific labeling of BamA and suppressor analysis suggest a cyclic mechanism for beta-barrel assembly in Escherichia coli. Proceedings of the National Academy of Sciences of the United States of America **110:**5151-5156.

185. **Justice SS, Hunstad DA, Harper JR, Duguay AR, Pinkner JS, Bann J, Frieden C, Silhavy TJ, Hultgren SJ.** 2005. Periplasmic peptidyl prolyl cis-trans isomerases are not essential for viability, but SurA is required for pilus biogenesis in Escherichia coli. J Bacteriol **187:**7680-7686.

186. **Palomino C, Marin E, Fernandez LA.** 2011. The fimbrial usher FimD follows the SurA-BamB pathway for its assembly in the outer membrane of Escherichia coli. J Bacteriol **193:**5222-5230.

187. **Gupta K, Hooton TM, Naber KG, Wullt B, Colgan R, Miller LG, Moran GJ, Nicolle LE, Raz R, Schaeffer AJ, Soper DE, Infectious Diseases Society of A, European Society for M, Infectious D.** 2011. International clinical practice guidelines for the

treatment of acute uncomplicated cystitis and pyelonephritis in women: A 2010 update by the Infectious Diseases Society of America and the European Society for Microbiology and Infectious Diseases. Clinical infectious diseases : an official publication of the Infectious Diseases Society of America **52:**e103-120.

188. **Wang A, Nizran P, Malone MA, Riley T.** 2013. Urinary tract infections. Primary care **40:**687-706.

189. **Busch A, Phan G, Waksman G.** 2015. Molecular mechanism of bacterial type 1 and P pili assembly. Philosophical transactions. Series A, Mathematical, physical, and engineering sciences **373**.

190. **Roberts JA, Kaack MB, Baskin G, Chapman MR, Hunstad DA, Pinkner JS, Hultgren SJ.** 2004. Antibody responses and protection from pyelonephritis following vaccination with purified Escherichia coli PapDG protein. The Journal of urology **171:**1682-1685.

191. **Salminen A, Loimaranta V, Joosten JA, Khan AS, Hacker J, Pieters RJ, Finne J.** 2007. Inhibition of P-fimbriated *Escherichia coli* adhesion by multivalent galabiose derivatives studied by a live-bacteria application of surface plasmon resonance. The Journal of antimicrobial chemotherapy **60:**495-501.

192. **Wellens A, Garofalo C, Nguyen H, Van Gerven N, Slattegard R, Hernalsteens JP, Wyns L, Oscarson S, De Greve H, Hultgren S, Bouckaert J.** 2008. Intervening with urinary tract infections using anti-adhesives based on the crystal structure of the FimH-oligomannose-3 complex. PloS one **3:**e2040.

193. **Han Z, Pinkner JS, Ford B, Obermann R, Nolan W, Wildman SA, Hobbs D, Ellenberger T, Cusumano CK, Hultgren SJ, Janetka JW.** 2010. Structure-based drug design and optimization of mannoside bacterial FimH antagonists. Journal of medicinal chemistry **53:**4779-4792.

194. **Schwardt O, Rabbani S, Hartmann M, Abgottspon D, Wittwer M, Kleeb S, Zalewski A, Smiesko M, Cutting B, Ernst B.** 2011. Design, synthesis and biological evaluation of mannosyl triazoles as FimH antagonists. Bioorganic & medicinal chemistry **19:**6454-6473.

195. **Pinkner JS, Remaut H, Buelens F, Miller E, Aberg V, Pemberton N, Hedenstrom M, Larsson A, Seed P, Waksman G, Hultgren SJ, Almqvist F.** 2006. Rationally designed small compounds inhibit pilus biogenesis in uropathogenic bacteria. Proceedings of the National Academy of Sciences of the United States of America **103:**17897-17902.

196. **Svensson A, Larsson A, Emtenas H, Hedenstrom M, Fex T, Hultgren SJ, Pinkner JS, Almqvist F, Kihlberg J.** 2001. Design and evaluation of pilicides: Potential novel antibacterial agents directed against uropathogenic Escherichia coli. Chembiochem **2:**915-918.

197. **Cegelski L, Pinkner JS, Hammer ND, Cusumano CK, Hung CS, Chorell E, Aberg V, Walker JN, Seed PC, Almqvist F, Chapman MR, Hultgren SJ.** 2009. Small-molecule inhibitors target Escherichia coli amyloid biogenesis and biofilm formation. Nature chemical biology **5:**913-919.

198. **Lo AW, Van de Water K, Gane PJ, Chan AW, Steadman D, Stevens K, Selwood DL, Waksman G, Remaut H.** 2014. Suppression of type 1 pilus assembly in uropathogenic Escherichia coli by chemical inhibition of subunit polymerization. The Journal of antimicrobial chemotherapy **69:**1017-1026.

199. **Greene SE, Pinkner JS, Chorell E, Dodson KW, Shaffer CL, Conover MS, Livny J, Hadjifrangiskou M, Almqvist F, Hultgren SJ.** 2014. Pilicide ec240 disrupts virulence circuits in uropathogenic Escherichia coli. mBio **5:**e02038.

200. **Cegelski L, Marshall GR, Eldridge GR, Hultgren SJ.** 2008. The biology and future prospects of antivirulence therapies. Nat Rev Micro **6:**17-27.

201. **Dobrindt U, Hacker J.** 2008. Targeting virulence traits: potential strategies to combat extraintestinal pathogenic *E. coli* infections. Curr. Opin. Microbiol. **11:**409-413.

202. **Boguski MS, Mandl KD, Sukhatme VP.** 2009. Repurposing with a Difference. Science **324:**1394-1395.

203. **White CA, Jr.** 2004. Nitazoxanide: a new broad spectrum antiparasitic agent. Expert review of anti-infective therapy **2:**43-49.

204. **Stockis A, De Bruyn S, Gengler C, Rosillon D.** 2002. Nitazoxanide pharmacokinetics and tolerability in man during 7 days dosing with 0.5 g and 1 g b.i.d. Int J Clin Pharm Th **40:**221-227.

205. **Rossignol JF.** 2014. Nitazoxanide: a first-in-class broad-spectrum antiviral agent. Antiviral research **110:**94-103.

206. **Nikolova K, Gluud C, Grevstad B, Jakobsen JC.** 2014. Nitazoxanide for chronic hepatitis C. The Cochrane database of systematic reviews **4:**CD009182.

207. **Di Santo N, Ehrisman J.** 2014. A functional perspective of nitazoxanide as a potential anticancer drug. Mutation research **768:**16-21.

208. **McVay CS, Rolfe RD.** 2000. In vitro and in vivo activities of nitazoxanide against Clostridium difficile. Antimicrob Agents Chemother **44:**2254-2258.

209. **Hoffman PS, Sisson G, Croxen MA, Welch K, Harman WD, Cremades N, Morash MG.** 2007. Antiparasitic drug nitazoxanide inhibits the pyruvate oxidoreductases of Helicobacter pylori, selected anaerobic bacteria and parasites, and Campylobacter jejuni. Antimicrob Agents Chemother **51:**868-876.

210. **Dubreuil L, Houcke I, Mouton Y, Rossignol JF.** 1996. In vitro evaluation of activities of nitazoxanide and tizoxanide against anaerobes and aerobic organisms. Antimicrob Agents Chemother **40:**2266-2270.

211. **Warren CA, van Opstal E, Ballard TE, Kennedy A, Wang X, Riggins M, Olekhnovich I, Warthan M, Kolling GL, Guerrant RL, Macdonald TL, Hoffman PS.** 2012. Amixicile, a novel inhibitor of pyruvate: ferredoxin oxidoreductase, shows efficacy against Clostridium difficile in a mouse infection model. Antimicrob Agents Chemother **56:**4103-4111.

212. **Sisson G, Goodwin A, Raudonikiene A, Hughes NJ, Mukhopadhyay AK, Berg DE, Hoffman PS.** 2002. Enzymes associated with reductive activation and action of nitazoxanide, nitrofurans, and metronidazole in Helicobacter pylori. Antimicrob Agents Chemother **46:**2116-2123.

213. **Shamir ER, Warthan M, Brown SP, Nataro JP, Guerrant RL, Hoffman PS.** 2010. Nitazoxanide Inhibits Biofilm Production and Hemagglutination by Enteroaggregative Escherichia coli Strains by Blocking Assembly of AafA Fimbriae. Antimicrob Agents Ch **54:**1526-1533.

214. **Okhuysen PC, DuPont HL.** 2010. Enteroaggregative Escherichia coli (EAEC): A Cause of Acute and Persistent Diarrhea of Worldwide Importance. Journal of Infectious Diseases **202:**503-505.

215. **Wakimoto N, Nishi J, Sheikh J, Nataro JP, Sarantuya J, Iwashita M, Manago K, Tokuda K, Yoshinaga M, Kawano Y.** 2004. Quantitative biofilm assay using a microtiter plate to screen for enteroaggregative Escherichia coli. Am J Trop Med Hyg **71:**687-690.

216. **Bolick DT, Roche JK, Hontecillas R, Bassaganya-Riera J, Nataro JP, Guerrant RL.** 2013. Enteroaggregative Escherichia coli strain in a novel weaned mouse model: exacerbation by malnutrition, biofilm as a virulence factor and treatment by nitazoxanide. Journal of medical microbiology **62:**896-905.

217. **Baba T, Ara T, Hasegawa M, Takai Y, Okumura Y, Baba M, Datsenko KA, Tomita M, Wanner BL, Mori H.** 2006. Construction of Escherichia coli K-12 in-frame, single-gene knockout mutants: the Keio collection. Mol Syst Biol **2**.

218. **Baneyx F, Georgiou G.** 1990. In vivo degradation of secreted fusion proteins by the Escherichia coli outer membrane protease OmpT. J Bacteriol **172:**491-494.

219. **Cherepanov PP, Wackernagel W.** 1995. Gene disruption in Escherichia coli: TcR and KmR cassettes with the option of Flp-catalyzed excision of the antibiotic-resistance determinant. Gene **158:**9-14.

220. **Thomason LC, Costantino N, Court DL.** 2007. E. coli genome manipulation by P1 transduction. Current protocols in molecular biology / edited by Frederick M. Ausubel ... [et al.] **Chapter 1:**Unit 1 17.

221. **Strauch KL, Johnson K, Beckwith J.** 1989. Characterization of degP, a gene required for proteolysis in the cell envelope and essential for growth of Escherichia coli at high temperature. J Bacteriol **171:**2689-2696.

222. **Roman-Hernandez G, Peterson JH, Bernstein HD.** 2014. Reconstitution of bacterial autotransporter assembly using purified components. Elife **3:**e04234.

223. **Blomfield IC, McClain MS, Eisenstein BI.** 1991. Type 1 fimbriae mutants of Escherichia coli K12: characterization of recognized afimbriate strains and construction of new fim deletion mutants. Mol Microbiol **5:**1439-1445.

224. **Saulino ET, Bullitt E, Hultgren SJ.** 2000. Snapshots of usher-mediated protein secretion and ordered pilus assembly. Proceedings of the National Academy of Sciences of the United States of America **97:**9240-9245.

225. **Thanassi DG, Stathopoulos C, Dodson KW, Geiger D, Hultgren SJ.** 2002. Bacterial outer membrane ushers contain distinct targeting and assembly domains for pilus biogenesis. J Bacteriol **184:**6260-6269.

226. **Datsenko KA, Wanner BL.** 2000. One-step inactivation of chromosomal genes in Escherichia coli K-12 using PCR products. Proceedings of the National Academy of Sciences of the United States of America **97:**6640-6645.

227. **Hultgren SJ, Lindberg F, Magnusson G, Kihlberg J, Tennent JM, Normark S.** 1989. The PapG adhesin of uropathogenic Escherichia coli contains separate regions for receptor binding and for the incorporation into the pilus. Proceedings of the National Academy of Sciences of the United States of America **86:**4357-4361.

228. **Thanassi DG, Saulino ET, Lombardo MJ, Roth R, Heuser J, Hultgren SJ.** 1998. The PapC usher forms an oligomeric channel: implications for pilus biogenesis across the outer membrane. Proceedings of the National Academy of Sciences of the United States of America **95:**3146-3151.

229. **Jacob-Dubuisson F, Pinkner J, Xu Z, Striker R, Padmanhaban A, Hultgren SJ.** 1994. PapD chaperone function in pilus biogenesis depends on oxidant and chaperone-like activities of DsbA. Proc. Natl. Acad. Sci. USA **91:**11552-11556.

230. **Henderson NS, Thanassi DG.** 2013. Purification of the outer membrane usher protein and periplasmic chaperone-subunit complexes from the P and type 1 pilus systems. Methods in molecular biology **966:**37-52.

231. **Rose RE.** 1988. The nucleotide sequence of pACYC184. Nucleic acids research **16:**355.

232. **Morales VM, Backman A, Bagdasarian M.** 1991. A series of wide-host-range low-copy-number vectors that allow direct screening for recombinants. Gene **97:**39-47.

233. **Jones CH, Danese PN, Pinkner JS, Silhavy TJ, Hultgren SJ.** 1997. The chaperone-assisted membrane release and folding pathway is sensed by two signal transduction systems. The EMBO journal **16:**6394-6406.

234. **Sauer FG, Mulvey MA, Schilling JD, Martinez JJ, Hultgren SJ.** 2000. Bacterial pili: molecular mechanisms of pathogenesis. Current opinion in microbiology **3:**65-72.

235. **Cusumano CK, Hultgren SJ.** 2009. Bacterial adhesion--a source of alternate antibiotic targets. IDrugs : the investigational drugs journal **12:**699-705.

236. **Steadman D, Lo A, Waksman G, Remaut H.** 2014. Bacterial surface appendages as targets for novel antibacterial therapeutics. Future microbiology **9:**887-900.

237. **Geibel S, Waksman G.** 2014. The molecular dissection of the chaperone-usher pathway. Biochimica et biophysica acta **1843:**1559-1567.

238. **Boisen N, Struve C, Scheutz F, Krogfelt KA, Nataro JP.** 2008. New adhesin of enteroaggregative Escherichia coli related to the Afa/Dr/AAF family. Infection and immunity **76:**3281-3292.

239. **Jansen AM, Lockatell V, Johnson DE, Mobley HL.** 2004. Mannose-resistant Proteus-like fimbriae are produced by most Proteus mirabilis strains infecting the urinary tract, dictate the in vivo localization of bacteria, and contribute to biofilm formation. Infection and immunity **72:**7294-7305.

240. **Tomaras AP, Dorsey CW, Edelmann RE, Actis LA.** 2003. Attachment to and biofilm formation on abiotic surfaces by Acinetobacter baumannii: involvement of a novel chaperone-usher pili assembly system. Microbiology **149:**3473-3484.

241. **Vallet I, Olson JW, Lory S, Lazdunski A, Filloux A.** 2001. The chaperone/usher pathways of Pseudomonas aeruginosa: identification of fimbrial gene clusters (cup) and their involvement in biofilm formation. Proceedings of the National Academy of Sciences of the United States of America **98:**6911-6916.

242. **Murphy CN, Mortensen MS, Krogfelt KA, Clegg S.** 2013. Role of Klebsiella pneumoniae Type 1 and Type 3 Fimbriae in Colonizing Silicone Tubes Implanted into the Bladders of Mice as a Model of Catheter-Associated Urinary Tract Infections. Infection and immunity **81:**3009-3017.

243. **Romero Cabello R, Guerrero LR, Munoz Garcia MR, Geyne Cruz A.** 1997. Nitazoxanide for the treatment of intestinal protozoan and helminthic infections in Mexico. Transactions of the Royal Society of Tropical Medicine and Hygiene **91:**701-703.

244. **Gilles HM, Hoffman PS.** 2002. Treatment of intestinal parasitic infections: a review of nitazoxanide. Trends Parasitol **18:**95-97.

245. **Pankuch GA, Appelbaum PC.** 2006. Activities of tizoxanide and nitazoxanide compared to those of five other thiazolides and three other agents against anaerobic species. Antimicrob Agents Chemother **50:**1112-1117.
246. **Marklund BI, Tennent JM, Garcia E, Hamers A, Baga M, Lindberg F, Gaastra W, Normark S.** 1992. Horizontal gene transfer of the *Escherichia coli pap* and *prs* pili operons as a mechanism for the development of tissue-specific adhesive properties. Mol Microbiol **6:**2225-2242.
247. **Ge X, Wang R, Ma J, Liu Y, Ezemaduka AN, Chen PR, Fu X, Chang Z.** 2014. DegP primarily functions as a protease for the biogenesis of beta-barrel outer membrane proteins in the Gram-negative bacterium Escherichia coli. FEBS J **281:**1226-1240.
248. **Bardwell JC, McGovern K, Beckwith J.** 1991. Identification of a protein required for disulfide bond formation *in vivo*. Cell **67:**581-589.
249. **Norgren M, Baga M, Tennent JM, Normark S.** 1987. Nucleotide sequence, regulation and functional analysis of the papC gene required for cell surface localization of Pap pili of uropathogenic Escherichia coli. Mol Microbiol **1:**169-178.
250. **Fairman JW, Noinaj N, Buchanan SK.** 2011. The structural biology of beta-barrel membrane proteins: a summary of recent reports. Curr Opin Struct Biol **21:**523-531.
251. **Dong H, Xiang Q, Gu Y, Wang Z, Paterson NG, Stansfeld PJ, He C, Zhang Y, Wang W, Dong C.** 2014. Structural basis for outer membrane lipopolysaccharide insertion. Nature **511:**52-56.
252. **Qiao S, Luo QS, Zhao Y, Zhang XJC, Huang YH.** 2014. Structural basis for lipopolysaccharide insertion in the bacterial outer membrane. Nature **511:**108-U523.
253. **Mogensen JE, Otzen DE.** 2005. Interactions between folding factors and bacterial outer membrane proteins. Mol Microbiol **57:**326-346.
254. **Watts KM, Hunstad DA.** 2008. Components of SurA required for outer membrane biogenesis in uropathogenic Escherichia coli. PloS one **3:**e3359.
255. **Allen RC, Popat R, Diggle SP, Brown SP.** 2014. Targeting virulence: can we make evolution-proof drugs? Nature reviews. Microbiology **12:**300-308.
256. **Hunstad DA, Justice SS, Hung CS, Lauer SR, Hultgren SJ.** 2005. Suppression of bladder epithelial cytokine responses by uropathogenic Escherichia coli. Infection and immunity **73:**3999-4006.
257. **Justice SS, Lauer SR, Hultgren SJ, Hunstad DA.** 2006. Maturation of intracellular Escherichia coli communities requires SurA. Infection and immunity **74:**4793-4800.
258. **Sklar JG, Wu T, Kahne D, Silhavy TJ.** 2007. Defining the roles of the periplasmic chaperones SurA, Skp, and DegP in Escherichia coli. Genes Dev **21:**2473-2484.
259. **Aoki SK, Malinverni JC, Jacoby K, Thomas B, Pamma R, Trinh BN, Remers S, Webb J, Braaten BA, Silhavy TJ, Low DA.** 2008. Contact-dependent growth inhibition requires the essential outer membrane protein BamA (YaeT) as the receptor and the inner membrane transport protein AcrB. Mol Microbiol **70:**323-340.
260. **Onufryk C, Crouch ML, Fang FC, Gross CA.** 2005. Characterization of six lipoproteins in the sigmaE regulon. J Bacteriol **187:**4552-4561.
261. **Dwyer RS, Ricci DP, Colwell LJ, Silhavy TJ, Wingreen NS.** 2013. Predicting functionally informative mutations in Escherichia coli BamA using evolutionary covariance analysis. Genetics **195:**443-455.
262. **Roelofs KG, Wang J, Sintim HO, Lee VT.** 2011. Differential radial capillary action of ligand assay for high-throughput detection of protein-metabolite interactions.

Proceedings of the National Academy of Sciences of the United States of America **108:**15528-15533.

263. **Kim KH, Paetzel M.** 2011. Crystal structure of Escherichia coli BamB, a lipoprotein component of the beta-barrel assembly machinery complex. J Mol Biol **406:**667-678.
264. **Kim KH, Aulakh S, Paetzel M.** 2011. Crystal structure of beta-barrel assembly machinery BamCD protein complex. The Journal of biological chemistry **286:**39116-39121.
265. **Jansen KB, Baker SL, Sousa MC.** 2015. Crystal Structure of BamB Bound to a Periplasmic Domain Fragment of BamA, the Central Component of the beta-Barrel Assembly Machine. The Journal of biological chemistry **290:**2126-2136.